NASA Contractor Report 3916

NASA-CR-3916 19850025820

Design and Testing of an Energy-Absorbing Crewseat for the F/FB-111 Aircraft

Volume I—Final Report

S. Joseph Shane

LIBRARY COPY

SEP 1985

LANGLEY RESEARCH CENTER
LIBRARY, NASA
HAMPTON, VIRGINIA

CONTRACT NAS1-17387
AUGUST 1985

NASA

NASA Contractor Report 3916

Design and Testing of an Energy-Absorbing Crewseat for the F/FB-111 Aircraft

Volume I—Final Report

S. Joseph Shane
Simula Inc.
Phoenix, Arizona

Prepared for
Langley Research Center
under Contract NAS1-17387

National Aeronautics
and Space Administration

Scientific and Technical
Information Branch

1985

PREFACE

This report was prepared by Simula Inc. under Contract No. NAS1-17387 for the National Aeronautics and Space Administration, Langley Research Center, Hampton, Virginia. Mr. Claude B. Castle served as the Technical Monitor.

Several other organizations made contributions to this work. The effort of the Federal Aviation Administration was managed by Mr. Richard F. Chandler, Chief of the Protection and Survival Laboratory, Civil Aeromedical Institute. Contributions of the U.S. Army Applied Technology Laboratories (AVSCOM) were managed by Mr. Kent Smith. Efforts of the U.S. Air Force were supervised by Mr. Patrick Santucci, Sacramento Air Logistics Center (SM-ALC), McLellan Air Force Base.

TABLE OF CONTENTS

	Page
1.0 INTRODUCTION	1
1.1 BACKGROUND	1
1.1.1 System Description	1
1.1.2 Acceleration Environment	3
1.1.3 Injury Record	7
1.2 PROGRAM OBJECTIVES	9
2.0 ENERGY-ABSORBING SEAT DESIGN	12
2.1 OPERATIONAL F-111 SEAT	12
2.1.1 General	12
2.1.2 Restraint	14
2.1.3 Cushions	16
2.2 DESIGN GUIDELINES	16
2.2.1 Energy-Absorbing Function	16
2.2.2 Other Seat Requirements	18
2.3 TEST SEAT	19
2.4 SEAT PAN LOAD CELLS	24
2.4.1 Modified Operational Seat Pan	24
2.4.2 Modified Energy-Absorbing Seat Pan	24
3.0 SEAT TESTING	28
3.1 TEST OBJECTIVES	28
3.2 CONDUCT OF TESTING	28
3.2.1 Test Facility	28
3.2.2 Test Methods	28
3.2.3 Test Matrix	31
3.2.4 Acceleration Pulse Characteristics	34

TABLE OF CONTENTS (CONTD)

	Page
3.3 PERFORMANCE OF THE ENERGY-ABSORBING SEAT	36
3.3.1 Acceleration Levels	37
3.3.2 Energy-Absorbing Stroke	45
3.3.3 Structural Integrity	45
3.3.4 Conclusions	46
3.4 COMPARISON OF OPERATIONAL AND ENERGY-ABSORBING F-111 SEATS	47
3.4.1 Acceleration Levels	48
3.4.2 Spinal Loads	56
3.4.3 Seat Pan Loads	58
3.4.4 Conclusions	64
4.0 CAPSULE TESTING	73
4.1 TEST OBJECTIVES	73
4.2 CONDUCT OF TESTING	73
4.2.1 Test Facility	73
4.2.2 Test Methods	75
4.2.3 Test Matrix	90
4.3 RESULTS OF CAPSULE TESTING	95
4.3.1 Test Conditions	95
4.3.2 Occupant Acceleration Levels	99
4.3.3 Seat Pan Loads	105
4.3.4 Vertical Stroking	108
4.3.5 Structural Integrity	114
4.4 CONCLUSIONS	115

TABLE OF CONTENTS (CONTD)

	Page
5.0 RETROFIT SEAT	116
5.1 DESIGN GUIDELINES	116
5.2 SEAT DESCRIPTION	118
5.2.1 Overall Description	118
5.2.2 Bulkhead Attachment	122
6.0 CONCLUSIONS	128
6.1 DISCUSSION	128
6.2 CONCLUSIONS	132
6.3 RECOMMENDATIONS	133
7.0 REFERENCES	135

LIST OF ILLUSTRATIONS

Figure		Page
1	F-111 crew module (courtesy U.S. Air Force)	2
2	Vertical seat pan accelerations during ejection phase of F-111 escape sequence at 64.2 KEAS (courtesy U.S. Air Force)	4
3	Vertical seat pan accelerations during ejection phase of F-111 escape sequence at 302.8 KEAS (courtesy U.S. Air Force)	4
4	Dynamic Response Index during ejection phase of F-111 escape sequence (Reference 1)	5
5	Correlation between Dynamic Response Index and spinal injury rate for ejection seats (Reference 2)	5
6	Module vertical accelerations during ground impact (courtesy U.S. Air Force)	6
7	Values of Dynamic Response Index for ground impacts calculated during qualification testing of F-111 crew module (Reference 3)	6
8	F-111 seat and occupant after shoulder strap haul-back with harness yoke properly positioned (Reference 3)	10
9	F-111 seat and occupant after shoulder strap haul-back with harness yoke improperly positioned (Reference 3)	10
10	Operational F-111 crewseat (Reference 3)	13
11	F-111 crewseat adjustment geometry	14
12	F-111 crewseat restraint system (Reference 3)	15
13	Energy-absorbing test seat	20
14	Front view of energy-absorbing test seat	21
15	Side view of energy-absorbing test seat	21
16	Back view of energy-absorbing test seat	22
17	Operational seat pan modified to incorporate seat pan load cells (Reference 3)	25
18	Modification of test seat to incorporate seat pan load cells	26

LIST OF ILLUSTRATIONS (CONTD)

Figure		Page
19	Seat pan from test seat that incorporates seat pan load cells	27
20	CAMI wire-bending decelerator mechanism (Reference 12)	29
21	Test fixture used in dynamic seat testing at CAMI	30
22	Energy-absorbing seat prior to CAMI test	32
23	Energy-absorbing seat after CAMI test	33
24	Definition of notation used in test pulse description	36
25	Seat pan vertical acceleration trace from CAMI test of energy-absorbing seat	40
26	Acceptable duration-magnitude curve for seat pan acceleration levels (Reference 14)	42
27	Seat pan acceleration measured during qualification to MIL-S-58095(AV)	44
28	Seat pan acceleration and corresponding DRI for energy-absorbing seat	46
29	Dynamic Response Index as a function of energy-absorber limit load	47
30	Dynamic Response Index measurements from energy-absorbing seat tests at CAMI	48
31	Pretest photograph from CAMI Test No. A83-101	49
32	Bearing assembly, roller, and bolt from energy-absorbing seat	51
33	Seat pan z-axis acceleration levels from energy-absorbing and operational seat tests at CAMI	52
34	Peak acceleration levels along the seat back tangent line for energy-absorbing and operational seat tests at CAMI	53
35	Dummy pelvis z-axis peak acceleration levels from energy-absorbing and operational seat tests at CAMI	54

LIST OF ILLUSTRATIONS (CONTD)

Figure		Page
36	Dummy chest z-axis peak acceleration levels from energy-absorbing and operational seat tests at CAMI	55
37	Seat pan z-axis accelerations for energy-absorbing and operational seats in similar tests corresponding to NASA Test No. 5	56
38	Seat pan z-axis accelerations for energy-absorbing operational seats in similar tests corresponding to NASA Test No. 6	57
39	Seat pan z-axis accelerations for energy-absorbing and operational seats in similar tests corresponding to NASA Test No. 8	58
40	Dynamic Response Index determined from seat pan z-axis accelerations in CAMI tests	60
41	Dynamic Response Index determined from seat back tangent line accelerations in CAMI tests	61
42	Dynamic Response Index determined from dummy pelvis z-axis accelerations in CAMI tests	62
43	Seat pan z-axis accelerations and spinal compression loads for CAMI tests corresponding to NASA Test No. 5	65
44	Seat pan z-axis accelerations and spinal compression loads for CAMI tests corresponding to NASA Test No. 6	66
45	Seat pan z-axis accelerations and spinal compression loads for CAMI tests corresponding to NASA Test No. 8	67
46	Dummy spinal compression and center seat pan vertical loads in CAMI tests corresponding to NASA Test No. 5	69
47	Seat pan z-axis accelerations and spinal compression loads for CAMI tests corresponding to NASA Test No. 6	70
48	Seat pan z-axis accelerations and spinal compression loads in CAMI tests corresponding to NASA Test No. 8	71
49	Impact Dynamics Research Facility at NASA Langley Research Center (Reference 17)	74
50	Drop tower of Impact Dynamics Research Facility at NASA Langley Research Center	76

LIST OF ILLUSTRATIONS (CONTD)

Figure		Page
51	Structure at front of crew module added for attachment of attitude control cables.	77
52	Structure at rear of crew module added for attachment of attitude control cables.	78
53	Swing test set-up at NASA impact dynamics research facility	80
54	Diagram of NASA Impact Dynamics Research Facility (Reference 17)	81
55	Crew module immediately prior to swing test at NASA Impact Dynamics Research Facility	82
56	Bulkhead accelerometer mountings for crew module tests.	84
57	Capsule center of gravity accelerometer mounting for crew module tests.	85
58	Seat pan accelerometer attachment on energy-absorbing seat in crew module tests.	86
59	Seat pan accelerometer mounting on energy-absorbing seat with seat pan load cells used in crew module tests.	86
60	Modification used to mount energy-absorbing seat in crewseat module tests.	88
61	Doubler placed in air ventilation duct	88
62	Modification to capsule bulkhead	89
63	Lower bearing fitting for energy-absorbing seat.	90
64	Occupant position in energy-absorbing seat during crew module tests.	91
65	Occupant position in operational seat during crew module tests	92
66	Effect of parachute oscillations on crew module horizontal and vertical velocities (courtesy of U.S. Air Force).	94
67	Bulkhead z-axis acceleration from NASA Test No. 5.	98

LIST OF ILLUSTRATIONS (CONTD)

Figure		Page
68	Seat pan vertical acceleration from right seat in NASA Test No. 2 (data filtered with class 180 filter)	101
69	Peak seat pan vertical accelerations in crew module drop tests	102
70	Peak acceleration levels along the seat back tangent line in crew module drop tests	103
71	Peak dummy pelvis z-axis acceleration levels in crew module drop tests	104
72	Seat pan z-axis Dynamic Response Index (DRI) measurements from module drop tests	107
73	Seat back tangent line Dynamic Response Index (DRI) measurements in module drop tests	108
74	Dynamic Response Index (DRI) measurements from pelvis z-axis accelerations in module drop tests	109
75	Comparison of total seat pan loads in module drop tests	111
76	Seat pan z-axis acceleration and center seat pan vertical load for NASA Test No. 8 (32 ft/sec drop test)	112
77	Seat pan z-axis acceleration and center seat pan vertical load for NASA Test No. 9 (25 ft/sec drop test)	113
78	Conceptual design of energy-absorbing retrofit seat for F-111 crew module	119
79	Hardware behind pilot's seat in some F-111 aircraft	124
80	Upper bearing attachment on pilot outboard side during crew module tests	125
81	Upper bearing attachment on WSO inboard side during crew module tests	126
82	Inflatable body and head restraint (Reference 10)	129
83	Vertical stroke versus energy absorber limit load (Reference 10)	131

LIST OF TABLES

Table		Page
1	F/FB-111 Major Injuries, October 1967 - December 1978 (Reference 6)	8
2	Vertebral Fractures Among F/FB-111 Ejectors (Reference 8)	8
3	Velocity at Ejection From F-111 Aircraft	17
4	Weight of Test Seat	23
5	Seat Test Matrix	35
6	Test Acceleration Pulse Description	35
7	Input Acceleration Pulses for Dynamic Seat Testing	37
8	Peak Vertical Accelerations Measured on Seat Pan During Energy-Absorbing Seat Testing at CAMI	38
9	Eiband and Dynamic Response Index Evaluation of Energy-Absorbing Seat Testing at CAMI	45
10	Stroke Measured in CAMI Seat Tests	50
11	Comparison of Peak Accelerations Measured on Operational (F-111) and Energy-Absorbing (E/A) Seats in CAMI Tests	51
12	Comparison of Dynamic Response Index Measurements for Operational (F-111) and Energy-Absorbing (E/A) Seats in CAMI Tests	59
13	Comparison of Eiband Measurements for Operational (F-111) and Energy-Absorbing (E/A) Seats in CAMI Tests	63
14	Lumbar Load Cell Measurements for Operational (F-111) and Energy-Absorbing (E/A) Seats in CAMI Tests	64
15	Seat Pan Load Cell Measurements for Operational (F-111) and Energy Absorbing Seats (E/A)	68
16	Peak Vertical Footrest Loads Measured in CAMI Tests	68
17	Crew Module Test Matrix	93

LIST OF TABLES (CONTD)

Table		Page
18	Crew Module Swing Test Conditions.	96
19	Velocity Change and Peak Acceleration Measured Along a Vertical Axis on Capsule Bulkhead.	97
20	Peak Vertical Accelerations Measured in Crew Module Tests	100
21	Duration above 23 G of Seat Pan Accelerations Measured in Crew Module Tests.	105
22	Dynamic Response Index (DRI) Measurements from Crew Module Tests.	106
23	Peak Seat Pan Loads Recorded During Module Tests	110
24	Vertical Stroke Measured During Crew Module Tests.	114

1.0 INTRODUCTION

1.1 BACKGROUND

1.1.1 System Description

The F/FB-111 aircraft uses a crew module escape system developed between 1963 and 1967. In this system, the crew remains inside the aircraft cockpit during the ejection sequence, which consists of two main phases. The first phase, or ejection, severs the module from the aircraft and rockets it away from the aircraft. The second phase, or descent, consists of a controlled parachute descent of the module and the inevitable ground impact.

Under normal conditions, the crew module is an integral part of the forward fuselage. When the ejection handles are pulled and the sequence is initiated, gas-powered inertia reels retract the shoulder straps, pulling the occupant back into the seat. Shaped charges then fire, separating the module from the aircraft as the module is lifted away by the thrust from a rocket motor. While the rocket motor is firing, a stabilization-brake parachute is deployed. Stabilization flaps are at the fore and aft ends of the module. However, none of these items are controlled by the crew; the flight path of the module is determined by aerodynamic forces on the module and brake parachute, as well as the direction of the rocket thrust.

The rocket motor thrust can be directed through two different ducts, depending predominantly on the aircraft speed at ejection. In the low-speed mode, below approximately 300 KEAS (Knots Equivalent Air Speed), most of the rocket thrust is directed toward lifting the module up from the aircraft. In the high-speed mode however, it was anticipated that the forward portion of the module (shown in Figure 1) would provide significant aerodynamic lift, and therefore more of the exhaust gases would be ducted to the exit port in the aft bulkhead. This prevents a severe pitching-up of the module in the high-speed ejection mode. After rocket motor burnout, which occurs between one and two seconds after the ejection sequence is initiated, the descent phase starts and the recovery chute is deployed. A recent modification to the escape system also cuts away the stabilization brake parachute at the same moment. This prevents entanglement of the two chutes, which could prevent the recovery chute from opening.

After the recovery chute lines have stretched, the impact attenuation bag (IAB) is filled from high-pressure nitrogen gas bottles located behind the pilot seat. This bag, designed to cushion the module landing, has blow-out plugs to allow the controlled release of the nitrogen gas. The IAB has been designed for both ground and water impacts.

While the IAB is filling, the parachute reaches the fully open condition with the capsule repositioned to a descent attitude of two degrees nose-up. The IAB becomes fully inflated, and the capsule ready for ground impact, between 7 and 16 sec (depending on speed and temperature) after initiation of the escape sequence.

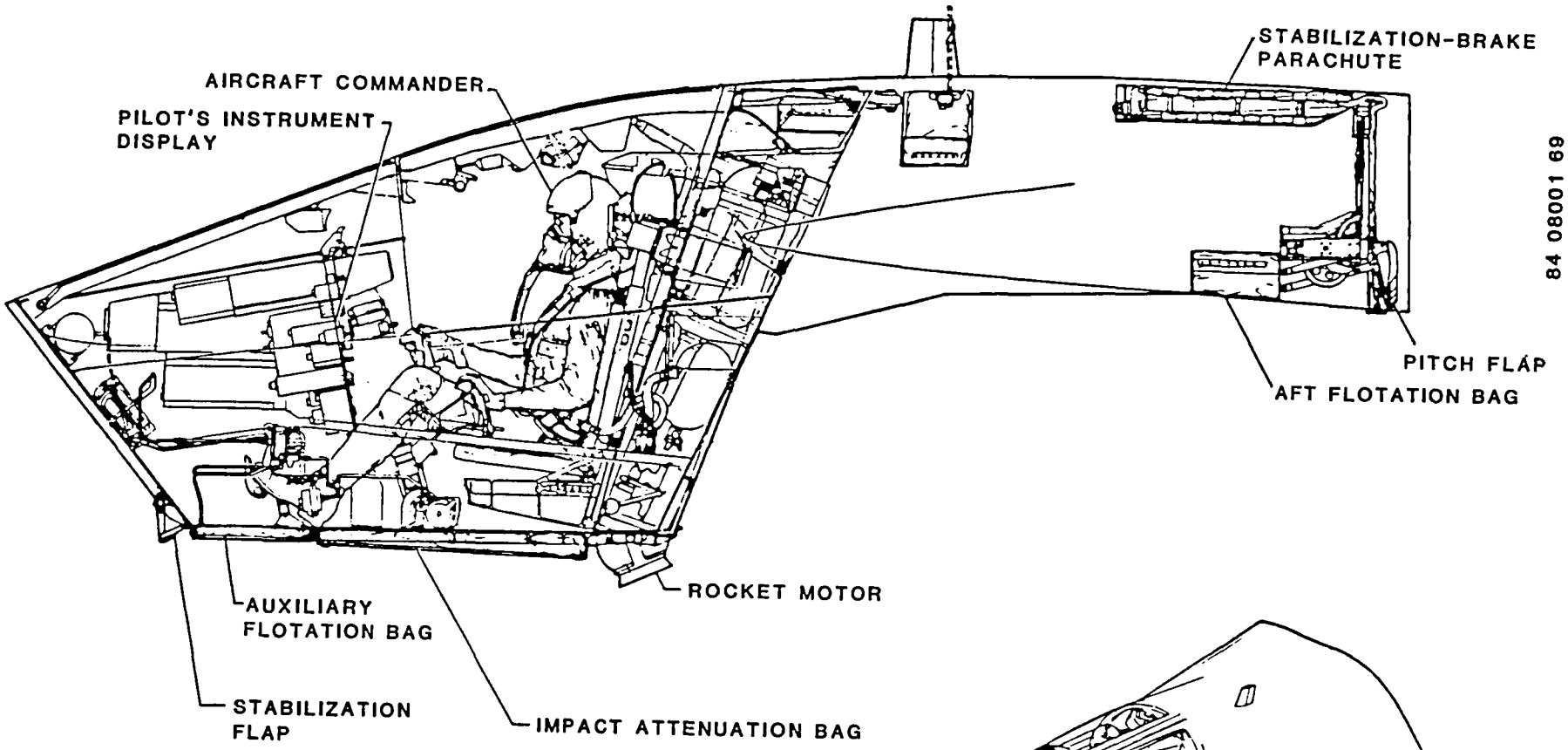

- PRE-EJECTION CONFIGURATION (EXCEPT FOR DEPLOYED STABILIZATION FLAP)
- 95TH- PERCENTILE OCCUPANT
- SEAT ADJUSTED FULL DOWN AND AFT
- RUDDER PEDALS ADJUSTED FULL FORWARD

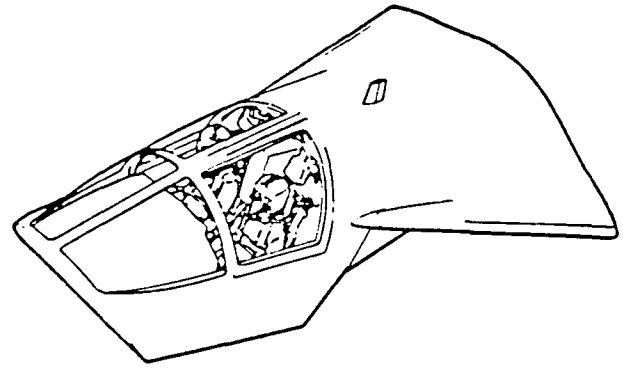

Figure 1. F-111 crew module (courtesy U.S. Air Force).

1.1.2 Acceleration Environment

The F-111 crew module was developed to contend with a hazard inherent in all open-seat ejection systems: windblast. While the module has been successful in this respect, it has had other problems that involve the high accelerations to which the occupants are subjected.

1.1.2.1 Ejection. The acceleration environment in the crew module was studied during initial qualification testing of the escape system. It was shown that during the module separation from the aircraft, the amplitude and duration of the vertical accelerations to which the occupants are subjected increase as the aircraft velocity increases. This is shown in Figures 2 and 3, which present vertical acceleration measurements from recent tests of the F-111 crew module.

The results of the increased acceleration levels are illustrated in Figure 4, which shows the Dynamic Response Index (DRI) for the ejection pulse plotted as a function of airspeed. The DRI value is the result of a simple lumped parameter mathematical model of human response to vertical accelerations. The model has been correlated with the probability of vertebral fracture in operational U.S. Air Force ejection seats. The relationship in ejection seats between DRI and spinal injury is shown in Figure 5.

In examining Figure 5, one can see that a DRI value of 18 corresponds to a spinal injury rate of 5 percent. Figure 4 thus shows that the expected spinal injury rate would remain below 5 percent through an ejection airspeed of 450 KEAS. Above 450 KEAS, the DRI, and thus the expected spinal injury rate, climb very steeply.

1.1.2.2 Ground Impact. As the capsule descends to the earth, it is supported by a single recovery parachute with a nominal vertical descent rate of 32 ft/sec. The capsule is designed for proper operation within the following maximum values for the given impact parameters:

- 20-knot wind
- Capsule swing under the parachute of 10 degrees
- Landing surface slope of 5 degrees.

The combination of a 20-knot wind and a capsule swing of 10 degrees can allow the horizontal velocity of the capsule to reach a very severe 43 ft/sec.

Shown in Figure 6 is a typical ground impact pulse for a sled test series conducted at Holloman Air Force Base, New Mexico. Since these tests were only conducted under conditions of low wind speed and with a level landing area, the ground impact pulse shown is a relatively mild one. Changes in the wind speed, aircraft attitude, and landing surface could all have some effect on the magnitude and shape of the ground impact pulse.

Figure 7 shows the DRI for various ground impacts during the initial testing of the F-111 crew module. Conclusions at the time were that under the most likely landing conditions, the spinal injury rate was going to be higher than 5 percent but probably less than 20 percent (Reference 3).

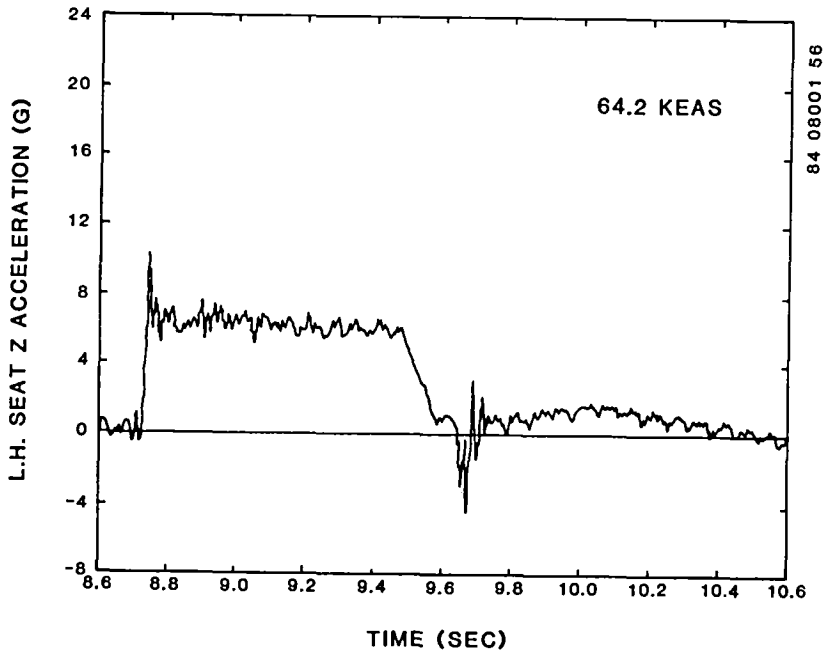

Figure 2. Vertical seat pan accelerations during ejection phase of F-111 escape sequence at 64.2 KEAS (courtesy U.S. Air Force).

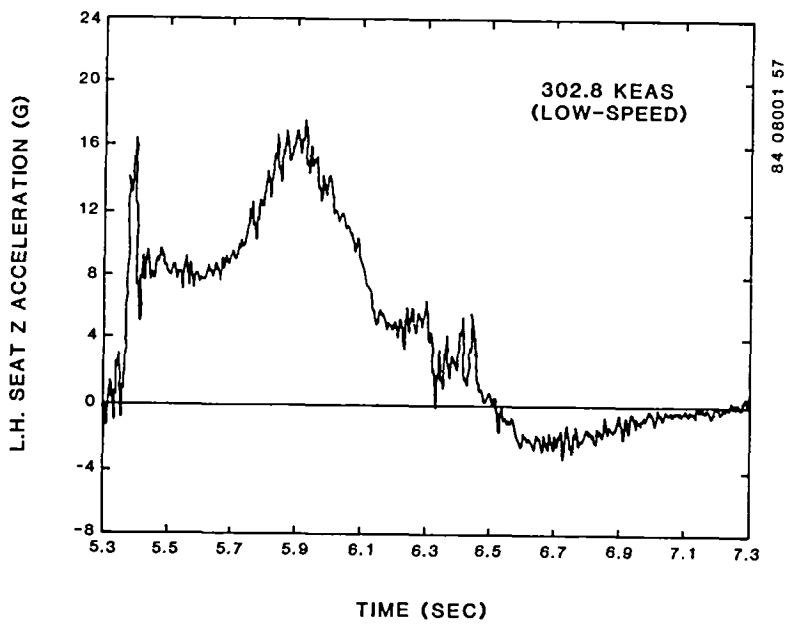

Figure 3. Vertical seat pan accelerations during ejection phase of F-111 escape sequence at 302.8 KEAS (courtesy U.S. Air Force).

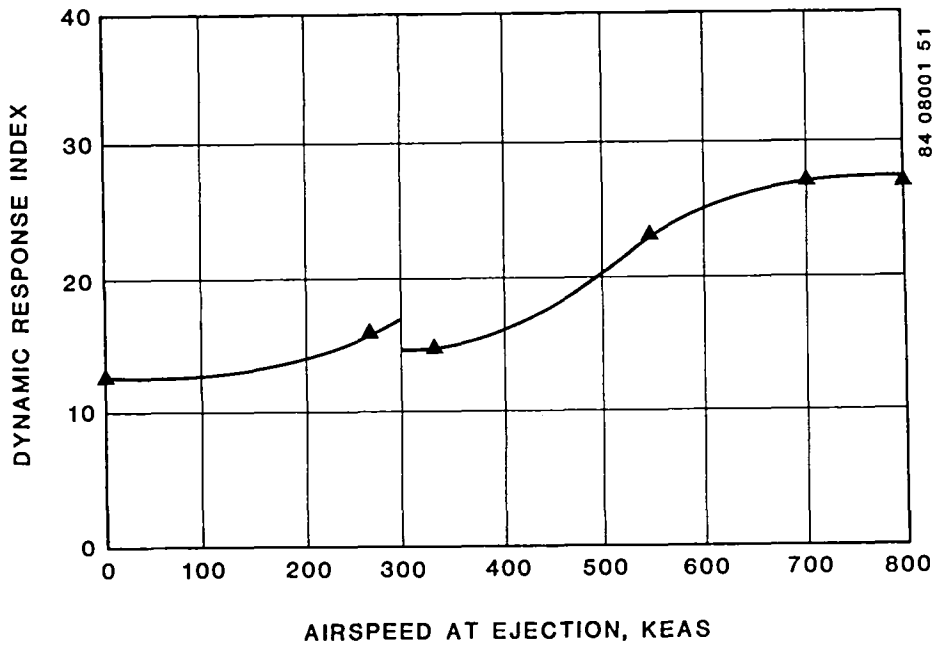

Figure 4. Dynamic Response Index during ejection phase of F-111 escape sequence (Reference 1).

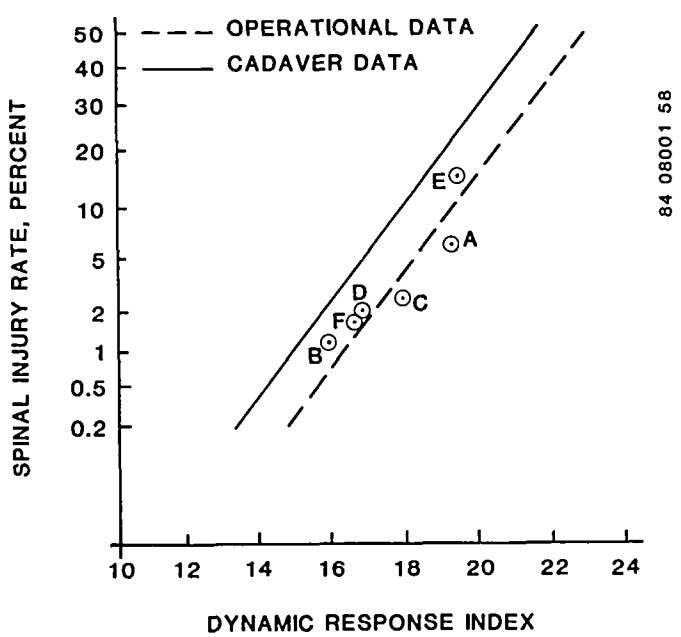

Figure 5. Correlation between Dynamic Response Index and spinal injury rate for ejection seats (Reference 2).

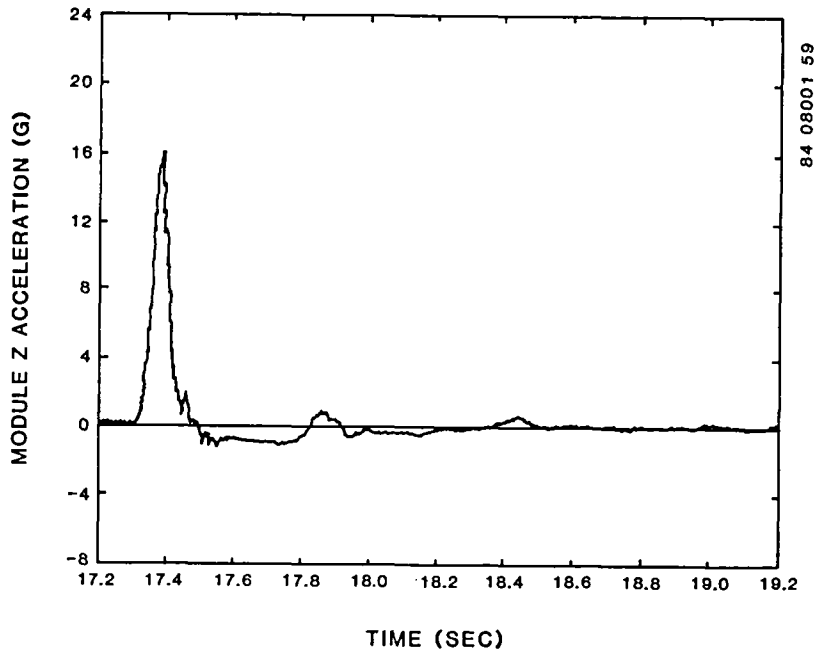

Figure 6. Module vertical accelerations during ground impact (courtesy U.S. Air Force).

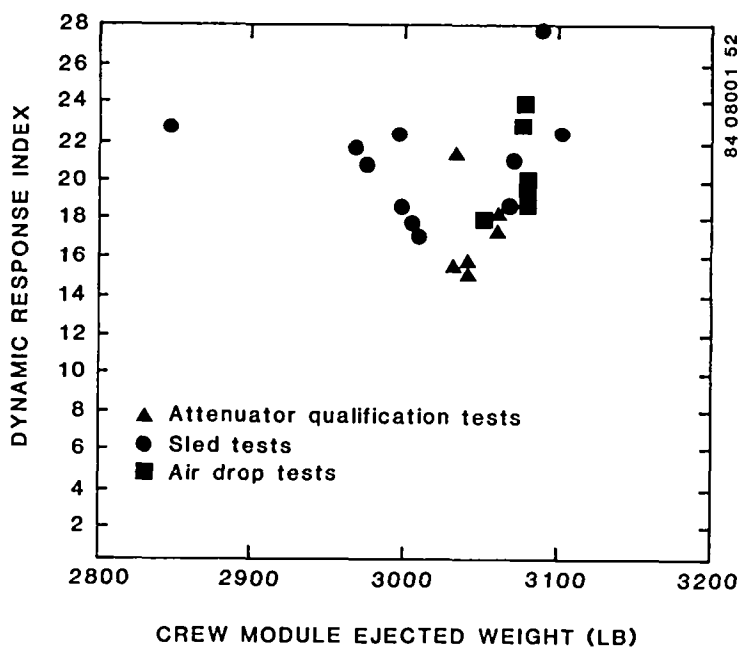

Figure 7. Values of Dynamic Response Index for ground impacts calculated during qualification testing of F-111 crew module (Reference 3).

1.1.3 Injury Record

Several examinations of injuries sustained during use of the F-111 escape module have been made (References 4, 5, 6, 7, and 8). All evaluations consider three main factors: ejection forces, the restraint system, and ground impact forces.

Kazarian (References 4 and 5) studied the first 39 F-111 ejections (October 19, 1967 to June 30, 1977), 31 of which were considered sucessful (the ejection occurred in the design envelope and the ejection system functioned properly). During these successful ejections, 27 occupants suffered two types of back injuries, resulting in a total back injury rate of 43.5 percent. Negative shoulder strap angles, reduced back support, and the position of the headrest were described as causes of hyperextension injuries during the power haul-back of the occupant by the inertia reel. Also, the high vertical ground impact forces had resulted in hyperflexion injuries to the spine.

Slightly after Kazarian's evaluation, another examination of the F-111 injury record by Harrison included 43 ejections that occurred between October 1967 and December 1978 (Reference 6). During the 35 successful ejections, only 24 occupants suffered a total of 33 major injuries. Some re-evaluation must have been completed by this time. Kazarian had listed 27 occupants as suffering spinal injuries in the first 31 successful ejections, but Harrison lists only 24 occupants suffering spinal injury in the first 35 successful ejections. Harrison categorizes the injuries as shown in Table 1, and cites "the position of the restraint system, namely the shoulder harness, along with the forces of ejection . . ." as responsible for four of the injuries. The ejection forces or landing forces are listed as the causes of the other injuries.

The Air Force Aerospace Medical Research Laboratory (AFAMRL) has more recently re-evaluated the injury history of the F-111. Hearon (References 7, 8) reports on the first 50 ejections, of which 39 were nonfatal with proper module functions. This analysis included re-examination of selected x-rays by several orthopedic and radiologic consultants. The results of this analysis are shown in Table 2. Retraction and ejection injuries are listed together because Hearon found it impossible to distinguish between the two.

Brinkley (Reference 3) and Hearon (Reference 1) also tested a proposed modification to the F-111 restraint system. The modification was based on the recommendations of Kazarian. The major points of the modification (which was never incorporated) were to raise the anchor point for the reflected shoulder straps and to raise the height of the support provided by the seat back. Their testing of the modification, examination of the ejection and ground impact accelerations, and subsequent analysis of the spinal injuries that have occurred during use of the F-111 escape module, resulted in several important conclusions. Some of these conclusions are as follows:

- The accelerations imposed on the crewmen are sufficient, both at high-speed ejection and ground impact, to cause a significant spinal injury rate (Reference 3).

- There is no evidence to indicate a hyperextension injury mechanism during retraction of the inertia reel straps (Reference 8). However, significant spinal flexion is possible during the retraction-ejection phase (Reference 7).

TABLE 1. F/FB-111 MAJOR INJURIES
OCTOBER 1967 - DECEMBER 1978
(REFERENCE 6)

Number of Injuries	Cause	Injury
15	Ejection Force	Vertebral Fracture
13	Module Landing Force	Vertebral Fracture
4	Restraints	Vertebral Fracture
1	Struck Cockpit	Rib Fracture
33		

TABLE 2. VERTEBRAL FRACTURES AMONG
F/FB-111 EJECTEES
(REFERENCE 8)

	Number
Survived Ejectees	78
No Vertebral Fracture	55
Vertebral Fracture	23
Retraction - Ejection	9
Landing Impact	11
Unknown Cause	3

- Future design changes in the ejection system should address reducing the high ground impact accelerations (References 1, 3, 7, and 8).

- Future proposed restraint system modifications should address all the unconventional design features of the present system (Reference 1).

Kazarian had identified some of the problems to which this last conclusion refers. However, a major problem identified by Brinkley is illustrated in Figures 8 and 9. It is possible to adjust the shoulder harness yoke in such a way that when the inertia reel retracts, a vertical load is applied to the spine. Figures 8 and 9 show an occupant after shoulder strap haul-back with the yoke properly and then improperly positioned. Putting a compression load on the spine in this manner would increase the chance of spinal injury when other upward vertical loads are applied, such as during ejection or ground impact.

1.2 PROGRAM OBJECTIVES

In recent years an increasing amount of effort has been directed toward the survival aspects of aviation crash safety. Good examples are the U.S. Army's Black Hawk and Apache helicopters. From the initial aircraft design, consideration was given to factors that affect survivability during a crash, such as: maintaining the living space around the occupants; preventing any cargo, equipment, or structure from breaking loose; delethalizing the area in close proximity to the occupants, minimizing the threat of postcrash hazards (fire, drowning, exposure, etc.), and reducing the intensity and duration of accelerations experienced by the occupant. The purpose of this program was to determine if this crashworthy technology could be used to reduce the injury potential of F-111 capsule ejections.

More specifically, since acceleration levels in the F-111 ejection sequence have been targeted as the primary cause of the spinal injury rate, the program objective was to determine if the technology used to reduce the severity of the acceleration levels experienced by occupants of an aircraft in a crash was applicable to the environment inside the F-111 capsule during an ejection sequence.

When an aircraft is designed with crash survivability in mind from the beginning, three items are intended to absorb a substantial amount of the crash energy and thus reduce the severity of the environment experienced by the occupant. These items are the landing gear, the aircraft fuselage structure, and the seat. Each of these items absorbs energy by applying a force through a distance. The landing gear is designed to deform according to a particular load-versus-deflection curve. After the landing gear has reached its maximum design deflection, it will no longer serve as an efficient energy absorber. Also, the fuselage structure will crush, applying a force through a distance to the aircraft structure above it. Similarly, the energy-absorbing seat is designed to deform, allowing the occupant to move towards the floor at a predetermined load and thus absorb more of the crash energy.

In the F-111 capsule the situation is somewhat different. During the ejection phase, there are no items designed to absorb energy and thus reduce the severity of the acceleration levels to which the occupant is subjected. The occupant sits in his rigid seat in a non-deforming capsule and escapes injury when the loads to which he is subjected are below injurious levels. Conversely, he is injured when the environment is too severe. During ground impact, the IAB

Figure 8. F-111 seat and occupant after shoulder strap haul-back with harness yoke properly positioned (Reference 3).

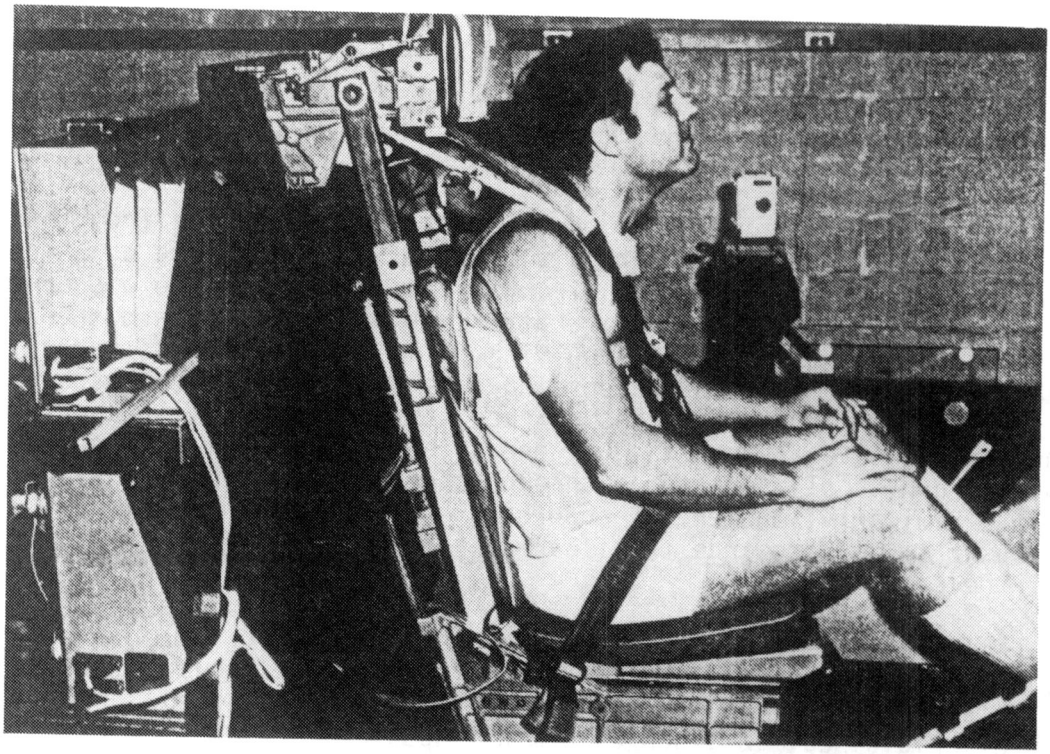

Figure 9. F-111 seat and occupant after shoulder strap haul-back with harness yoke improperly positioned (Reference 3).

does provide an energy-absorbing function. When the IAB hits the ground, the force of the capsule on top of it raises the pressure in the bag until the blow-out plugs release. Then the nitrogen gas is forced through the resulting holes. During this time, the IAB is applying an upward force on the capsule, absorbing energy as the capsule pushes its way to the ground. However, when the capsule hits the ground, there is no more energy absorption. There is only a sheet metal floor above the IAB, and the seat is rigidly mounted to the bulkhead.

Efforts have been considered to modify the IAB to determine if it could absorb more energy; there are two ways in which the IAB could be changed. One would be to increase the load at which the energy is being absorbed. This could be done by reducing the size of the ports, which would raise the bag pressure during impact, and thus raise the load applied to the capsule. This assumes however, that the loads presently applied by the IAB produce loads inside the capsule that are below the threshold of injury for the occupants. Since the injury rate in F-111 ejections is already unacceptably high, this may not be the case. The second method of increasing the energy absorbed by the bag would be to increase the distance over which the bag absorbs energy. However, an IAB with a longer energy-absorbing stroke may require a larger space in which to be contained. The probability of capsule rollover may also be increased. Thus while changing the IAB is a possible method of reducing the severity of the environment to which the occupants are subjected, there are many questions that need to be answered.

It was not within the scope of this program to examine changes to the IAB. The main purpose of this program was to adapt an energy-absorbing seat to the F-111 capsule and determine over what performance envelope the seat could absorb the energy required to reduce the intensity and duration of the accelerations experienced by the occupants to non-injurious levels.

Towards this goal, the program was divided into two phases. During the first phase, Simula Inc., with monitoring by Sacramento Air Logistics Center and NASA Langley Research Center, examined the existing seat design in detail. Many possible concepts for incorporating an energy-absorbing seat into the F-111 crew module were examined.

The concept that would be the most appropriate for a retrofit seat was used in designing a test seat that was subjected to a thorough dynamic test series by the FAA Civil Aeromedical Institute (CAMI).

The second phase of the project mounted the test seat inside the crew module, which was then subjected to a series of swing and drop tests. This testing was conducted at the Impact Dynamics Research Facility at NASA Langley Research Center by NASA and the U.S. Army Applied Technology Laboratories (AVSCOM).

Volume I provides a discussion of the program, including the design of the test seat, evaluation of the data from the test series, a description of a concept for a retrofit seat, and the overall conclusions of the program. Volume II presents the data from the dynamic seat testing conducted at CAMI. Data from the crew module test series at NASA Langley is in Volume III.

2.0 ENERGY-ABSORBING SEAT DESIGN

The test seat designed for this program used many parts from the operational F-111 seat. This chapter will first present the operational F-111 seat, outline guidelines used in the design of the energy-absorbing test seat, and then present the test seat.

2.1 OPERATIONAL F-111 SEAT

2.1.1 General

The operational F-111 seat is shown in Figure 10. It consists of three major assemblies: the carriage assembly, the seat pan/back assembly, and the headrest assembly. The seat carriage is an aluminum frame enclosed by sheet metal. The carriage has four sets of claws that enable it to slide up and down the bulkhead on two sets of tracks. Vertical support of the carriage comes from the seat adjustment actuator, an electromechanical device that can move the carriage, guided by the tracks, along the bulkhead over an adjustment range of 5 in. The top of the seat adjustment actuator is pinned to a fixed clevis on the bulkhead while the bottom of the actuator is pinned to a clevis on the carriage.

The seat pan has an aluminum base with grooved slots on each side that mate with slots in the carriage, allowing the seat pan to slide horizontally inside the carriage. The horizontal adjustment is actuated by a handle in front of the seat pan and the position is fixed by pins extending out from the seat pan into holes on both sides of the carriage. The horizontal adjustment range is 5 in. Proper adjustment for leg comfort is provided for not only in the seat pan but in the 6 in. fore and aft adjustment of the rudder pedals. The top of the seat pan is covered by fiberglass over a foam core, the shape of which is contoured to provide for thigh support and comfort.

The seat back is a box-like structure with an aluminum honeycomb core. Rectangular aluminum tubes, open at the top, run along the sides of the back. At the bottom of each tube is a fitting that is used to attach the seat back to the seat pan with two bolts. This method of attachment allows the seat back to rotate around the pitch axis relative to the seat pan. Rotation is necessary since as the seat pan slides forward, the bottom of the seat back moves forward with it.

The headrest is supported by structure rigidly mounted to the bulkhead. While the headrest can be adjusted horizontally over a range of 6 in., it remains at the same vertical position for all seat adjustments. As the seat carriage is moved up and down, rectangular tubes hanging from the headrest assembly slide inside tubes that are part of the seat back. Conversely, when the headrest is adjusted, these same tubes pull the top of the seat back with the headrest, pivoting the seat back around the bolts that connect it to the seat pan.

One can see that with provisions for horizontal adjustment of both seat pan and headrest, as well as vertical adjustment of the seat pan, various angles of the seat back are possible. Figure 11 is a side view showing the geometry of the described adjustments. The headrest support surface remains vertical

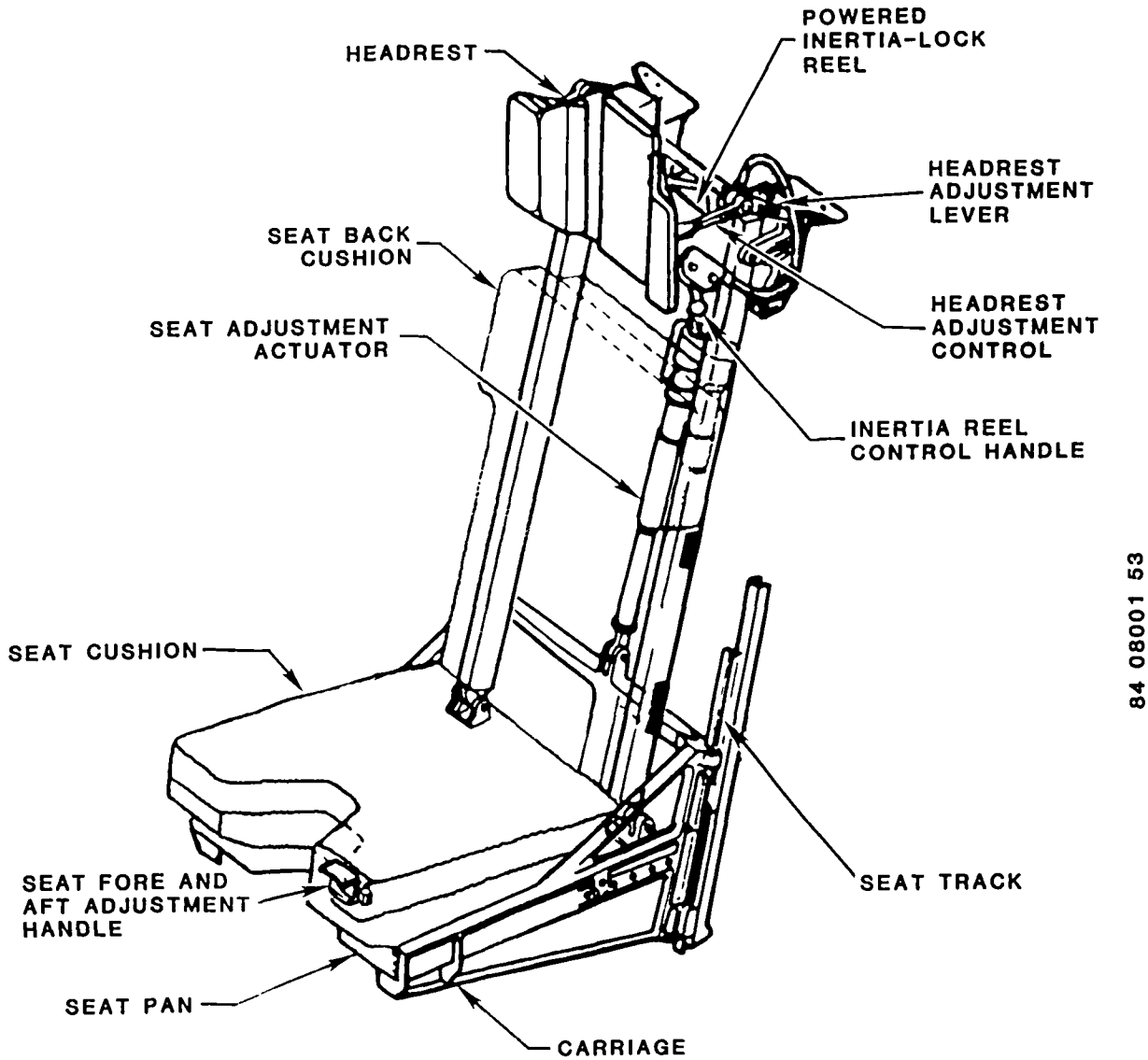

Figure 10. Operational F-111 crewseat (Reference 3).

and is in front of the back tangent line. As the seat is tilted back, the head support point remains in front of the seat back tangent line by an amount that depends on the seat adjustment position and the seated height of the occupant. The headrest support plane can be as much as 2-1/4 in. in front of the seat back tangent line. This does not conform to MIL-C-25969, "General Requirements for Capsule Energy Escape Systems" (Reference 9), which calls for the head support to be 1 in. aft of the seat back tangent line. Pushing the head forward

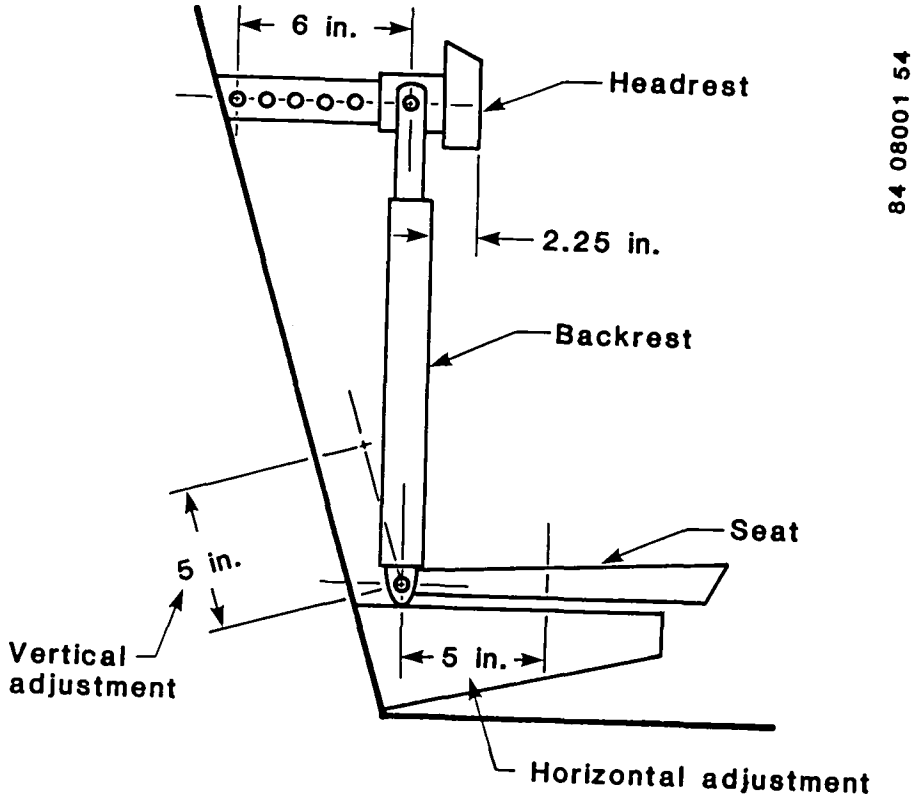

Figure 11. F-111 crewseat adjustment geometry.

as the F-111 headrest does leads to downward and forward rotation of the head and chest during a vertical impact (Reference 10). The loads associated with this movement increase the risk of injury during ejection and ground impact.

2.1.2 Restraint

The restraint system for the operational F-111 seat, shown in Figure 12, has a lap belt, two shoulder straps, and a crotch strap, sometimes referred to as a negative-G strap. The lap belts and crotch strap are connected to the seat pan. Operation of the single-point release box knob, attached to the top of the crotch strap, releases the four buckles of the lap belts and shoulder straps. Adjustment is provided in the shoulder and lap belts.

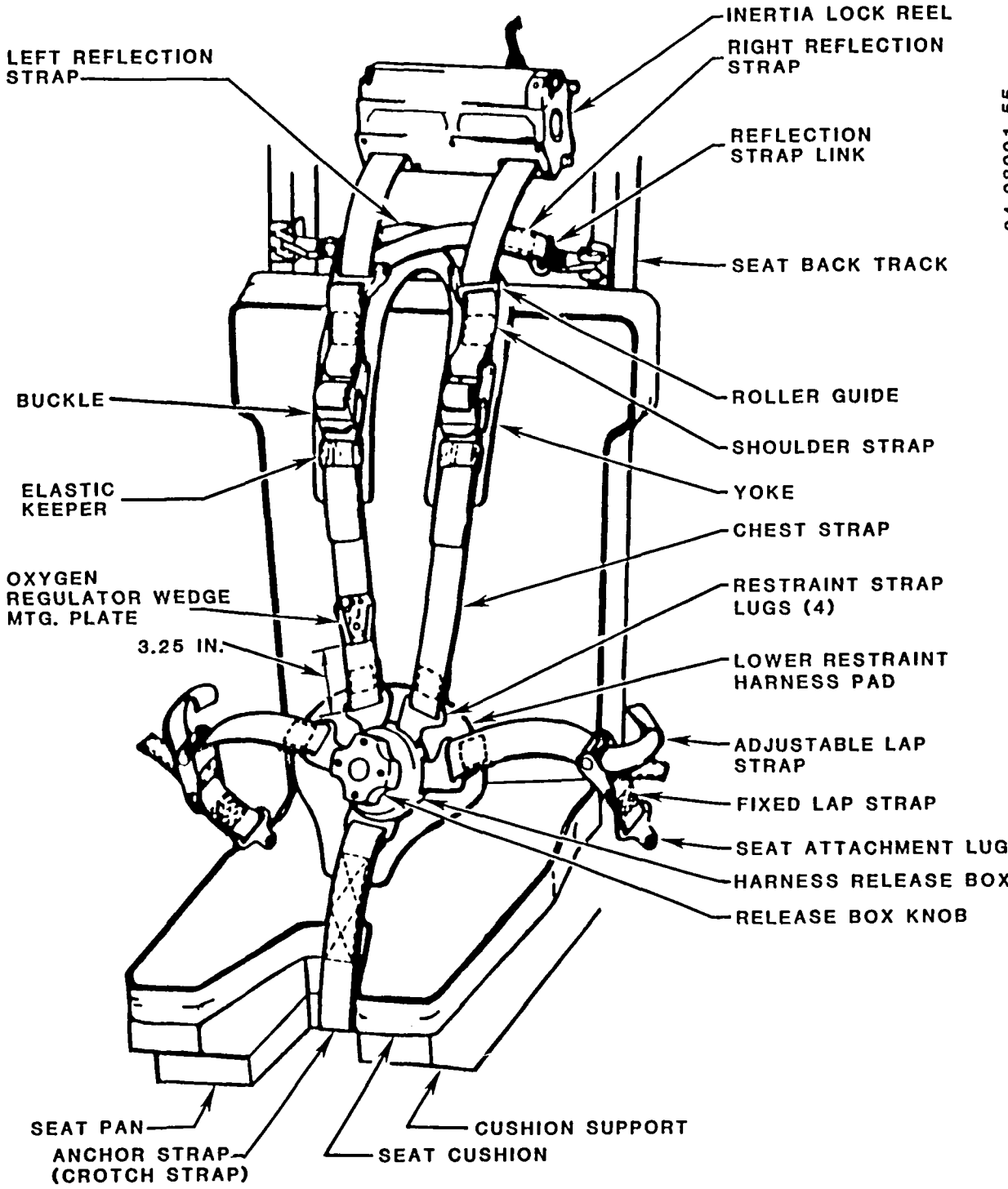

Figure 12. F-111 crewseat module restraint system (Reference 3).

Both shoulder straps attach to a yoke that sits like a "horse collar" on the crewman's shoulders. Straps from the inertia reel, which is fixed in one position on the bulkhead, also attach to the yoke by passing around a roller and

then attaching to the seat back on the opposite side at a point 24.09 in. above the seat reference point. This arrangement using the yoke and reflected inertia reel straps provides lateral restraint for the torso of the crewman. However, the attachment point of the reflected straps on the seat back is at or below the mid-shoulder sitting height of approximately 90 percent of the flying population (Reference 3). Therefore, in many cases power haul-back loads in these straps will apply compression loads on the spine (Reference 11). While several investigations have been done (References 1, 3, 10, and 12), a suitable modification to alleviate this problem has not yet been found.

2.1.3 Cushions

Cushions are provided for the headrest, seat back, and seat pan.

The headrest is covered with three cushions. The cushions are 7/16-in. thick, made from a closed-cell Ensolite foam, and are covered with leather before they are bonded to the headrest.

The back cushion is a single layer of polyurethane foam and is 1-1/2 in. thick. The cushion has a fabric cover and is held in place by Velcro strips. Because of the short height of the seat back, the cushion is only 21 in. high, providing support to a height of 23 in. above the seat reference point.

The seat pan cushion is made of two layers of foam bonded together. The top layer of foam is 1/2-in.-thick polyethylene. The lower layer is a 1-1/2-in.-thick pad of the same polyurethane foam used in the seat back. Crewmen have been known to remove the cushion from its stretchable fabric cover and invert the foam so that the polyurethane is on top.

2.2 DESIGN GUIDELINES

As stated earlier, the main objective of the program was to examine how crashworthy technology could be used to reduce the injury potential in F-111 aircraft ejections. In order to do this, an energy-absorbing test seat was designed. The seat designed was not meant to be a retrofit seat. A retrofit seat would meet all the flight requirements of the aircraft, while the test seat was designed only for use in the tests conducted during this program. To minimize cost, it was built using as much of the existing seat hardware as possible. Because of this, the test seat is heavier than an energy-absorbing retrofit seat would be, yet still demonstrates the capabilities of an energy-absorbing seat.

2.2.1 Energy-Absorbing Function

Previous evaluations of the F-111 ejection sequence discussed in Section 1.0 have identified the vertical inertial loads applied to the occupant as the primary cause of the high spinal injury rate. Horizontal loads in both the forward and lateral directions are below levels that would be injurious to the occupant. Therefore, an energy-absorbing retrofit seat should absorb energy only in the vertical direction. However, Section 1.0 identified both the vertical accelerations on module ejection and ground impact as capable of causing spinal injury (Reference 3). Therefore, it would be most desirable to have an energy-absorbing seat that would be prepared to operate both during ejection

and ground impact. Because of the limited distance available for energy-absorbing stroke, such a system may need to "reset" itself after the ejection and prior to ground impact. This system would operate by first allowing any stroke necessary during the ejection sequence. During the parachute descent the occupant would then be lifted back up through any energy-absorbing stroke that had occurred, or possibly to the full-up seat position. Such a system would provide maximum protection during both the ejection and ground impact phases. However, this system would also be more complex to build than one that operated during either ejection or ground impact. Therefore, the injury potential in each phase of the ejection sequence must be examined.

Table 3 shows a listing of the first 67 ejections from F-111 aircraft divided in terms of aircraft velocity at ejection. Figure 4 shows that at a 450 KEAS ejection velocity the acceleration pulse to which the occupant was subjected has a DRI of 18. The U.S. Air Force considers the DRI of 18 to be acceptable for ejection seats. Figure 5 shows that for an ejection seat, this DRI corresponds to an injury rate of 5 percent. While the acceleration environment in a capsule ejection may be slightly different from an ejection seat, and this would affect the accuracy of the injury rate prediction, the DRI does give a good understanding of how the severity of the environment increases as the aircraft velocity at ejection increases. Therefore, Table 3 uses the 450 KEAS ejection velocity as a dividing line to show that a relatively low percentage of ejections occur at the higher velocities.

TABLE 3. VELOCITY AT EJECTION FROM F-111 AIRCRAFT

	Velocity Below 450 KEAS	Velocity at or Above 450 KEAS	Velocity Unknown
Number of Ejections	59	5	3
Percentage of Ejections	88.1	7.5	4.5

On the other hand, every ejection has the potential for injury from ground impact. The qualification test data (Figure 7) show that the injury rate on ground impact would probably be too high. Also, several studies from the Air Force Aerospace Medical Research Laboratory (References 1, 3, 7, and 8) state the need for reducing high ground-impact accelerations.

There are several factors that influence the potential for injury during ground impact. The wind velocity, magnitude of parachute oscillations, slope and hardness of the landing surface, and the module attitude at impact all affect the risk of injury. While the pilot may be able to slow the aircraft and thus minimize the injury risk during ejection, he has little or no control over the factors affecting the injury risk at ground impact. For these reasons, the Air Force was interested in examining the use of the energy-absorbing seat to reduce high ground-impact accelerations.

At this time, it appears that the difficulties involved in allowing the occupant to stroke during ejection and then lifting him back up during module descent, and providing stroke again during ground impact, outweigh the benefits that could be gained by providing protection needed only in a certain percentage of ejections. Therefore, the seat design and testing have concentrated on the ground impact problem.

2.2.2 Other Seat Requirements

Although the test seat is not a retrofit seat, it was necessary to choose a design concept for a retrofit seat before building the test seat. This was a requirement for two reasons. First, the concepts to be used for absorbing energy and guiding the stroking seat in a retrofit seat should also be used in the test seats. Doing so helps to uncover any interference or performance problems particular to a design concept. Second, a retrofit seat should be installed with minimum modification to the aircraft. Only by examining the concepts to be used for the retrofit seat can the required aircraft modifications be determined. The extent of the necessary modifications can then be used as criteria in evaluating seat designs. Also, some specific aircraft modifications are not acceptable, and will eliminate some design concepts.

Since a specification for an energy-absorbing retrofit seat for the F-111 does not exist at this time, it was necessary to establish certain design guidelines. A discussion of these guidelines, as well as the final design chosen after the evaluation of many possible concepts, are presented in Section 5.0. The retrofit seat would use four bearing assemblies fixed to the bulkhead. Tubes pass through these bearings, guiding the seat as it performs its energy-absorbing stroke. Inversion-tube energy absorbers are used. The test seat is designed to perform in the same manner as the retrofit seat.

Variable-load energy absorbers would be a requirement on the retrofit seat. A variable-load energy absorber is adjusted by the occupant to provide the proper attenuating load for his individual weight. This load should be set as high as possible, but below the threshold of injury, since a higher load can absorb more vertical energy as the seat strokes. Experience with Simula energy-absorbing seats in the U.S. Army's UH-60 Black Hawk helicopter has demonstrated the effectiveness of vertical energy absorber loads corresponding to acceleration levels of 14.5 G.

The energy absorbers in Simula Black Hawk seats are fixed-load energy absorbers, and are set at loads corresponding to 14.5-G acceleration levels for the 50th-percentile occupant. Thus, a heavier occupant experiences a lower deceleration level when the seat strokes, but requires a correspondingly longer stroking distance. The lighter occupant experiences a higher deceleration level and a shorter stroking distance. Variable-load energy absorbers allow the load to correspond to a deceleration level of 14.5 G for all occupants; therefore, all occupants require approximately the same stroking distance for a given crash pulse. This system makes the most efficient use of the space available and is therefore needed in the F-111 capsule because of the short available stroking distance.

The reliability of Simula's variable-load energy absorbers was demonstrated under U.S. Naval Air Development Center Contract No. N62269-79-C-0241; they would be suitable for use on a retrofit F-111 seat. In order to simplify the seat design and the testing required, variable-load energy absorbers were not used on the test seat. Instead, the energy absorbers were sized for the 50th-percentile occupant, and all testing was done with a 50th-percentile anthropomorphic dummy. Since variable-load energy absorbers would be used in the retrofit seat, the vertical stroking distances measured in the tests apply to all occupant sizes.

Some other design constraints were typical to both the retrofit seat and the test seat:

- In the present configuration, the headrest remains at a constant waterline (horizontal position), and moves fore and aft with the seat. The seat back angle is adjustable, moving with the headrest. The power haul-back inertia reel is mounted to the bulkhead. The retrofit seat need not incorporate these design features.

- The seat back should provide a 13-degree back angle, either as a fixed back or as one of the adjustment positions.

2.3 TEST SEAT

A drawing of the test seat is provided in Figure 13. Figures 14, 15, and 16 show front, side, and rear views of the test seat. It is a bulkhead-mounted seat with the roller bearing assemblies mounted on the bulkhead. The seat consists of a seat back and seat pan assembly connected by diagonal tubes and mounted on guide tubes. A headrest is mounted on the top of the seat back, and the power haul-back inertia reel is mounted between the tops of the guide tubes. The attenuators are mounted between the clevis on the bulkhead and the seat pan assembly.

Since this seat is designed only for testing, adjustment in the vertical and horizontal directions is not provided. The height of the headrest is designed for a 50th-percentile occupant, and the seat reference point is approximately in the middle of the fore-and-aft adjustment range provided on the existing seat. The seat is in the full-up position to provide for measurement of the maximum energy-absorbing stroke.

The seat pan assembly uses the existing F-111 seat pan with only minor modifications. Along both sides of the seat pan are machined aluminum angles, which grip the seat pan in the same manner that the seat-pan carriage does on the existing F-111 seat. The seat-pan carriage was not used because it reduces the available stroking distance. Underneath the seat pan, three 1/4-in.-thick aluminum straps connect the left and right tray supports.

The seat back from the existing F-111 seat is used and is fixed at a 13-degree angle. The headrest is mounted at the top of the seat back and adjusted to the proper height for a 50th-percentile occupant. Parts of the headrest previously needed for adjustment have been removed. Also, since only a 50th-percentile occupant was used, the range of support provided by the headrest could be reduced in the vertical direction. As in the existing seat, the headrest is still mounted to the seat back with a sliding rectangular tube-in-tube

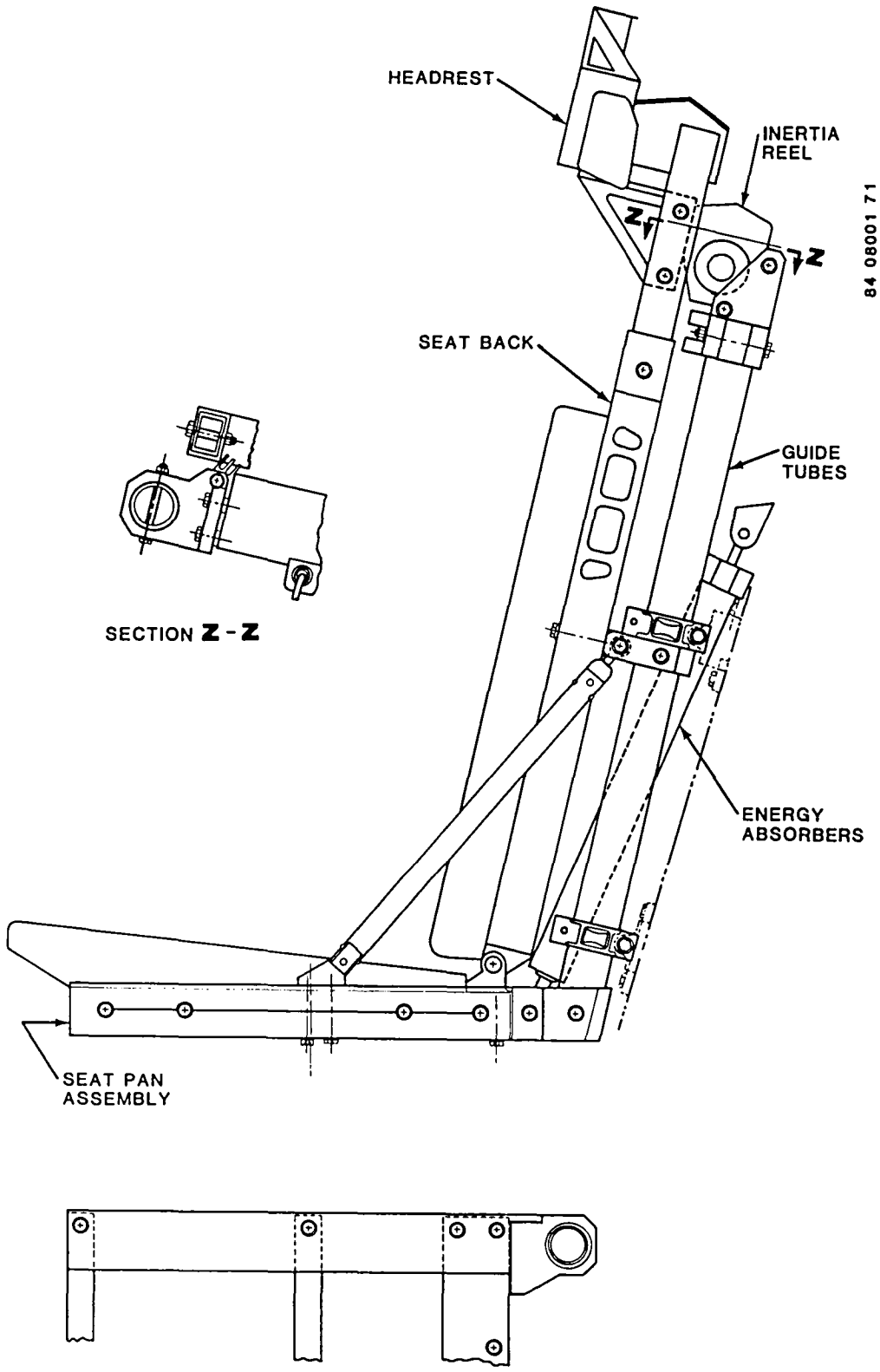

Figure 13. Energy-absorbing test seat.

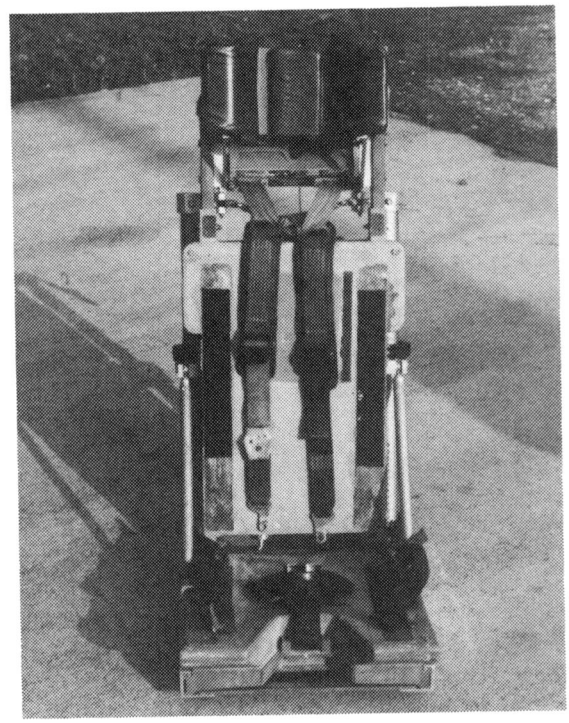

Figure 14. Front view of energy-absorbing test seat.

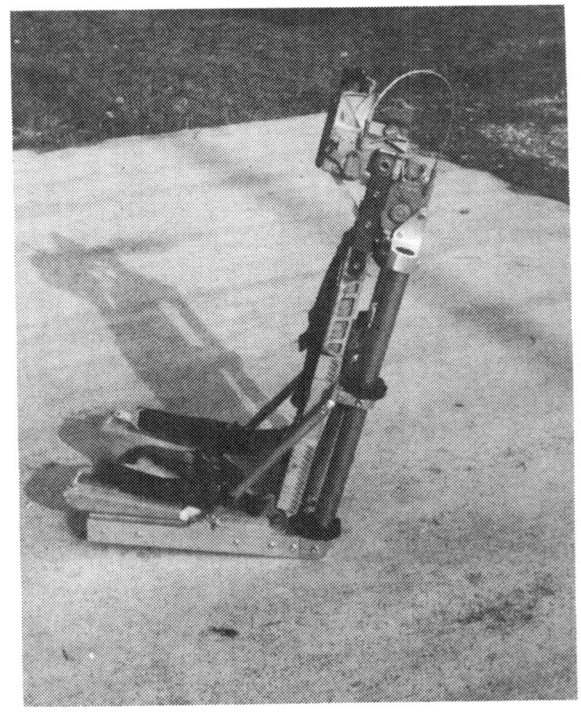

Figure 15. Side view of energy-absorbing test seat.

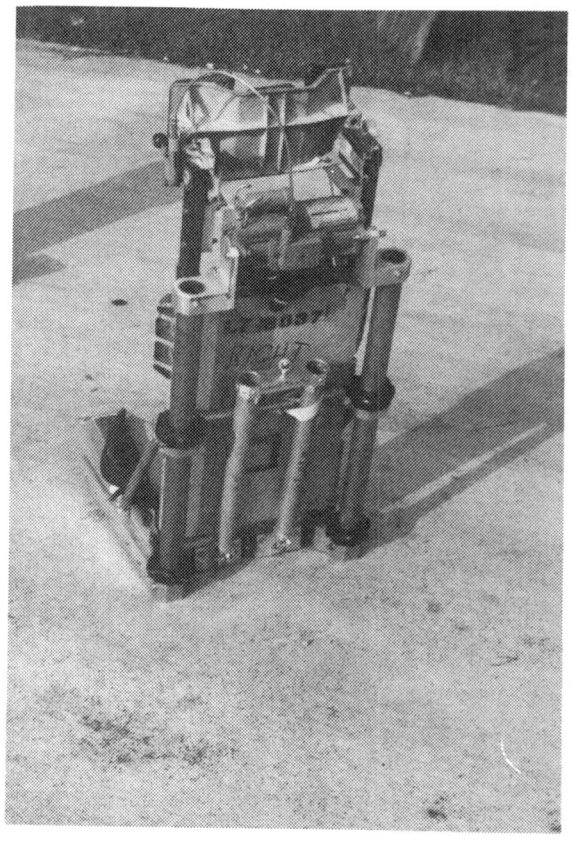

Figure 16. Back view of energy-absorbing test seat.

arrangement. The height of the headrest is fixed by a bolt through each set of tubes. Rotational movement of the headrest is prevented by an aluminum bracket. The headrest surface is fixed parallel to, and is 1-1/4 in. in front of, the seat back tangent line.

The seat pan and seat back assemblies are mounted to the heat-treated 4130 steel guide tubes. At the bottom of the seat, an aluminum fitting connects the guide tubes to the seat pan and seat pan tray. Another fitting, located about halfway up each of the guide tubes, joins the guide tubes to the seat back. Behind the seat back, an aluminum tube runs across the seat and is riveted to each of these fittings, defining the distance between the guide tubes. Also, from each fitting, a tube runs diagonally forward and down to a point approximately 1 in. in front of the buttocks reference point. The upper fitting on the diagonal tube supports a rod end to release the top of this tube from bending loads. The bottom of the diagonal tube is riveted to a fitting that is bolted through both the seat pan and the seat pan carriage. The triangular truss formed by the diagonal tube, seat pan carriage, and the guide tube support the loads applied to the seat pan by the occupant.

The power haul-back inertia reel is mounted to the top of the guide tubes. With the inertia reel cantilevered at the top of the guide tubes, the guide tubes are subjected to high bending moments. The guide tubes serve as races for the four linear roller bearing assemblies. Each bearing assembly contains four contoured rollers located at 90-degree increments to surround the guide tube. This assembly minimizes friction during the vertical energy-absorbing stroke while still transferring loads to the bulkhead.

Two energy absorbers, which restrain the seat bucket in its vertical position, are attached to fittings at the rear of the seat pan. The top of the attenuators are connected by a fitting that attaches to the clevis provided on the bulkhead for the existing F-111 seat vertical adjustment mechanism. The test seat uses energy absorbers sized for the 50th-percentile occupant.

The cushions presently used on the F-111 seat are also used on the test seat. Some of the headrest cushions are cut to fit the modified headrest; however, the cushioning effect for the occupant's head is the same.

The restraint system on the test seat is that presently used on the F-111 aircraft. It was described in Section 2.1.2, and has a five-point rotor-release buckle with tiedown strap, lap belt, and shoulder straps. The shoulder straps attach to a yoke that sits around the back of the occupant's neck. Straps from the inertia reel pass through fittings on the yoke and back to the upper guide tube fittings on the opposite side, not to the points on the seat back that are used by the operational seat. Since the inertia reel and the reflection strap anchor points are mounted to the upper guide tube fittings, the restraint system moves with the occupant during the energy-absorbing stroke of the seat.

The weights of the various seat parts are listed in Table 4. Since the test seat was made using as much of the existing seat as possible, it is much heavier than a retrofit seat would be.

TABLE 4. WEIGHT OF TEST SEAT

Item	Weight (lb)
Seat Pan Assembly	19.2
Diagonal Strut Assembly	1.0
Seat Back	6.2
Guide Tubes	10.1
Headrest	4.7
Mid-Cross-Tube Assembly	1.5
Inertia Reel Fittings	2.6
Inertia Reel	7.4
Restraint System	4.0
Cushions	2.0
Roller Bearings	2.4
Attenuator Assembly	1.9
TOTAL	63.0

2.4 SEAT PAN LOAD CELLS

During the time that the concepts for a retrofit seat were being examined, it was decided to also conduct some of the planned tests with the operational F-111 seat. The seat provided by the Air Force was an operational F-111 seat modified to incorporate seat pan load cells. In order to provide corresponding data during testing, one of the energy-absorbing test seats was also modified to incorporate seat pan load cells.

2.4.1 Modified Operational Seat Pan

Figure 17 shows a picture of the modified operational F-111 seat pan. The majority of the seat pan material between the side rails has been cut away. At the back of the seat pan, the seat back and lap belts are still attached in the same manner. At the front of the seat pan, the crotch strap is attached in the same manner as on the operational F-111 seat. Horizontal and vertical adjustment has not been changed by the modification.

The modified seat pan assembly is divided into upper and lower portions. The lower portion, really the seat pan support, has two aluminum plates running between the side rails. The rear plate has mounting provisions for one vertical load cell and two strain-gaged load links, which measure horizontal loads.

The front plate has mounting points for two vertical load cells and one load link. The other end of each of the three load links is attached to the upper portion of the new seat pan assembly. This upper part has really become the new seat pan, and has the same foam core fiberglass-covered contour as all operational F-111 seats. However, the bottom consists of a 1/2-in.-thick aluminum plate. The load links attach to fittings that are threaded into holes in this plate.

When assembled, the seat pan sits on the three load buttons of the vertical load cells mounted in the seat pan support. Hard points have been added to the bottom of the seat pan to reduce wear. The load links were used in the assembly, since they prevent the seat pan from sliding off the vertical load cells; however, they were not used during the program to measure horizontal loads. The weight of the seat pan sitting on the load cells is 12.45 lb.

2.4.2 Modified Energy-Absorbing Seat Pan

An energy-absorbing test seat was modified in much the same way as the operational seat. Figure 18 shows how the same material between the side rails was removed and replaced with two machined plates. The crotch strap is attached in the same manner as on the operational seat. As is the case with the other test seats, horizontal adjustment of the seat pan is not provided.

With respect to the seat reference point, positions of the vertical load cells in the test seat are the same as in the modified Air Force seat. Since horizontal loads were not required, simpler load links were used. Other changes included provisions for accelerometers on the rear plate and different load buttons to provide easier adjustment and assembly.

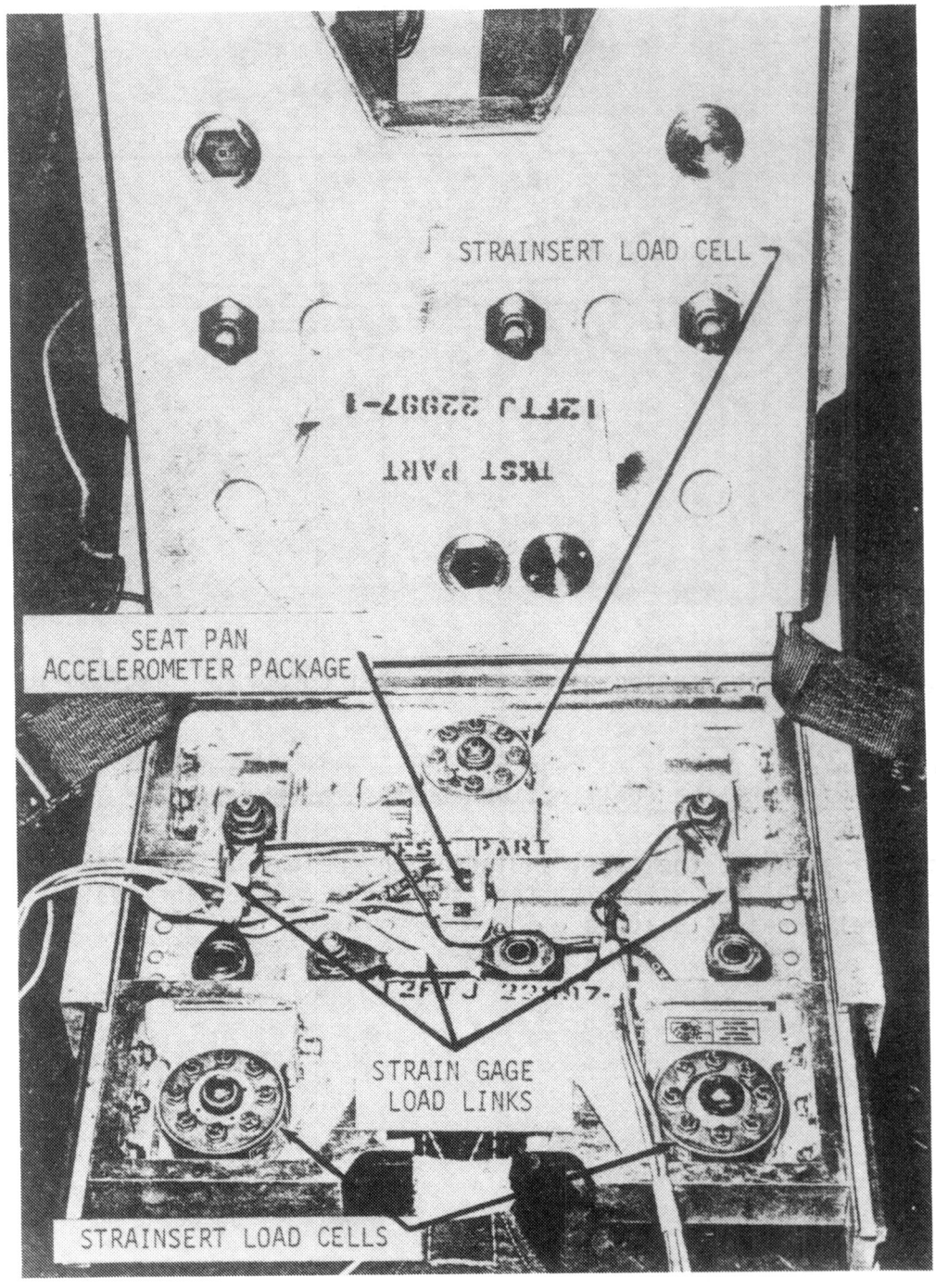

Figure 17. Operational seat pan modified to incorporate seat pan load cells (Reference 3.)

Figure 19 shows bottom and top views of the seat pan. The 5/16-in.-thick aluminum plate is bonded to the bottom of the F-111 contoured foam and fiberglass seat pan. The three fittings in the bottom view are the attachment points for

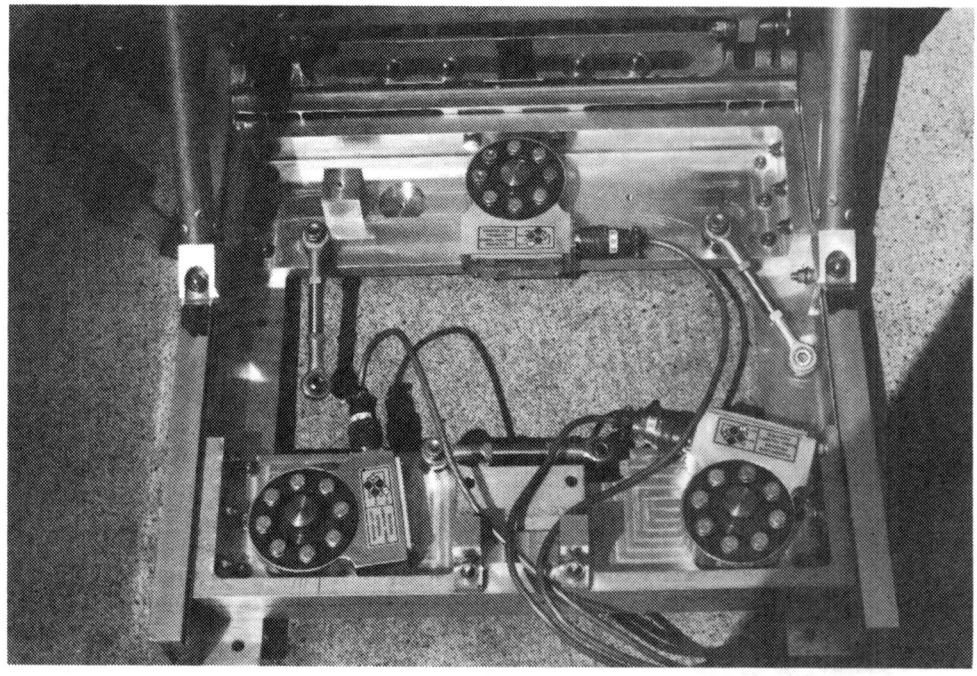

Figure 18. Modification of test seat to incorporate seat pan load cells.

the load links. Fittings to reduce surface wear were not needed at the points of contact with the load cell buttons because of the limited use of this seat.

This modification to the seat, including the weight of the load cells, increased the total weight of the test seat by 13.4 lb. The seat pan sitting on the load cells weighs 9.10 lb.

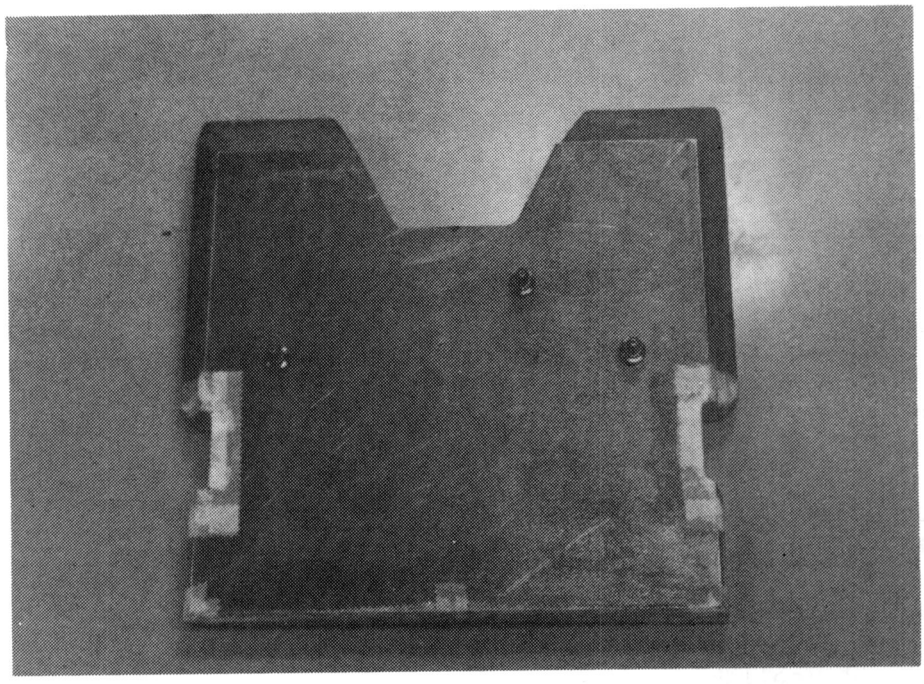

a. Bottom view

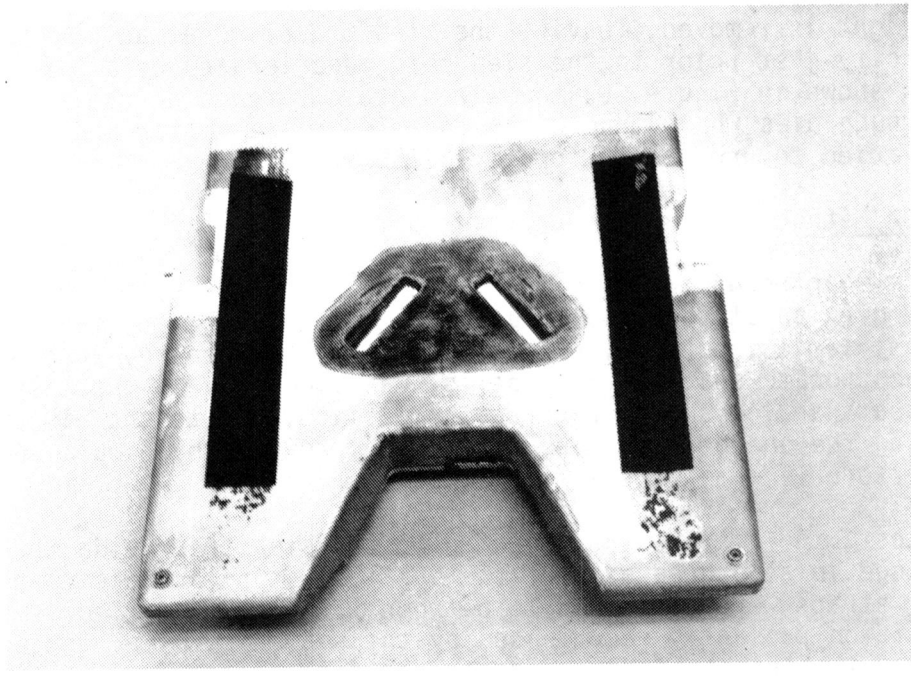

b. Top view

Figure 19. Seat pan from test seat that incorporates seat pan load cells.

3.0 SEAT TESTING

Dynamic testing of the Simula energy-absorbing seat and the operational F-111 seat was conducted at the FAA Civil Aeromedical Institute (CAMI) in December 1983 and March, 1984.

3.1 TEST OBJECTIVES

The primary objective of the dynamic testing done at CAMI was to demonstrate the energy-absorbing capability and structural integrity of the seat when subjected to loads within the design envelope of the possible ground impact conditions. The decision to study ground impact conditions was based on the discussion in Section 2.2.1 of the injury potential during ejection and ground impact.

The second objective of these tests was to provide data for a comparison of the existing F-111 seat and an energy-absorbing seat. Three tests were conducted in which the operational F-111 seat was subjected to the same acceleration pulses as the energy-absorbing seat.

3.2 CONDUCT OF TESTING

3.2.1 Test Facility

The CAMI test facility uses a sled guided along a set of horizontal rails while being accelerated by a cable attached to a falling weight. The load from the falling weight is removed, leaving the sled traveling at an essentially constant velocity just prior to the sled being decelerated by a wire bending mechanism. As shown in Figure 20, the wires are stretched across the track and pulled through dies when impacted by the sled. The number and location of the wires is varied to produce the proper pulse shape.

3.2.2 Test Methods

The fixture mounted on the sled in Figure 21 was provided by the Air Force. Two standard (without seat pan load cells) energy-absorbing seats were provided for the test series, but only one was used. A third energy-absorbing seat, modified to incorporate seat pan load cells, was used only in the tests where the vertical seat pan loads were recorded. Modifications to the fixture, necessary for mounting the energy-absorbing seat, were provided by Simula and incorporated by CAMI personnel.

For each test, the fixture was oriented on the sled to provide the proper velocity change in all three axes of the seat. Just prior to each test, the inertia reel straps were preloaded to between 10 and 15 lb. The arms were placed in the position presently recommended by the U.S. Air Force: extended with the hands on the knees. Input velocity was determined from the time it took the sled to break successive light beams in a velocity trap placed just before the wire-bending mechanism. Accelerometers on the sled measured the shape and peak of the deceleration pulse.

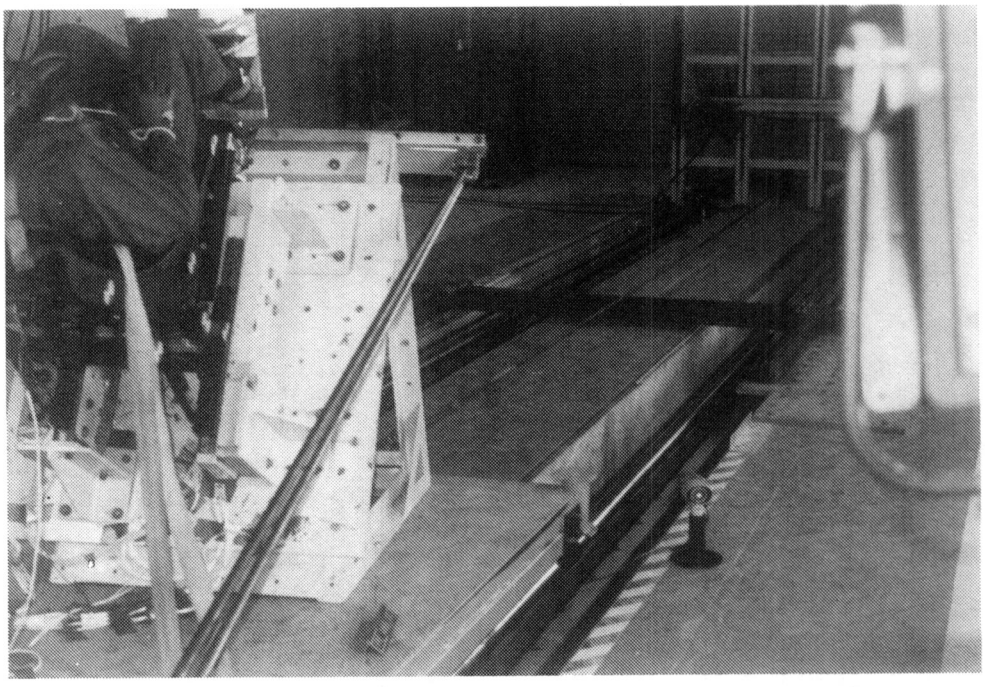

(a) Sled and wires prior to test

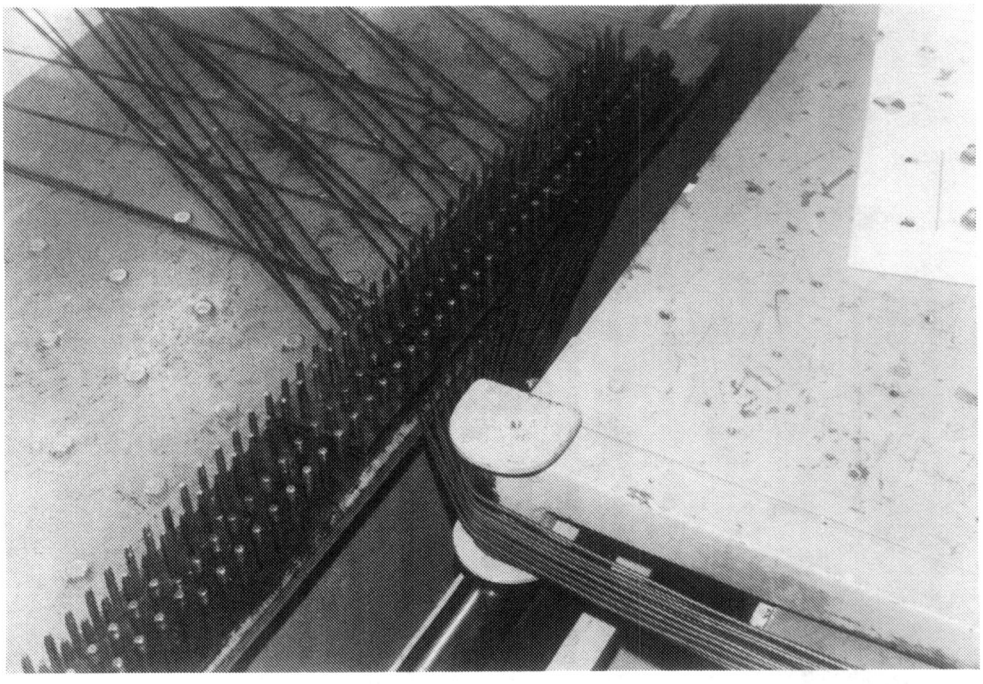

(b) Wires following test

Figure 20. CAMI wire-bending decelerator mechanism.

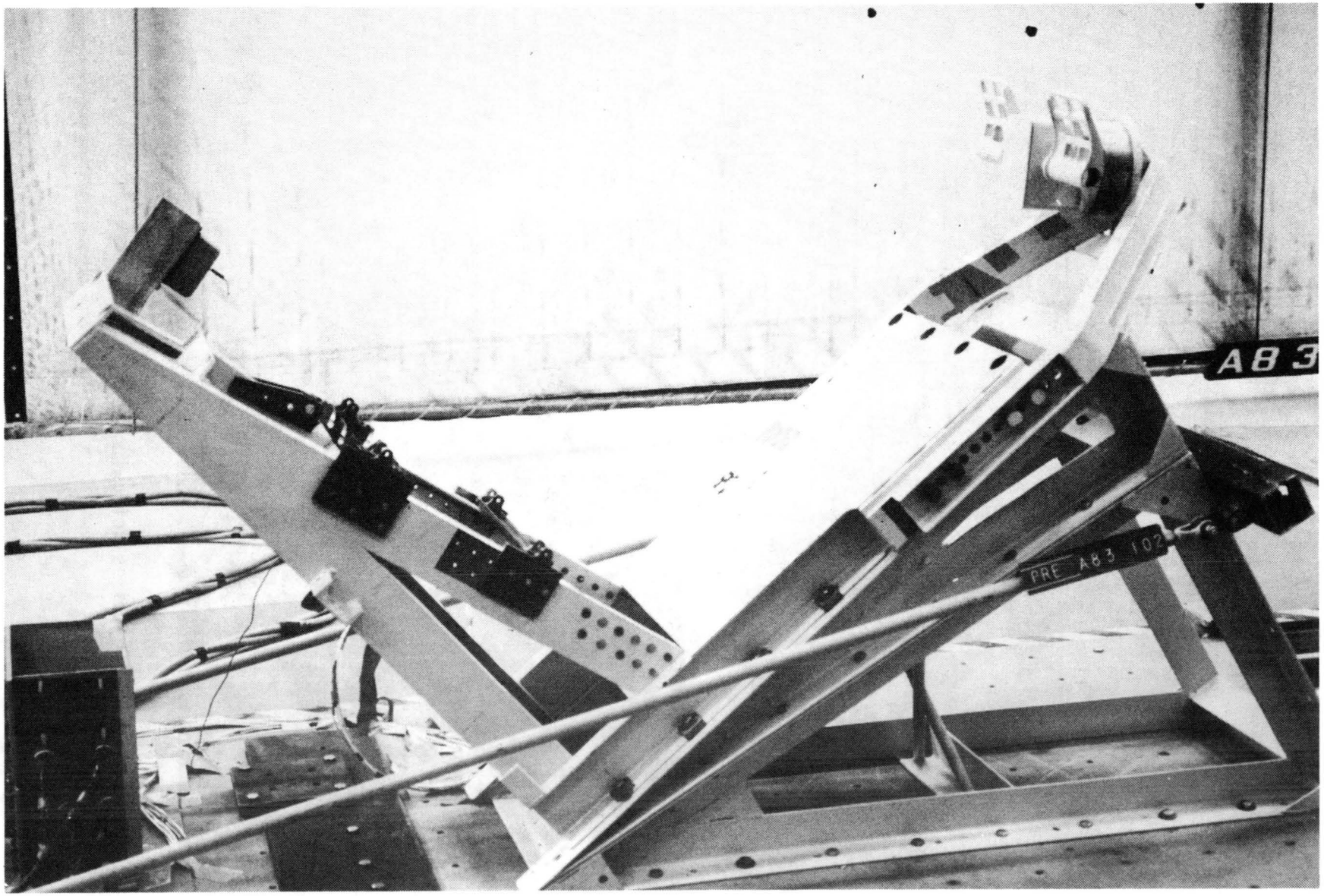

Figure 21. Test fixture used in dynamic seat testing at CAMI.

The seat performance was monitored by various instruments:

- Accelerometers
  - Seat pan, triaxial and along back tangent line, four channels
  - Dummy
    - -- Pelvis, triaxial, three channels
    - -- Chest, triaxial, three channels
    - -- Head, triaxial, three channels
  - Test fixture, triaxial (seat axes), three channels
  - Sled, forward (parallel to velocity vector), two channels
- Load Cells
  - Restraint system webbing tensiometers, lap belts and inertia reel straps, four channels
  - Restraint system strain-gaged end fittings, inertia reel straps, two channels
  - Seat pan, vertical, three channels
  - Dummy spine, triaxial, six channels
  - Footrest, triaxial, three channels
- String Potentiometer
  - Seat stroke along guide tubes, one channel

Still photographs (Figures 22 and 23) were taken to document the pre- and post-test conditions of the test items, while high-speed motion pictures recorded the dynamic response of the test articles.

3.2.3 Test Matrix

Both the seat testing conducted at CAMI, and the capsule testing conducted later at NASA Langley Research Center, were designed to evaluate the performance of the energy-absorbing seat over the full design envelope of ground impact conditions. Therefore, both test matrices considered the following variables for the ground impact conditions:

- Wind velocity (0-20 knots)
- Wind direction (±180 degrees)

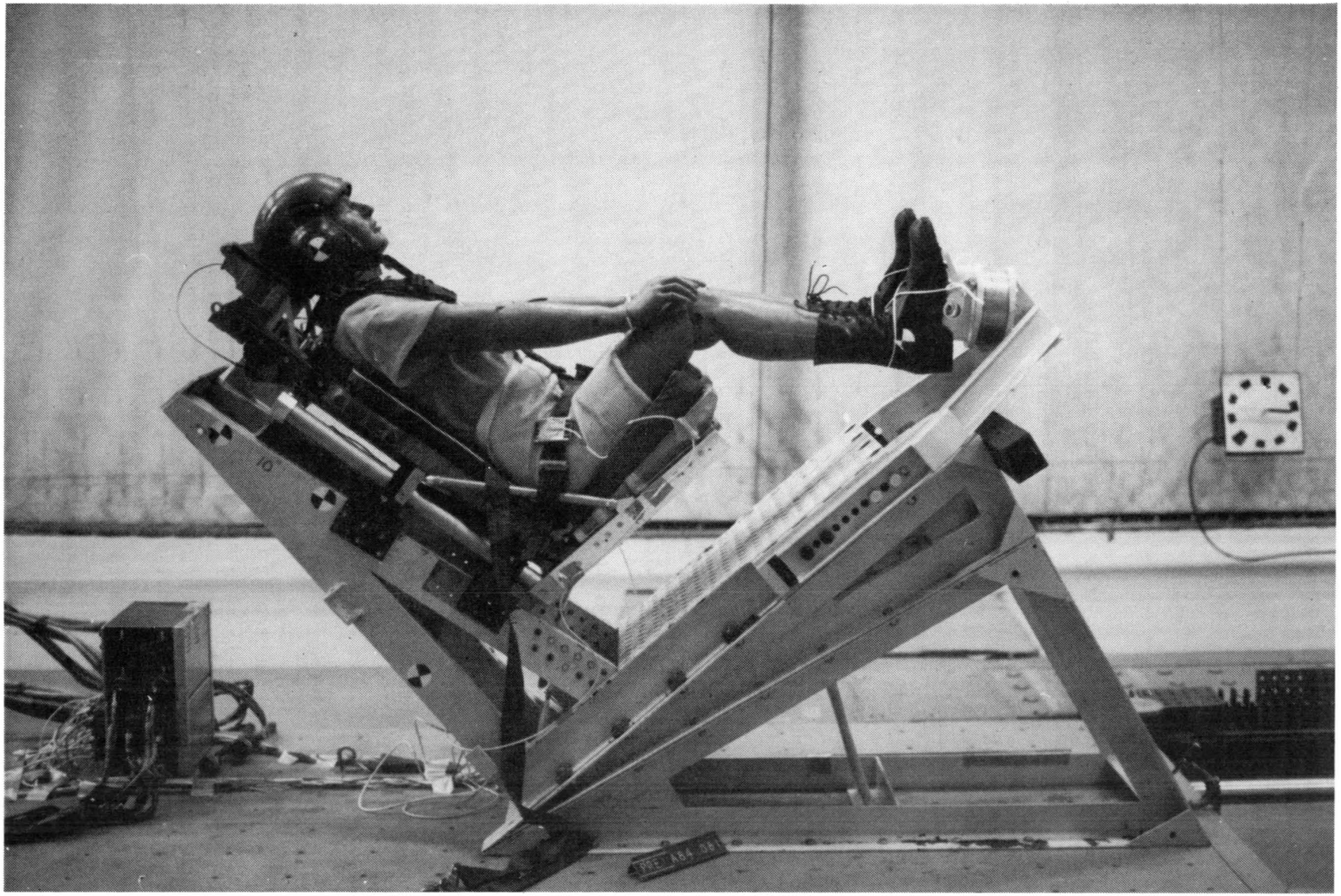

Figure 22. Energy-absorbing seat prior to CAMI test.

Figure 23. Energy-absorbing seat after CAMI test.

- Parachute oscillations (±10 degrees)
- Landing surface slope (±5 degrees).

The vertical descent rate was always 32 ft/sec.

Eight tests were defined for the capsule series using the previous parameters, and are discussed in detail in Section 4.2.3. During seat testing at CAMI, seven of these eight impact conditions were simulated. The conditions were simulated by placing the seat on the test sled at CAMI with the same orientation to the velocity vector that the seat would have in the corresponding NASA capsule test. In this orientation the seat was subjected to an estimate of the acceleration pulse in the corresponding capsule test. Thus, the variables for the seat testing were the seat (whether the operational F-111 seat or the energy-absorbing seat), the seat orientation to the velocity vector, and the acceleration pulse. Table 5 presents the test matrix for the 13 dynamic tests conducted. For convenience (or comparison), column one lists the NASA test numbers presented in Section 4.0. The CAMI tests in column two were designed to be as similar as possible to the NASA tests listed in column one.

Table 5 also lists the seat orientations for each test. Although the orientation of the seat and occupant to the velocity vector is basically the same in corresponding CAMI and NASA tests, some rounding off in seat orientation measurements was permitted to reduce the number of test fixtures required. However, even with these simplifications, velocity components along the major axes of the seat were always within 5 percent of the corresponding ideal capsule test.

The characteristics of the test acceleration pulses are given in Table 6, and the notation used is defined in Figure 24. The acceleration pulses were designed to be as similar as possible to the module bulkhead acceleration pulses expected during actual ground impacts. Estimates were made using Air Force data from capsule ejection tests conducted at Holloman AFB in New Mexico. Tests such as these are normally conducted only under low wind conditions. Indeed, films of the tests show the capsule landing under relatively mild conditions with respect to previously listed parameters. In spite of this, the data was the best available, and was therefore used as a starting point in estimating the bulkhead acceleration pulses even for the extreme conditions that were being tested. The velocity changes in the test pulses were the same as the impact velocities to be used in the crew module tests. This was done since no module rebound was evident in the reference data. The onset rates and peak accelerations were also similar to the reference data. The difference in pulses three and four was a judgement based on expected changes in IAB efficiency with changes in aircraft attitude.

3.2.4 Acceleration Pulse Characteristics

Table 7 presents a comparison of the measured test pulses to the test pulse description in Table 5. Rather than tabulate the values of T_1 and T_2, the range of onset rates defined by T_1 and T_2 is listed in column 4 of Table 7. The onset rate for the measured pulse was determined using an approximation technique described in Reference 11.

TABLE 5. SEAT TEST MATRIX

NASA Test Number	CAMI Test Number	Seat(1)	Pulse Number	Seat Orientation (deg) Pitch	Roll	Yaw
1	A83-110	E/A	3	40	0	30
2	A83-106	E/A	4	0	30	90
3	-	-	-	-	-	-
4	A83-108	E/A	3	60	0	45
5	A83-111	F-111	4	70	0	30
	A83-109	E/A	4	70	0	30
	A84-83	E/A	4	70	0	30
6	A83-113	F-111	2	40	0	0
	A83-103	E/A	2	40	0	0
	A84-81	E/A	2	40	0	0
7	A83-104	E/A	2	-30	0	180
8	A83-112	F-111	1	90	0	0
	A83-101	E/A	1	90	0	0
	A84-82	E/A	1	90	0	0

(1) E/A refers to energy-absorbing seat, F-111 refers to operational seat.

TABLE 6. TEST ACCELERATION PULSE DESCRIPTION

Pulse Number	ΔV (ft/sec)	T_1 (sec)	T_2 (sec)	G_{Min}	G_{Max}
1	32	.040	.046	16	18
2	53.6	.053	.061	23	25
3	46.7	.043	.048	23	25
4	46.7	.049	.056	22	24

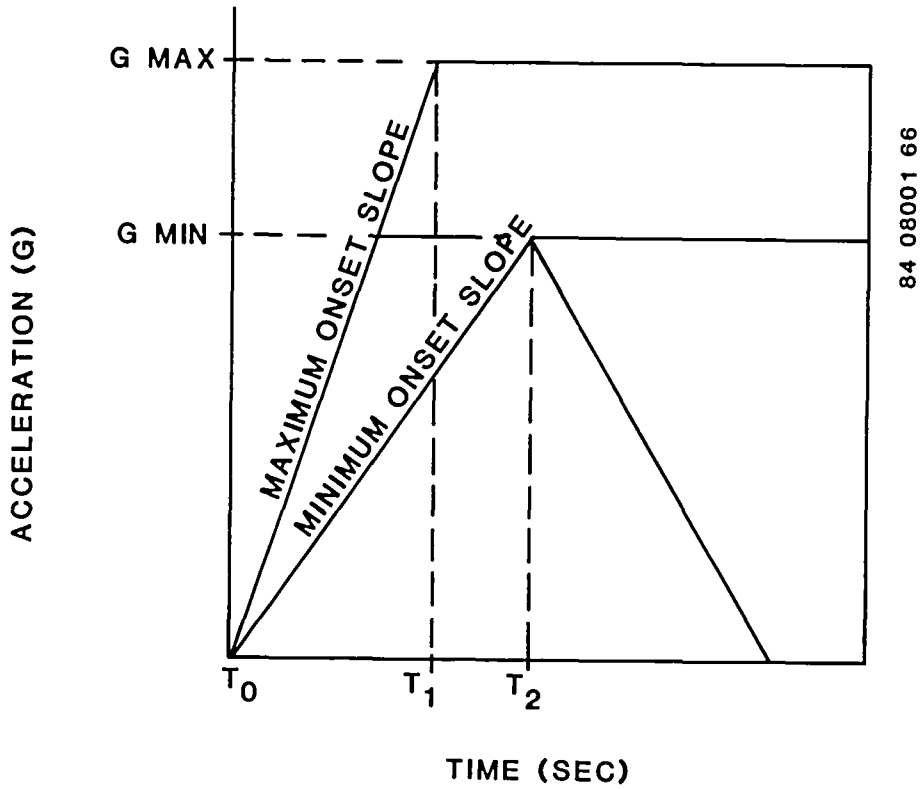

Figure 24. Definition of notation used in test pulse description.

Despite the small ranges defined for onset rate and peak acceleration in the definitions of the test pulse, the large majority of the test pulse characteristics fell within the specified values. The most important parameter, the velocity change, was held within 1 ft/sec of the specified value in every test except A84-81. Peak accelerations were within or slightly above the specified ranges. Some variations in the onset rates (Tests A83-112, A83-113, and A84-81) are noticeable. However, the test pulses were defined based on the available data, obtained under conditions different from that which was being simulated. Therefore, the measured test pulses were certainly within the precision necessary to provide an estimate of the capsule environment.

3.3 PERFORMANCE OF THE ENERGY-ABSORBING SEAT

Three main factors are involved in evaluating the performance of the energy-absorbing seat: acceleration levels, stroking distance, and structural integrity.

TABLE 7. INPUT ACCELERATION PULSES FOR DYNAMIC SEAT TESTING(1)

NASA Test Number	CAMI Test Number	Ideal Pulse			Measured Pulse		
		Δv (Ft/sec)	Onset Rate (G/sec)	Peak (G)	Δv (Ft/sec)	Onset Rate (G/sec)	Peak (G)
1	A83-110	46.7	480-580	23-25	47.1	567	25.1
2	A83-106	46.7	390-490	22-24	46.4	486	23.0
3	-	-	-	-	-	-	-
4	A83-108	46.7	480-580	23-25	45.9	556	24.6
5	A83-111	46.7	390-490	22-24	46.9	455	25.7
	A83-109	46.7	390-490	22-24	46.8	473	26.2
	A84-83	46.7	390-490	22-24	46.7	433	23.5
6	A83-113	53.6	380-470	23-25	54.5	329	27.6
	A83-103	53.6	380-470	23-25	54.4	478	26.9
	A84-81	53.6	380-470	23-25	54.8	514	25.7
7	A83-104	53.6	380-470	23-25	53.1	449	26.7
8	A83-112	32	350-450	16-18	31.9	521	17.7
	A83-101	32	350-450	16-18	32.3	415	19.5
	A84-82	32	350-450	16-18	32.3	401	17.7

(1) Data filtered with class 60 filter per SAE Recommended Practice SAE J211b.

3.3.1 Acceleration Levels

Table 8 presents four of the peak accelerations measured during each test of the energy-absorbing seat. Both the seat-pan-z and seat-back-z accelerometers were mounted on the bottom of the seat pan. The seat-pan-z accelerometer measures pure vertical accelerations while the seat-back-z accelerometer measures accelerations along the seat back tangent line. The pelvis and chest accelerometers are mounted inside the dummy.

The seat pan accelerations, both vertical and along the seat back tangent line, are the most commonly used measurements for evaluating seat performance. These peak acceleration values, ranging from 16.8 to 27.3 G, are well within the

TABLE 8. PEAK VERTICAL ACCELERATIONS MEASURED ON SEAT PAN DURING ENERGY-ABSORBING SEAT TESTING AT CAMI[1]

NASA Test Number	CAMI Test Number	Accelerometer Orientation			
		Seat Pan z (G)	Seat Back Tangent Line	Pelvis z (G)	Chest z (G)
1	A83-110	21.7	23.9	21.7	22.1
2	A83-106	21.1	20.9	15.4	15.8
3	-	-	-	-	-
4	A83-108	21.8	23.6	27.1	25.5
5	A83-109	22.2	24.3	25.8	24.0
	A84-83	22.9	23.4	27.5	27.1
6	A83-103	24.6	27.1	24.4	24.4
	A84-81	20.6	27.3	27.1	23.1
7	A83-104	21.1	16.8	18.1	16.3
8	A83-101	21.3	22.0	23.7	23.3
	A84-82	21.3	19.9	26.3	22.5

(1) Data filtered with class 180 filter per SAE Recommended Practice J211b.

range of values that would be expected with an energy-absorbing seat. The pelvis and chest accelerations tend to be slightly higher due to the dynamic amplification effects of the dummy as it compresses into the seat pan during the test. A typical seat pan acceleration trace from the test series is shown in Figure 25.

The shape of the seat pan acceleration curve is most easily explained under the conditions when the seat and occupant are being subjected to a purely vertical crash test. Initially, the seat and occupant are traveling downward at the same constant velocity with little or no loads being transferred between the occupant and the seat. The cushion, fleshy parts of the buttocks and torso, and the spine are uncompressed. When the aircraft strikes the ground, an upward acceleration is applied through the floor and seat structure to the seat pan. This is shown by the increasing acceleration between 20 and 40 msec.

At the time the accelerations start to increase, the occupant is not applying a significant load to the seat pan. However, the cushion and fleshy parts of the buttocks, as well as the torso and spine, start compressing as the accelerations continue to increase. The greater the compression of these elements, the higher is the load applied to the seat by the occupant. Thus, the seat pan is now being acted upon by two forces: the upward loads, or accelerative forces transferred through the seat structure, and the downward loads applied by the occupant. However, the upward loads are transferred through the energy absorbers and are therefore limited in magnitude.

One can see in Figure 25 that after the initial peak is reached, there is a small notch in the acceleration pulse around 50 msec. This is caused by a significant downward load applied to the seat pan by the pelvis. The cushion and fleshy part of the buttocks are compressed and the pelvis starts experiencing essentially the same deceleration as the seat pan. At this time the spine and torso have not yet fully compressed. In this case the added load from the pelvis is not enough to start stroking the seat. The accelerations drop for a short time, but the applied accelerations continue to increase and again start driving the accelerations upward.

This notch after the initial spike will not occur in all tests or with all seats. The three main factors influencing the shape of the pulse in this area are the stroking weight of the seat, the peak acceleration level, and the rate of onset of the acceleration pulse. For instance, if the stroking weight of the seat is heavy, such as with an armored bucket, and the onset rate of the applied pulse is steep enough, acceleration levels on the bucket will get high enough to stroke the seat before the occupant has fully compressed the cushion.

Obviously, other factors such as the cushion stiffness, seat pan stiffness, and anthropomorphic dummy properties are continuously influencing the shape of the pulse.

Figure 25 shows another peak around 60 msec followed by a sharp drop in the accelerations. It is at about the time of this peak that stroking starts. The energy absorbers are limiting the load applied through the floor to the seat structure while the spine continues to compress, applying more and more downward load to the seat pan. This increasing load applied by the occupant drives the seat pan accelerations downward. Eventually the accelerations drop to what is called the initial notch (70 msec). At this point the load applied to the seat by the occupant is the greatest. It is also around this

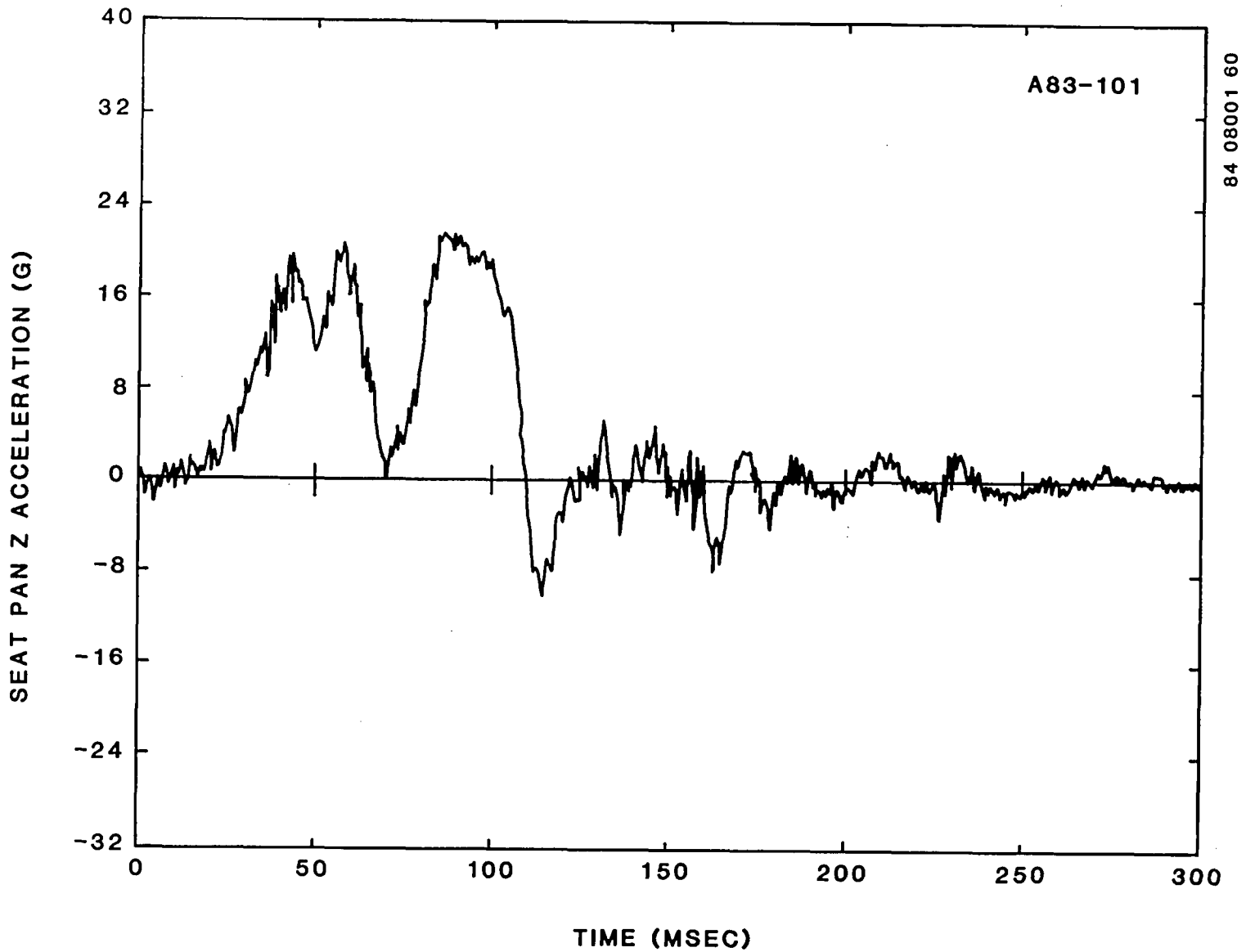

Figure 25. Seat pan vertical acceleration trace from CAMI test of energy-absorbing seat.

time that the compression on the spine reaches its first maximum. The exact time of maximum spinal load depends on the phase relationship between the head, torso, and pelvis. The dynamics of the pulse, as well as the application of loads in directions other than vertical, may cause the loads in different parts of the dummy to peak at different times.

After the initial notch the acceleration starts rising again. This is due to the rebound of the occupant off the seat pan. Up until this point in the crash the body has been compressed down towards the seat pan. Now some of the body is acting like a spring, such as a ball thrown against the ground acts, and is pushing up away from the seat pan. As the occupant rebounds, the downward load he applies to the seat decreases and the steady load applied through the energy absorbers causes the accelerations to rise to the secondary spike. After the secondary spike the spine and buttocks again start to compress and apply more downward load to the seat pan, causing the accelerations to drop.

If the applied pulse were severe enough to continue stroking, one would see the acceleration level continue to oscillate with decreasing magnitude until it steadied out at the energy absorber limit load. In this case however, the test input is not that severe. Stroking stops after approximately 110 msec and the accelerations drop down to 0.

Accelerations along the seat back tangent line will have a shape similar to the seat pan z-axis acceleration. However, depending on the direction of the applied load, the magnitudes of the accelerations along the back tangent will be different from the pure vertical accelerations. In most of the tests presented in Table 8, the seat orientation was such that the load vector was more in line with the seat back tangent line than with pure vertical. Thus the magnitudes of the accelerations seen along the seat back tangent line are greater than the accelerations along the seat pan z-axis.

Qualitatively, the acceleration trace shows the seat to be performing in the expected manner. As a more quantitative evaluation, the seat pan accelerations will be compared to the U.S. Army requirements for crashworthy crewseats presented in MIL-S-58095(AV) (Reference 14). Figure 26 shows the maximum acceptable duration-magnitude curve reprinted from MIL-S-58095(AV). This curve is based on data gathered by Eiband (Reference 15). Violations of the curve into the area of injury occur when the acceleration levels are at least 23 G for greater than .006 sec.

There are several deficiencies with this current criterion. One problem is that the flexion of the upper torso, which can be a major contributor to spinal injury, is not considered when examining the seat pan accelerations. However, occupants of the F-111 are pulled back into their seats by power-haul back inertia reels before the crew module blasts away from the aircraft. The upper torso flexion would be much less in the F-111 than in, for example, a helicopter pilot who was bent over the cyclic or collective sticks trying to maneuver the aircraft when it crashed.

A major problem with the Eiband curve is simply that it uses only the maximum seat pan accelerations as a measure of injury potential. From the discussion of the seat pan acceleration plot in Figure 25, the maximum accelerations do not occur when the load on the spine is the highest, but when the lowest loads are transmitted by the occupant to the seat. Therefore, the Eiband curves can at best be considered an empirical tool.

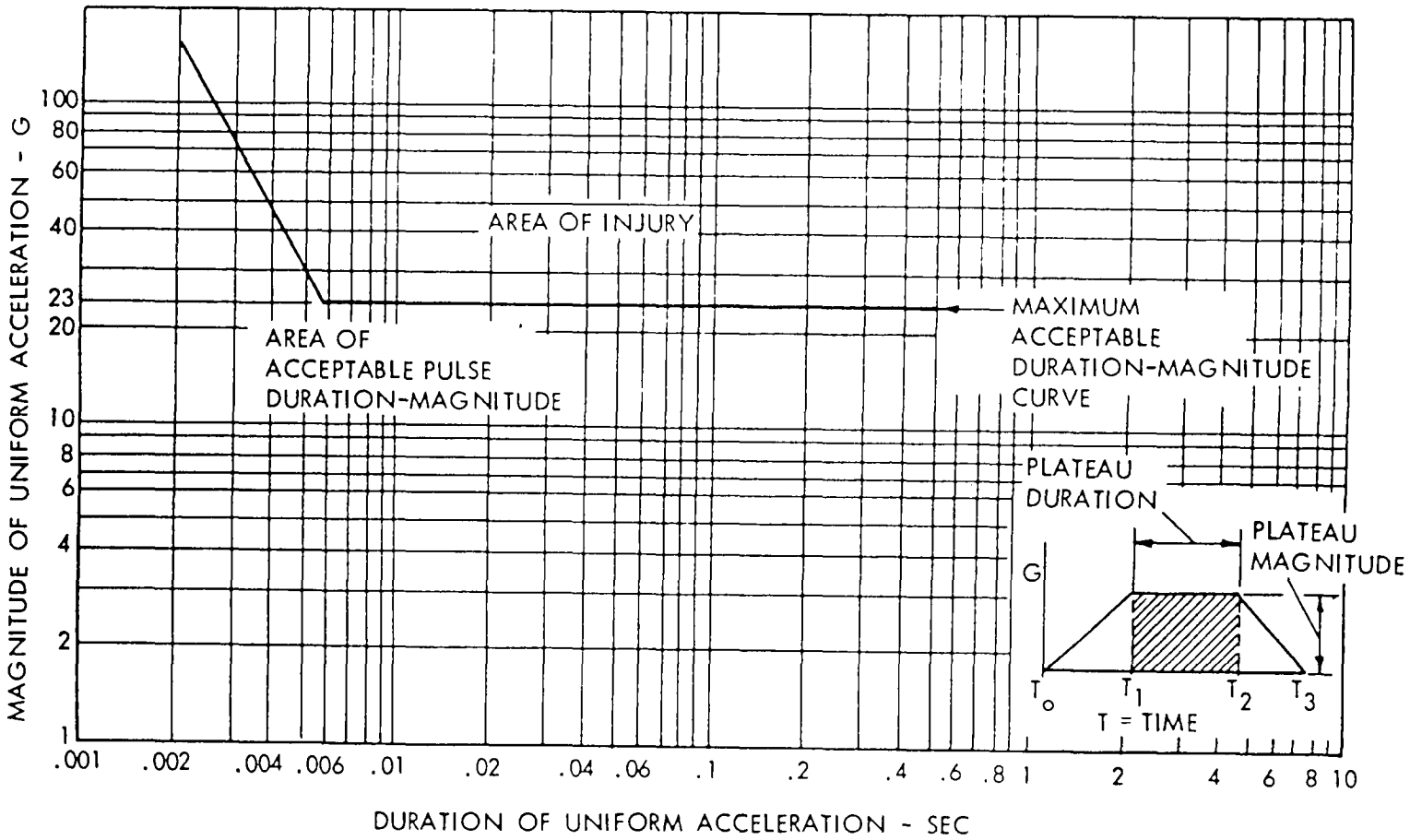

Figure 26. Acceptable duration-magnitude curve for seat pan acceleration levels (Reference 14).

Finally, problems have occurred in the interpretation of the Eiband curves. Figure 27 shows a seat pan vertical acceleration measured during qualification testing to MIL-S-58095(AV) of an energy-absorbing seat. These multiple spikes obviously raise the average acceleration above 23 G for more than .006 sec. The natural frequency of the human body is too low to respond to each of these individual spikes. It would respond, however, to the average of these spikes, which is obviously over 23 G for more than .006 sec. However, this seat would be judged to be in accordance with MIL-S-58095(AV) since none of the individual spikes violates the criterion. This interpretation impairs the use of Eiband's work even as an empirical tool.

With these factors in mind, Table 9 presents the durations during which the seat pan vertical and seat back tangent line accelerations were above 23 G. The maximum time above 23 G, determined using average accelerations as well as individual peaks, was recorded. Since only the vertical accelerations are used in MIL-S-58095(AV), this seat would easily meet the criterion. Because of the seat orientations during the testing, accelerations along the back tangent line tended to be higher. In only one case, A84-81, Eiband's criterion was violated as the acceleration level remained above 23 G for .017 sec.

Also presented in Table 9 are the values of the Dynamic Response Index (DRI). The DRI uses a single lumped mass, damped spring system to model the human body. The acceleration curve for which a DRI is being determined is used as input to the model. The maximum deflection of the spring, multiplied by a factor, is used as the DRI for that curve. The deflection of the spring is related to the deflection of the spine; thus, the higher the DRI is, the greater the potential is for injury. A typical DRI measurement for the energy-absorbing seat is presented along with a seat pan acceleration used as input in Figure 28.

Presented earlier in Figure 5 is the correlation made for ejection seats between the DRI and the spinal injury rate. Differences in pulse duration, onset rate, and the seat motion make the environment in an energy-absorbing seat different from the environment in an ejection seat. At this time no data correlating DRI to spinal injury rate in an energy-absorbing seat are available. Figure 29 is reprinted from Reference 13 to show what magnitude of DRI values can be expected from an energy-absorbing seat. The change in DRI with respect to a change in energy absorber load is not very steep. An energy absorber load of 14.5 G corresponds to a DRI of approximately 20.

Table 9 shows that the DRI's measured along the seat pan vertical axis are all less than 20. Values of the DRI along the seat back tangent line are, as would be expected from the seat orientations, slightly higher than the vertical DRI's. However, all but one is in the expected range. The pelvis DRI's, as were the pelvis peak accelerations, tend to be higher than the values measured on the seat pan.

The DRI tends to smooth out the sharp peaks that can cause inconsistent differences between the peak measurements of seat pan and pelvis accelerations. The result is pelvis DRI's that are consistently a few points higher than the seat pan DRI's. This is best seen by examining Figure 30. The pelvis DRI's show the greatest difference from the seat pan DRI's in Test Numbers A83-101 and A84-82. That is because the seat was lying on its back (Figure 31) for this test and the dummy was not preloading the cushion as well as in other tests. Because of this the dynamic amplification effects noticeably raise the

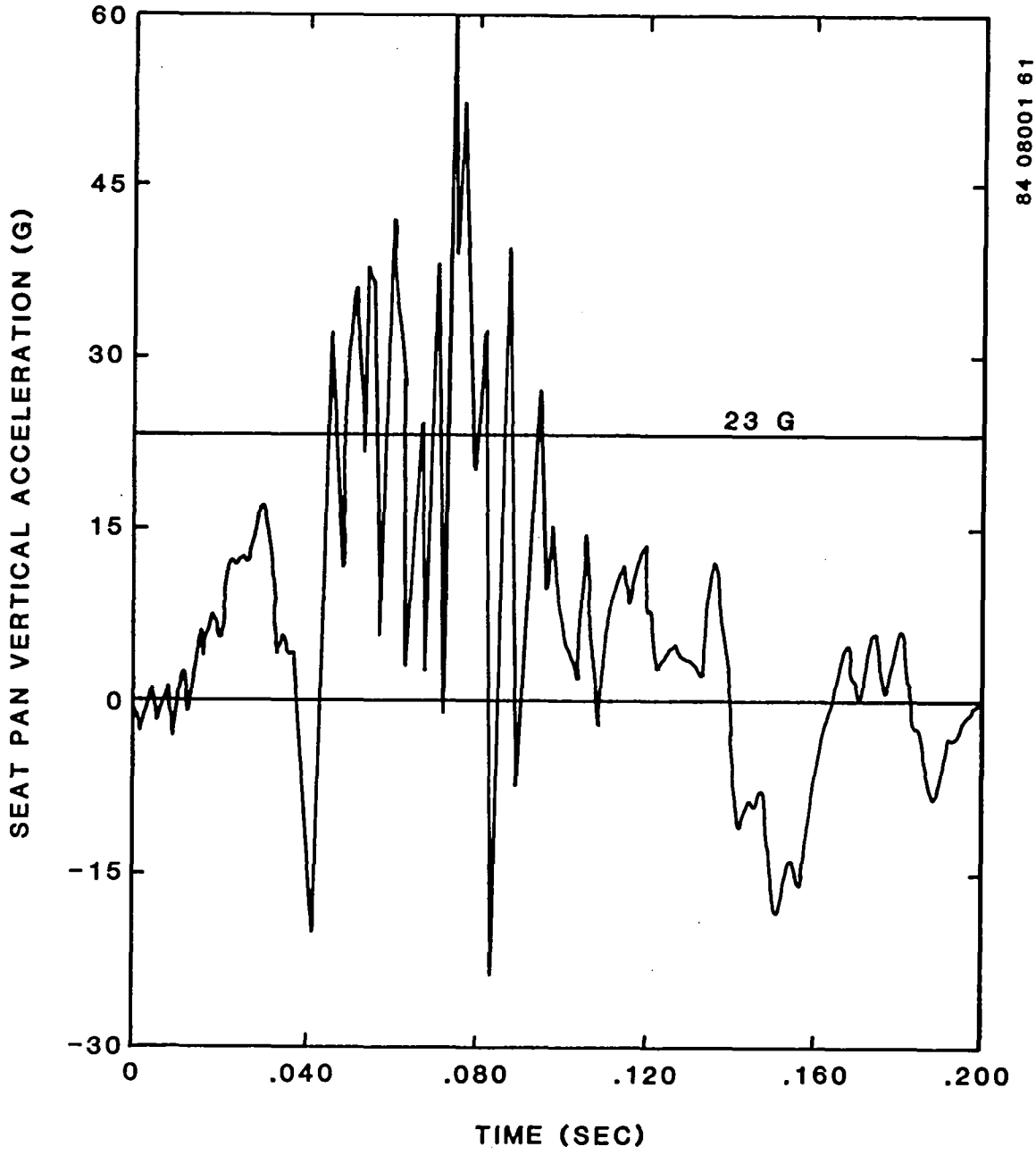

Figure 27. Seat pan acceleration measured during qualification to MIL-S-58095.

pelvis acceleration level and the resulting DRI value. One DRI value is inconsistent with the other values measured during testing. The seat back tangent line DRI test for A84-81 is higher than would be expected. However, this DRI is inconsistent with seat pan and pelvis DRI values from the same test, as well as the pattern of measurements in other tests. At this time it is not clear why this value is so much higher than the corresponding value in Test Number A83-103, where the test conditions were the same.

TABLE 9. EIBAND AND DYNAMIC RESPONSE INDEX EVALUATION OF ENERGY-ABSORBING SEAT TESTING AT CAMI

NASA Test Number	CAMI Test Number	Duration Above 23 G (sec)		Dynamic Response Index		
		Seat Pan z	Seat Back Tangent Line	Seat Pan z	Seat Back Tangent Line	Pelvis z (G)
1	A83-110	0	0.002	14.9	19.7	23.4
2	A83-106	0	0	18.9	17.3	14.8
3	-	-	-	-	-	-
4	A83-108	0	0.001	16.3	19.5	22.3
5	A83-109	0	0.004	18.2	20.7	24.6
	A84-83	0	0.002	18.1	19.9	22.5
6	A83-103	0.002	0.006	17.6	21.6	24.9
	A84-81	0	0.017	17.0	26.1	24.5
7	A83-104	0	0	16.0	10.6	13.4
8	A83-101	0	0	18.6	18.4	24.2
	A84-82	0	0	17.2	16.2	23.7

3.3.2 Energy-Absorbing Stroke

Table 10 lists the vertical energy-absorbing stroke measured in each of the seat tests. The measured stroke was the vertical movement of the seat reference point. Preliminary layouts have shown that a retrofit seat would have an available stroking distance of 6 to 11 in., depending on vertical seat position. In all cases the stroke measured was less than the minimum stroke that would be available.

If the required stroke is more than the available stroking distance, the seat will hit the floor before the impact energy has been dissipated. This will mean an increase in the loads to which the occupant is subjected and produce a spike on the seat pan acceleration plots. If significant energy is remaining in the impact pulse, the loads created by "bottoming out" can be injurious.

3.3.3 Structural Integrity

No structural failures of any seat parts occurred during the test series.

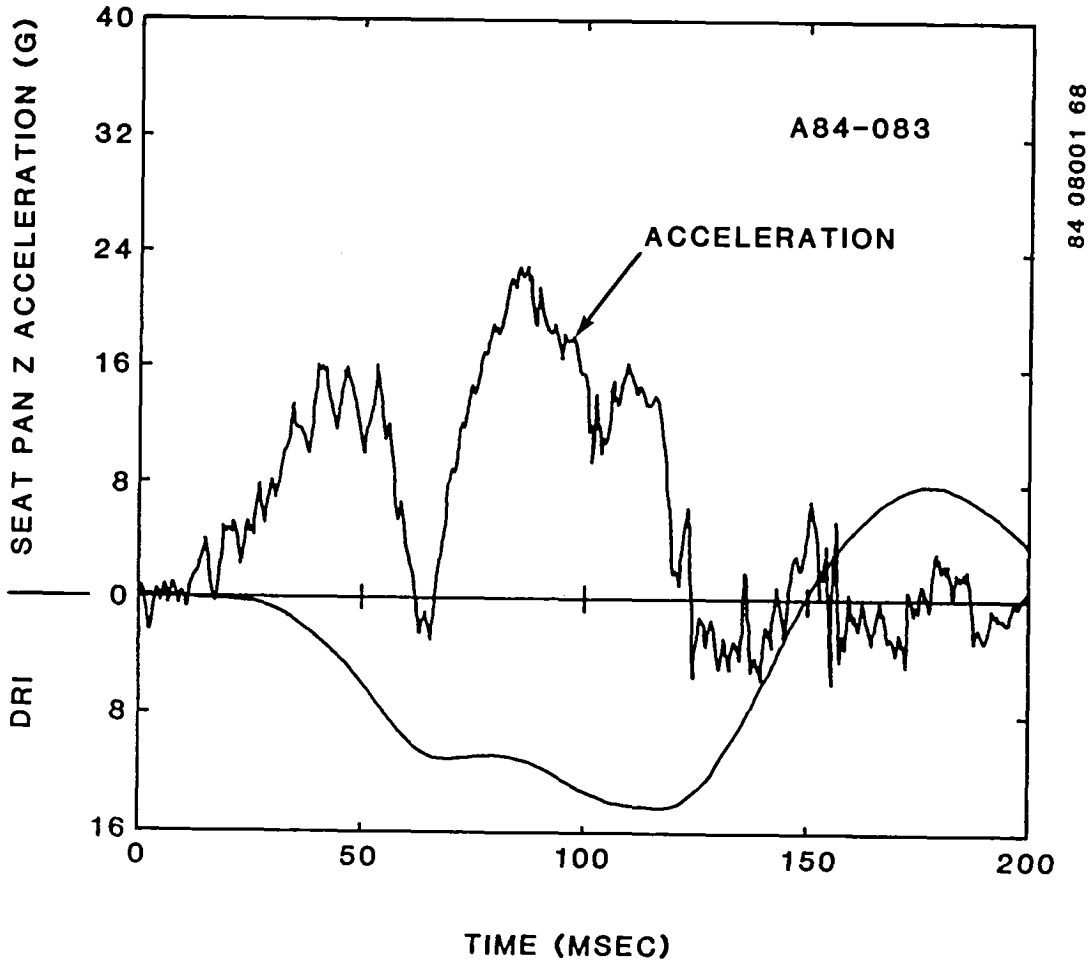

Figure 28. Seat pan acceleration and corresponding DRI for energy-absorbing seat.

Periodic maintenance of the seats during testing consisted of replacing stroked energy absorbers, and also roller bearings and bearing bolts (Figure 32) when necessary. Depending on the direction of the applied loads, the roller bearings may be subjected to very high loads in bearing against the guide tubes. Even while supporting these loads, they must roll freely so that the seat strokes with a minimum of frictional resisting force. After a few tests there is a tendency for a roller to turn less smoothly due to minor damage to the roller or the bolt that supports it. In either case, the part was replaced. This type of wear would cause no trouble in the field since it only occurs under very high loads such as during a ground impact after ejection.

3.3.4 Conclusions

Certain conclusions can be reached based only on the performance of the energy-absorbing seat.

- The seat pan vertical acceleration levels and the corresponding DRI's show the energy-absorbing seat to be functioning properly.

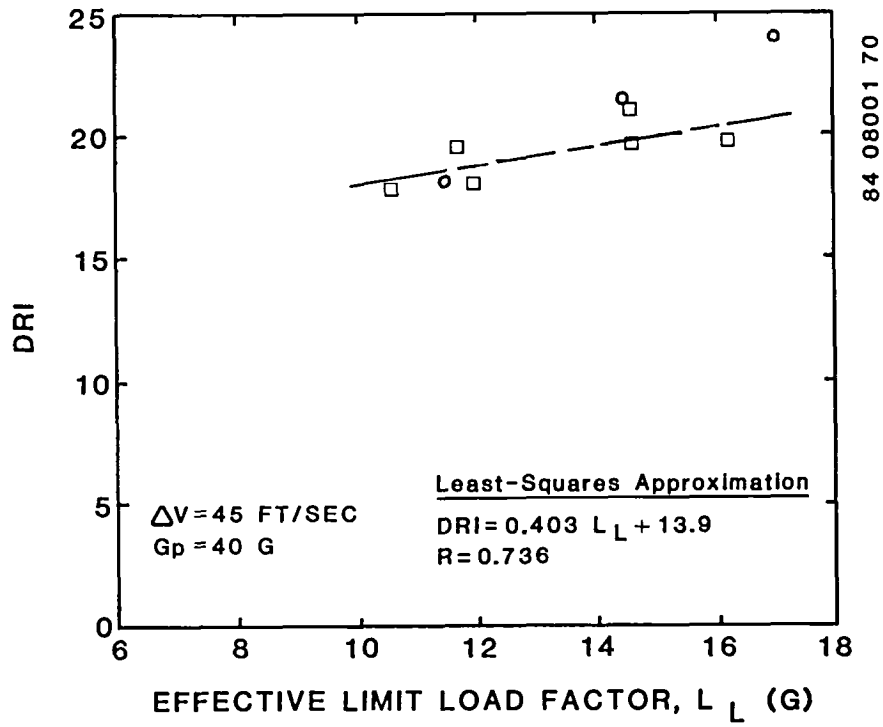

Figure 29. Dynamic Response Index as a function of energy absorber limit load.

- It has been estimated that if an energy-absorbing retrofit seat is placed in the F-111 capsule, the available stroking distance will range from 6 to 11 in., depending on vertical seat position. In every seat test the measured stroke was less than the minimum available stroke.

- The seat suffered no structural damage. Therefore, it was reasonable to assume that the seat is suitable for capsule testing at NASA Langley Research Center.

3.4 COMPARISON OF OPERATIONAL AND ENERGY-ABSORBING F-111 SEATS

Three of the test conditions were run with both the operational F-111 seat and the energy-absorbing test seat. In each case two tests were conducted with the energy-absorbing seat and one test with the operational seat. The second set of energy-absorbing seat tests, A84-81, -82, and -83, were conducted after seat pan load cells had been incorporated into the design.

Three major factors will be used in comparing the two seats. First, the vertical acceleration levels, including seat pan, seat back, pelvis, and chest, will be examined. Secondly, vertical loads measured by load cells placed under the seat pan will be compared. Finally, spinal load and moment measurements from a load cell placed inside the dummy will be presented.

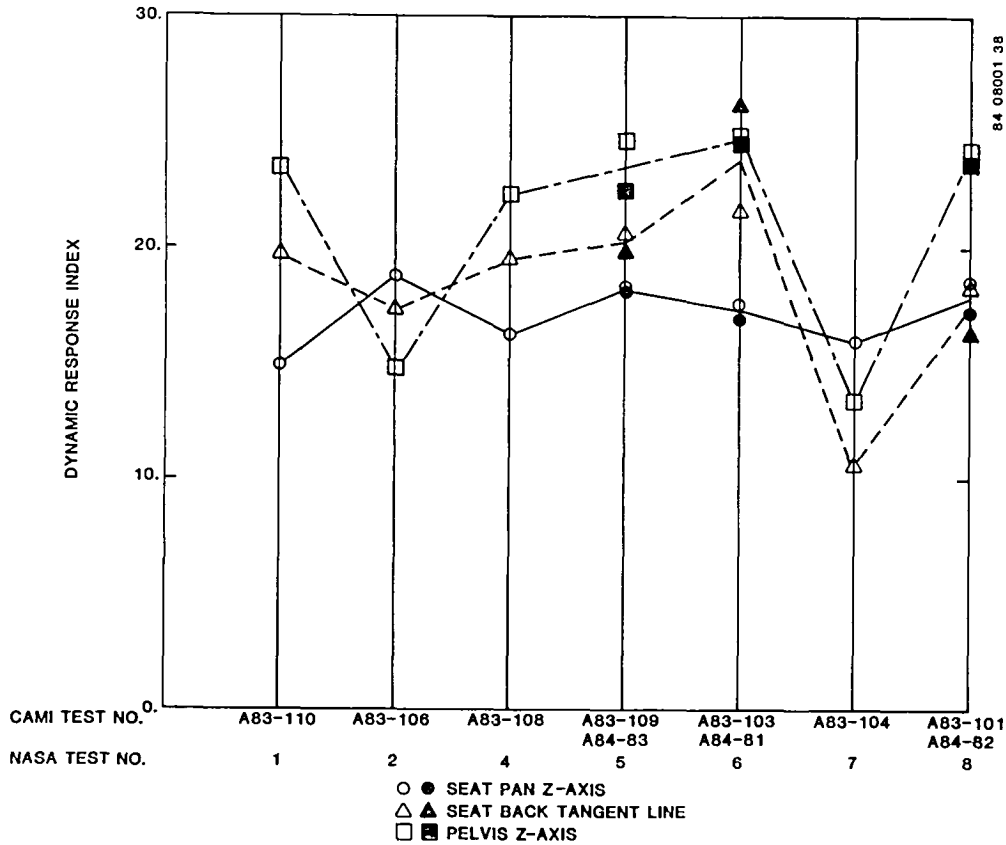

VALUES OF DYNAMIC RESPONSE INDEX RECORDED DURING CAMI TEST SERIES.

Figure 30. Dynamic Response Index measurements from energy-absorbing seat tests at CAMI.

3.4.1 Acceleration Levels

The first comparisons between the seats was done using the same measurements that were used to evaluate the performance of the energy-absorbing seat: peak acceleration levels in the vertical direction.

Table 11 presents the peak accelerations for the seat pan z-axis, seat back tangent line, pelvis z-axis, and chest z-axis. Figures 33 through 36 present the same information in graphical form. One can see that the peak accelerations for the energy-absorbing seat were below those for the operational seat in every case but one. This one case is the seat back tangent line for Tests A83-112 and -101, where both accelerations peaked at 22.0 G. In some cases the differences were not great, but they were significant and consistent.

The shape of the seat pan z-axis acceleration traces for both the energy-absorbing seat and the operational seat in similar tests are shown in Figures 37 through 39. Both traces follow the same path, rising steadily, for the first 30 to 40 msec. When the energy-absorbing seat starts to stroke, its seat pan acceleration drops off rapidly. However, the operational seat pan accelerations continue to rise slightly and then level off. After remaining at this level for 35 to 45 sec., the operational seat pan accelerations drop back to 0.

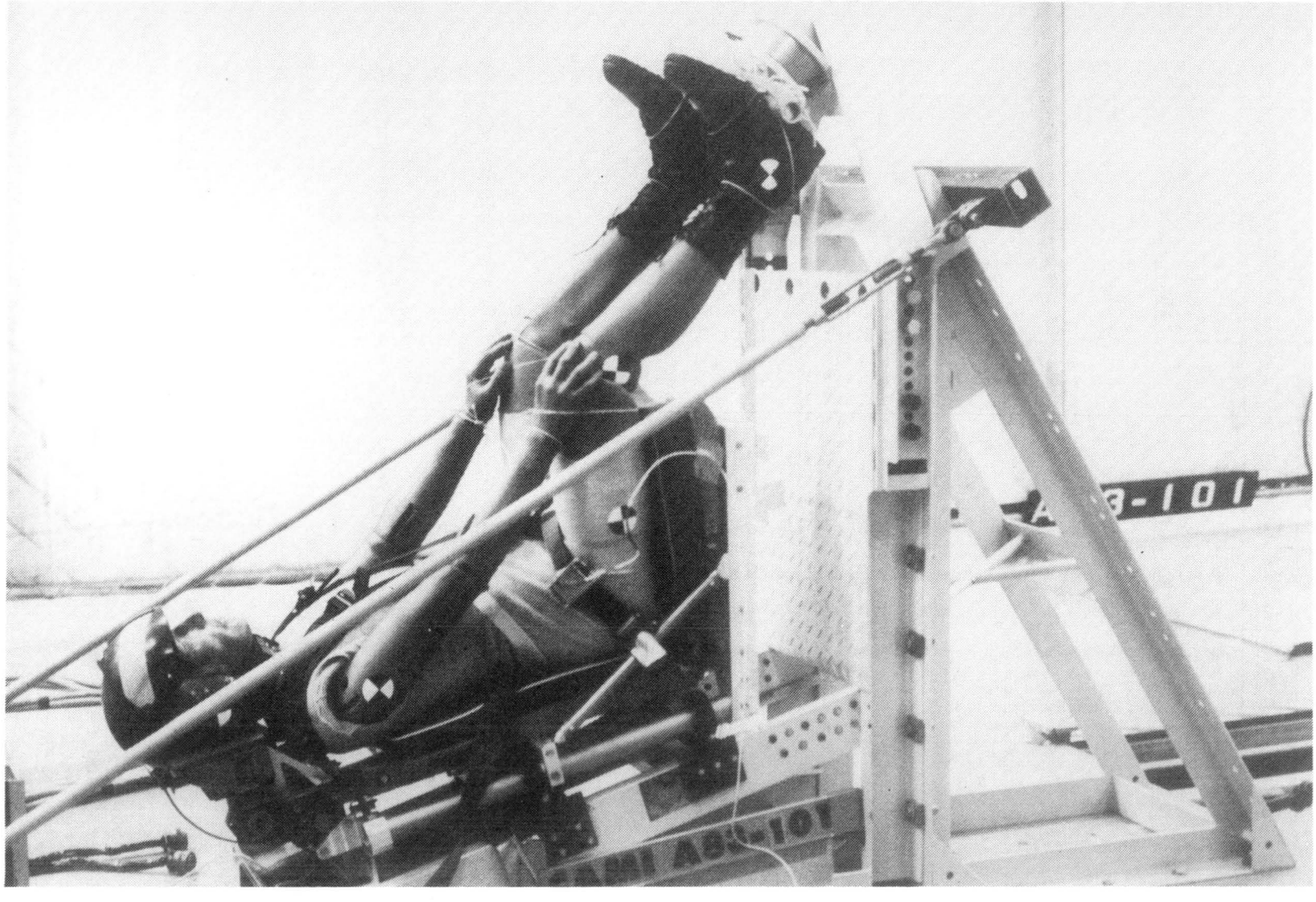

Figure 31. Pretest photograph from CAMI Test No. A83-101.

TABLE 10. STROKE MEASURED IN CAMI SEAT TESTS

NASA Test Number	CAMI Test Number	Stroking Distance (in.)
1	A83-110	2.1
2	A83-106	0
3	-	-
4	A83-108	1.8
5	A83-109	5.1
	A84-83	5.4
6	A83-103	4.35
	A84-81	3.95
7	A83-104	0
8	A83-101	2.9
	A84-82	2.9

In the other case, after the energy-absorbing seat pan acceleration drops to zero, it rises again to a value equal to or slightly higher than the initial peak. As discussed earlier in Section 3.3.1, the acceleration levels will now oscillate while steadily decreasing to the energy absorber limit load. However, before much oscillation occurs in this case, the acceleration drops back to 0.

One can see that while the peak levels for the energy-absorbing seat are lower, it is only by a matter of 2 to 4 G. What is more significant is that the energy-absorbing seat spreads the accelerations out over a longer time period. The area under these curves represents the total velocity change seen by the seat and occupant, and since the input conditions for these two tests were the same, the area under the curves must be equal. The acceleration trace for the energy-absorbing seat satisfies this requirement by lasting a longer time. The energy-absorbing seat subjects the occupant to the velocity change over a .015 to .020 sec longer time period than the operational seat. This lengthening of the pulse reduced the loads seen by the occupant and is reflected in the differences in the DRI's recorded for the two seats. Table 12 presents the DRI's for the seat pan and pelvis accelerations. The seat pan accelerations produce DRI's that are 6 to 11 points lower for the occupant of the energy-absorbing seat.

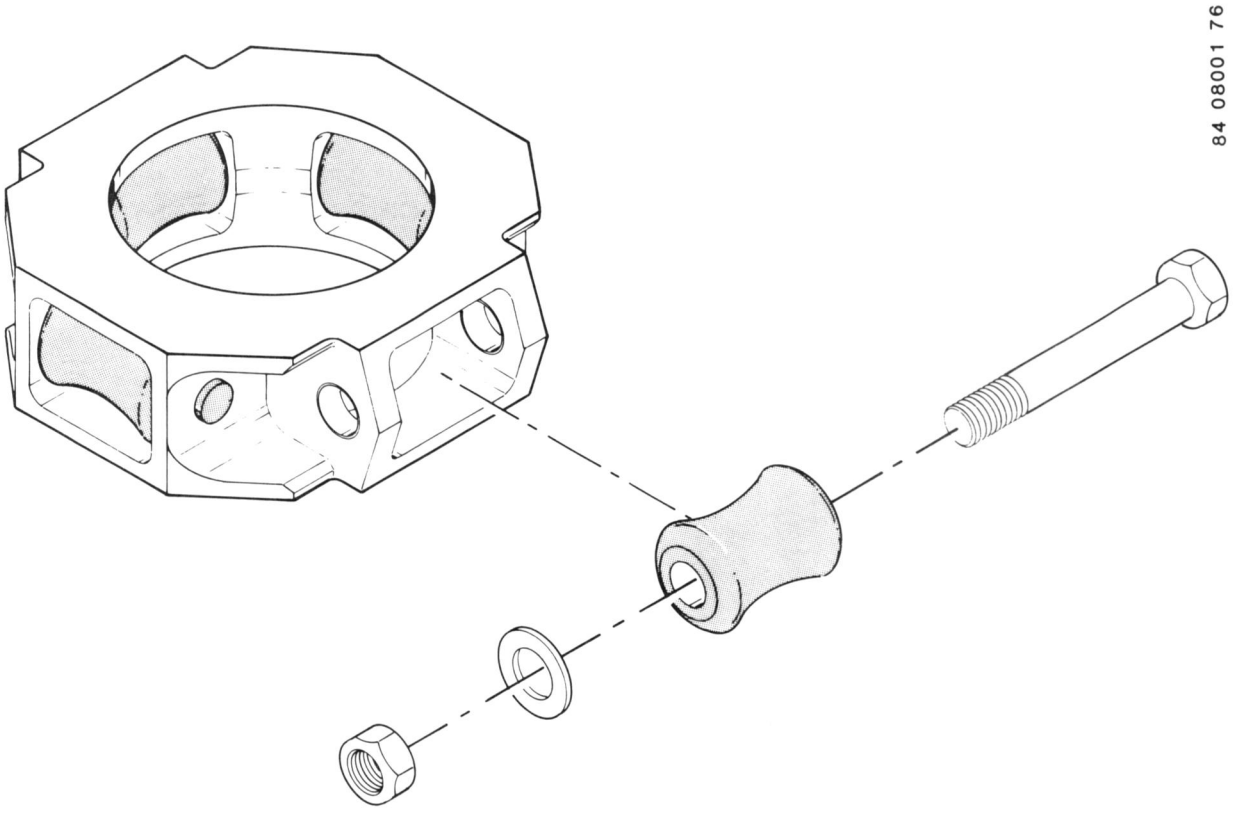

Figure 32. Bearing assembly, roller, and bolt from energy-absorbing seat.

TABLE 11. COMPARISON OF PEAK ACCELERATIONS MEASURED ON OPERATIONAL (F-111) AND ENERGY-ABSORBING (E/A) SEATS IN CAMI TESTS

NASA Test Number	CAMI Test Number	Seat	Peak Acceleration (G)			
			Seat Pan z	Seat Back Tangent Line	Pelvis z	Chest z
5	A83-111	F-111	26.9	28.2	34.4	33.4
	A83-109	E/A	22.2	24.3	25.8	24.0
	A84-83	E/A	22.9	23.4	27.5	27.1
6	A83-113	F-111	27.3	30.6	30.1	32.2
	A83-103	E/A	24.6	27.1	24.4	24.4
	A84-81	E/A	20.6	27.3	27.1	23.1
8	A83-112	F-111	23.1	22.0	32.6	30.6
	A83-101	E/A	21.3	22.0	23.7	23.3
	A84-82	E/A	21.3	19.9	26.3	22.5

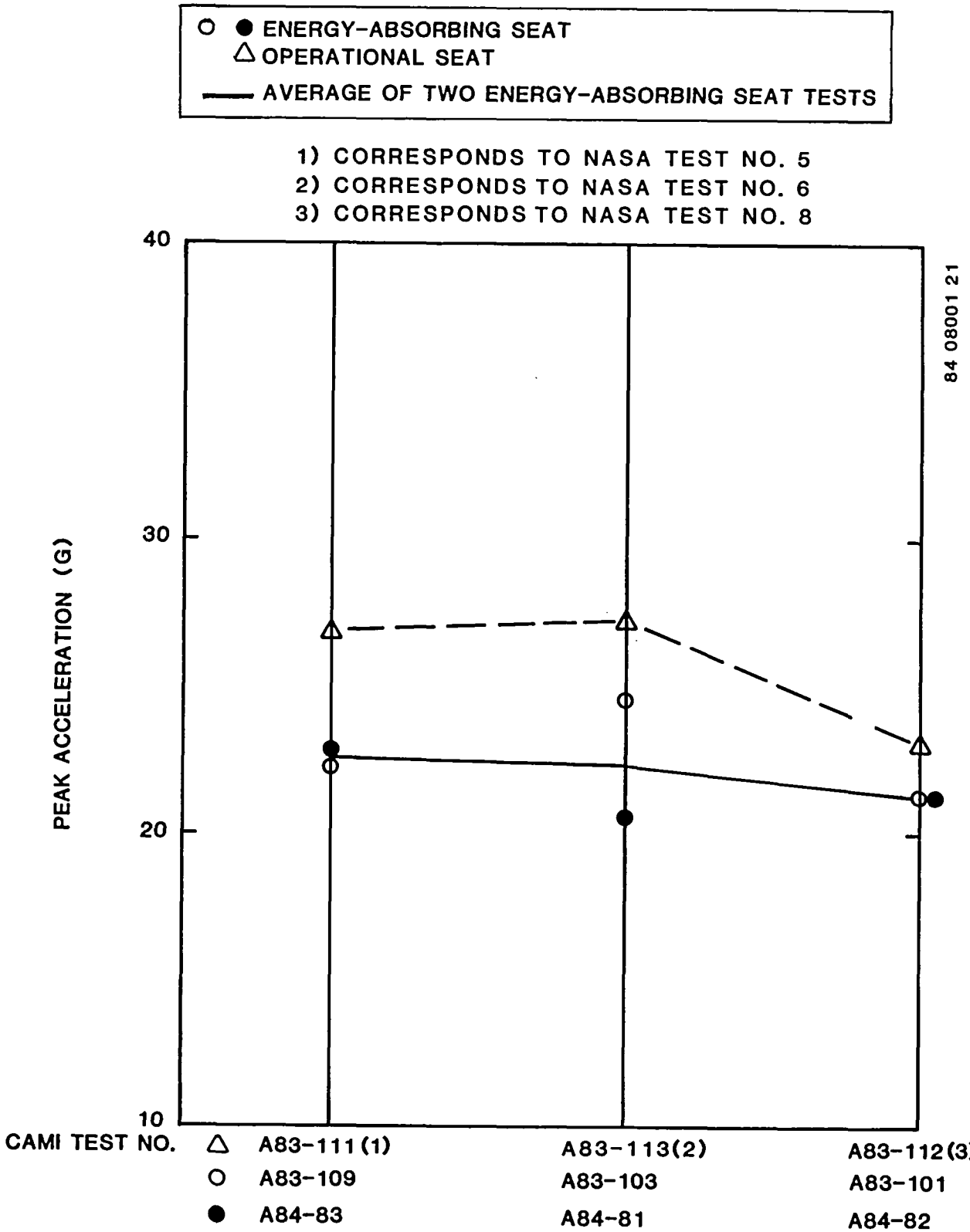

Figure 33. Seat pan z-axis acceleration levels from energy-absorbing and operational seat tests at CAMI.

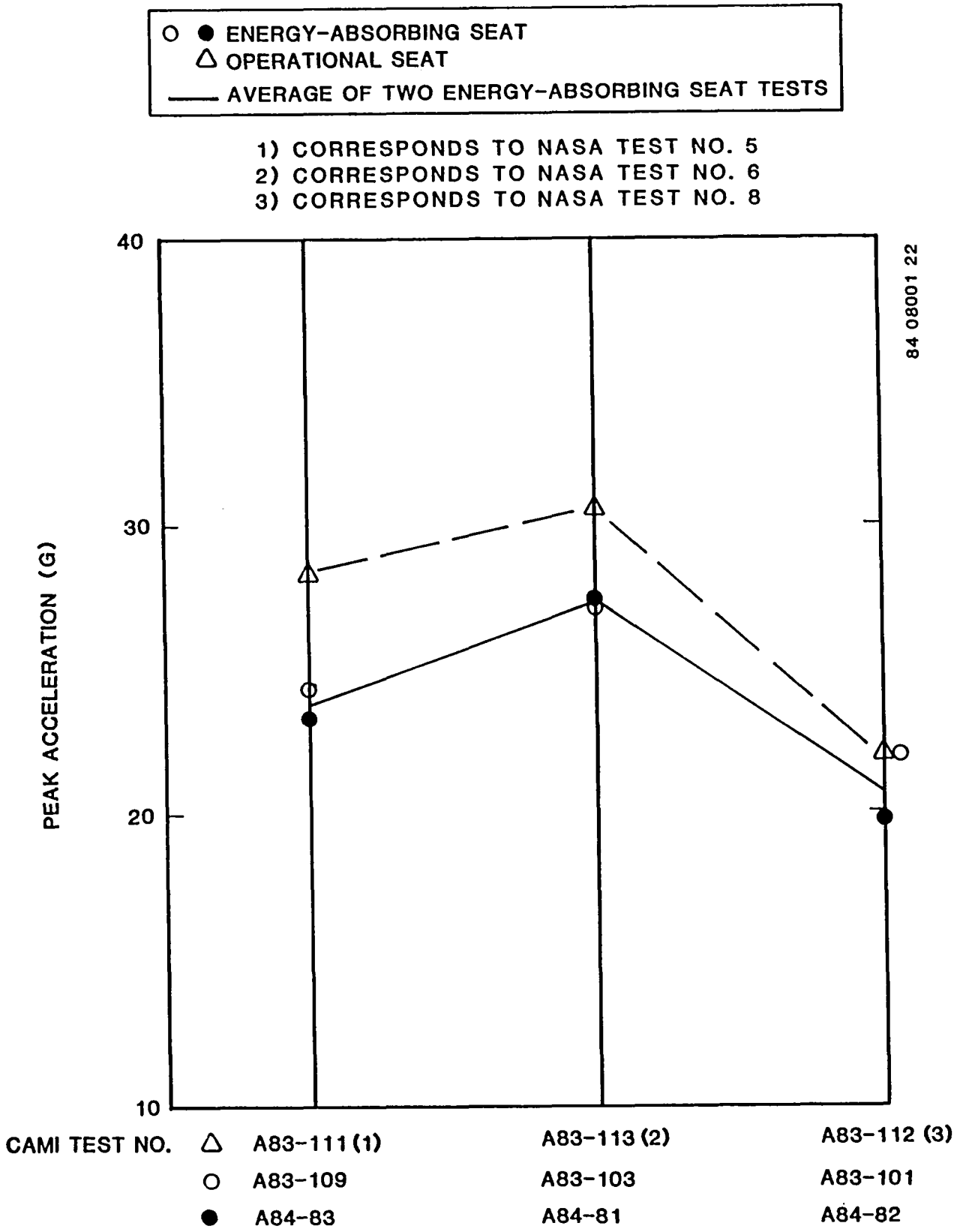

Figure 34. Peak acceleration levels along the seat back tangent line for energy-absorbing and operational seat tests at CAMI.

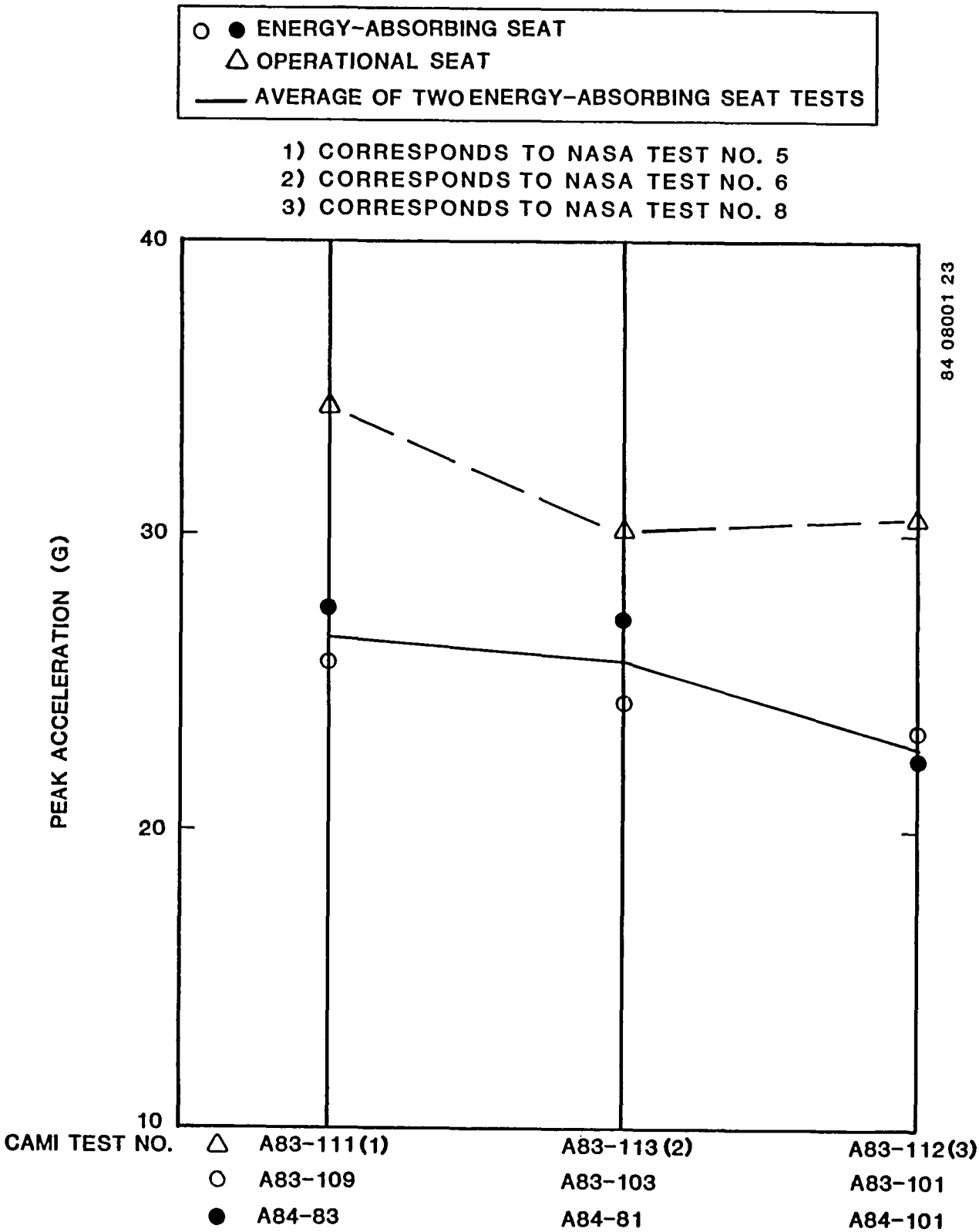

Figure 35. Dummy pelvis z-axis peak acceleration levels from energy-absorbing and operational seat tests at CAMI.

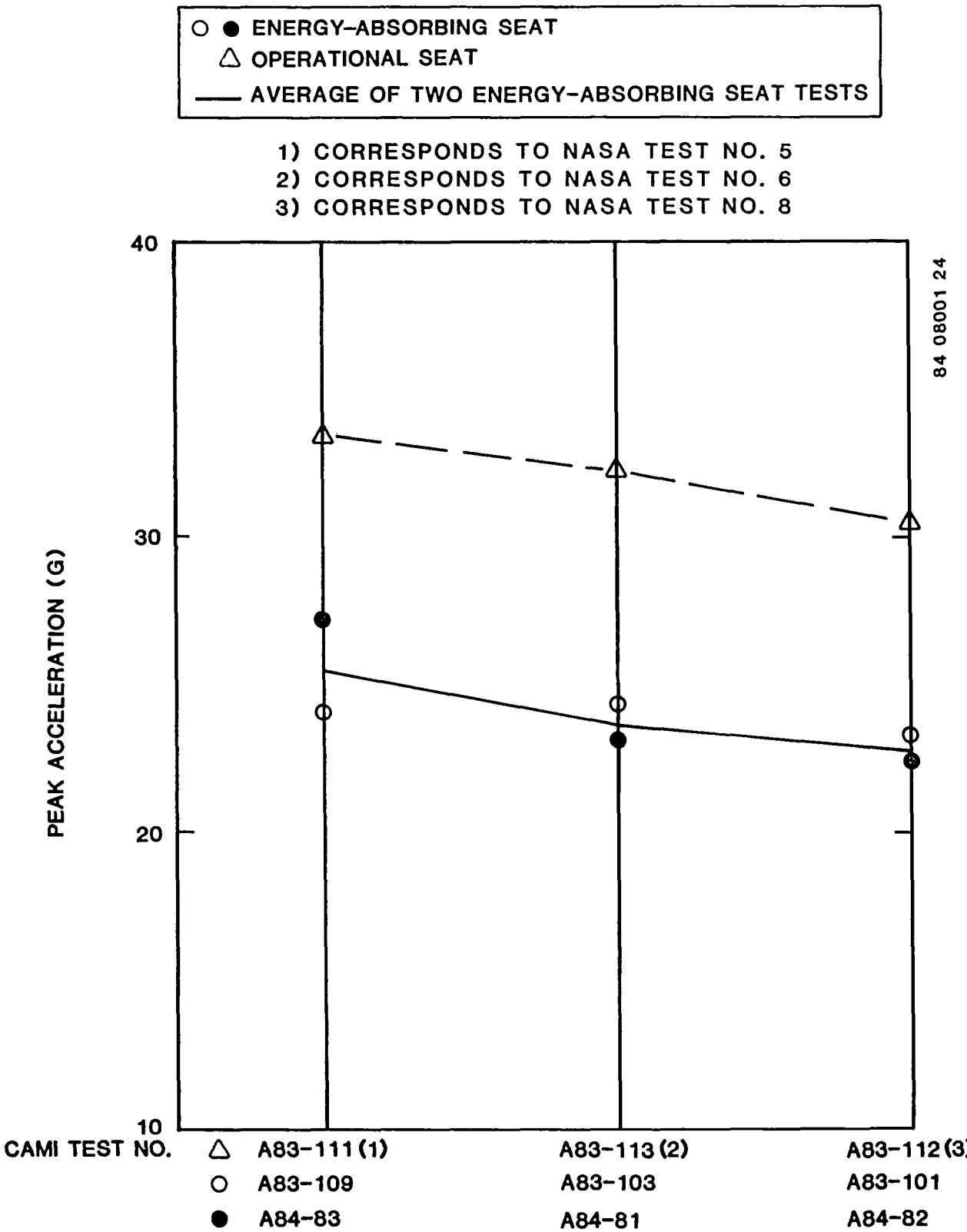

Figure 36. Dummy chest z-axis peak acceleration levels from energy-absorbing and operational seat tests at CAMI.

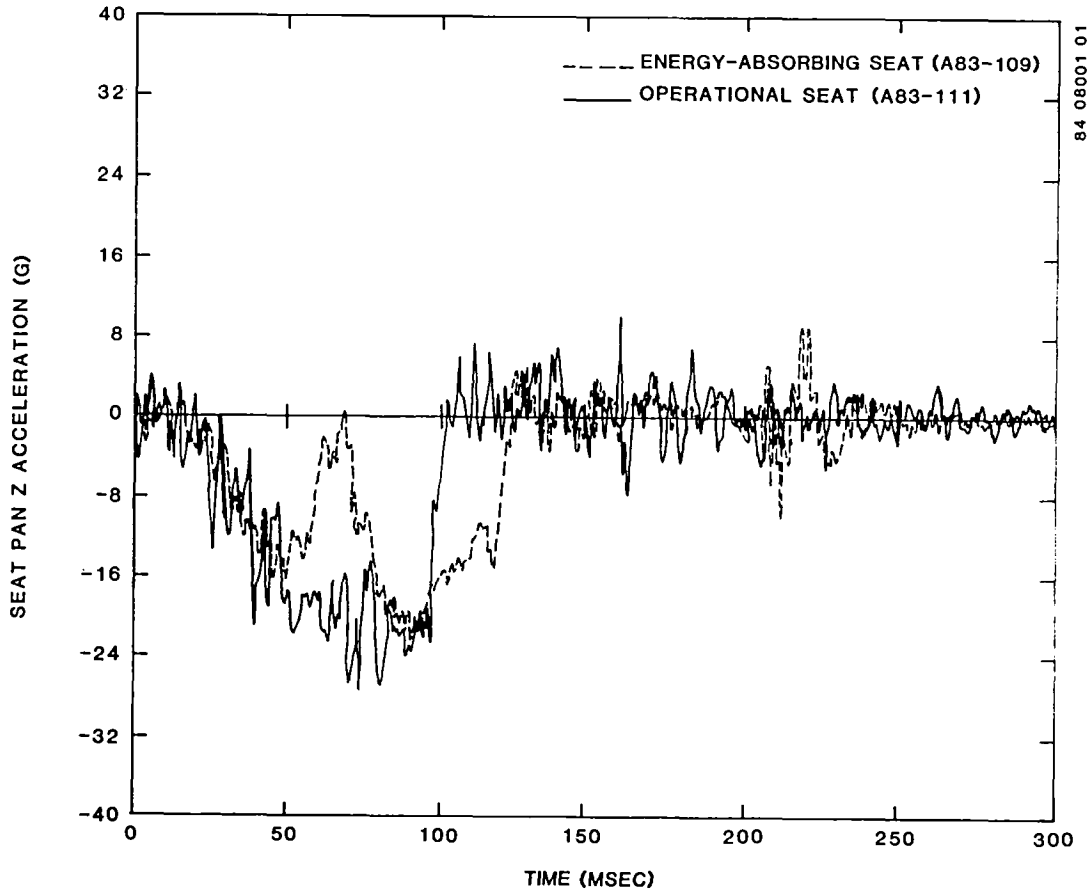

Figure 37. Seat pan z-axis accelerations for energy-absorbing and operational seats in similar tests corresponding to NASA Test No. 5.

The differences in the DRI are represented in Figures 40 through 42. Again, the DRI along the seat back tangent line in Test Number A84-81 is significantly higher than would be expected. The seat pan vertical and pelvis DRI's for the same test are consistent with the results of Test Number A83-103, which was conducted under the same conditions.

The durations spent above 23 G for the seat pan acceleration measurements are presented in Table 13. The only violation of the Eiband criterion is by the energy-absorbing seat in A84-81. However, the overall measurements are inconclusive in showing any differences between the two seats. Although these pulses were only an estimate of the capsule environment, it is interesting to note that the operational seat did not violate the Eiband criterion, although experience with the F-111 capsule shows the environment to be severe enough to cause spinal injuries.

3.4.2 Spinal Loads

The anthropomorphic dummy used in these tests had been previously modified to incorporate a six-axis load cell at the base of the lumbar spine. The installation of this load cell is described in Reference 16. The data gathered

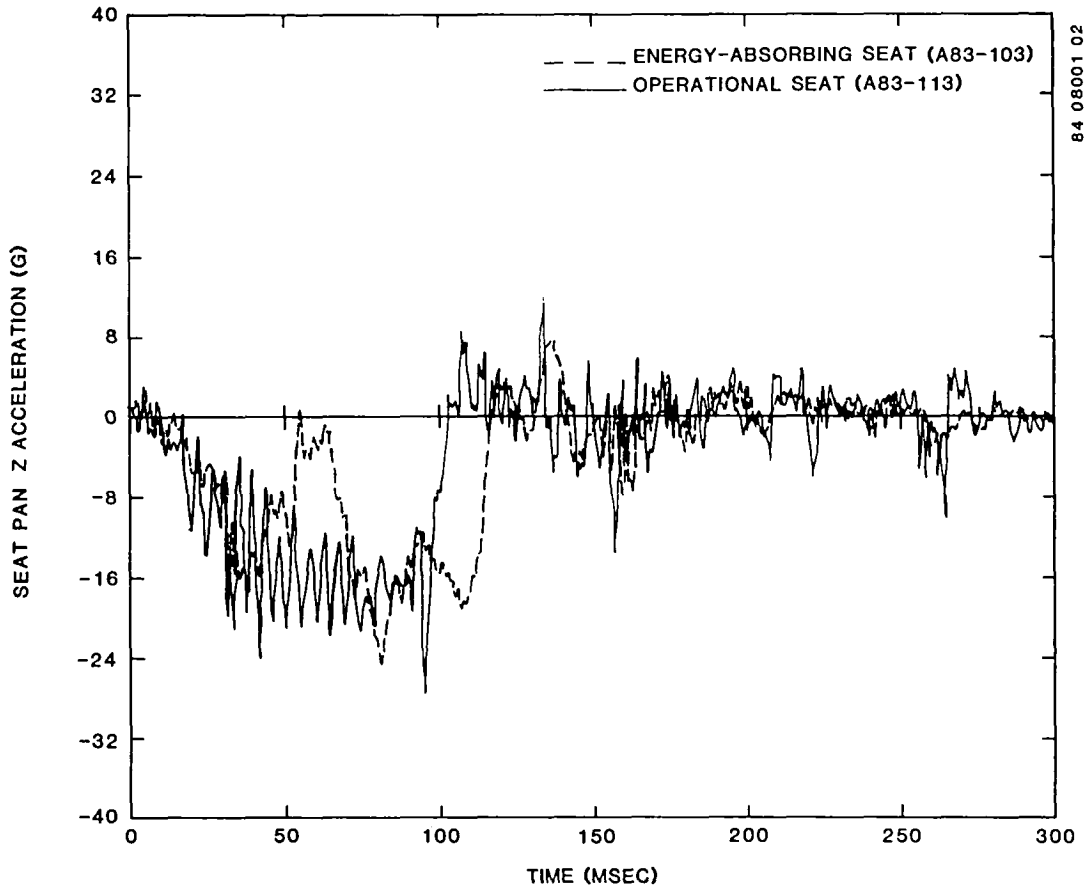

Figure 38. Seat pan z-axis accelerations for energy-absorbing and operational seats in similar tests corresponding to NASA Test No. 6.

through this dummy have not yet been correlated with an injury potential. However, the data gathered during this test series was consistent and reasonable. It is therefore being used as a comparative tool in examining differences between the energy-absorbing and operational seats. If the spinal loads and moments can be accurately and precisely measured, these values would be the best predictors of spinal injury potential.

Table 14 presents the lumbar measurements of both the z-axis peak load and the peak moment about the y-axis. These measurements were taken both during the original test series and after seat pan load cells had been added to the energy-absorbing seat. The spinal compression loads are consistently much less for the energy-absorbing seat: 1300 to 1500 lb when compared to 2000 to 2100 lb for the operational seat. Differences in the pitch-axis moments are not as dramatic, with a significant difference only being shown for the three CAMI tests with pure vertical loading, which corresponds to NASA Test Number 8. The CAMI tests which correspond to NASA Test Number 6 resulted in the seat being oriented on the sled in a pitch-up 40-degree condition. This combined forward and downward loading, as would be expected, produced the highest bending moments on the spine, but these peak moments did not occur at the same time as the peak compression loads. Figures 43a through 45a show the seat pan z-axis acceleration and the spinal z-force for the operational seat in all three tests.

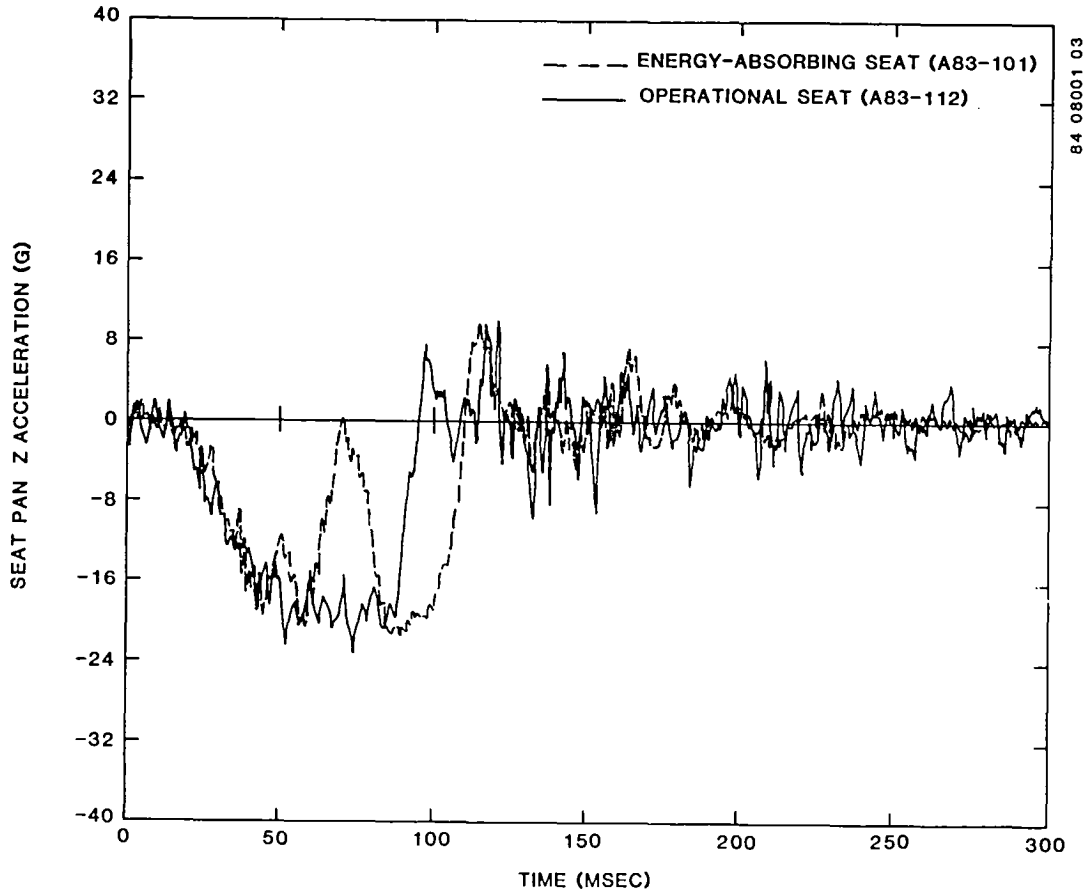

Figure 39. Seat pan z-axis accelerations for energy-absorbing and operational seats in similar tests corresponding to NASA Test No. 8.

One can see how the spinal loads continue to climb even after the vertical accelerations have leveled off around their peak value. Figures 43b and c through 45b and c show similar plots with the energy-absorbing seat. One can see that the spinal loads peak after the seat has started stroking, during the initial notch when the acceleration levels have dropped down to about zero. However, the stroking of the seat prevents the spinal compression loads from rising to as high a value as they did in the operational seat.

These traces also emphasize a point made earlier about problems with Eiband evaluation traces. The peaks in spinal load occur at minimum values of seat pan acceleration, while the Eiband evaluation uses the acceleration peaks to determine the severity of the pulse.

3.4.3 Seat Pan Loads

The modification that added seat pan load cells to the operational seat and energy-absorbing seat is described in Section 2.4. The load cells measured only the vertical loads applied downward from the bottom of the seat pan. The maximum measurements recorded from each load cell, as well as the maximum summation of the three load cells at one time, are listed in Table 15. Total loads for the energy-absorbing seat were much less than the operational seat by amounts ranging from 1000 to 2200 lb.

TABLE 12. COMPARISON OF DYNAMIC RESPONSE INDEX MEASUREMENTS FOR OPERATIONAL (F-111) AND ENERGY-ABSORBING (E/A) SEATS IN CAMI TESTS

NASA Test Number	CAMI Test Number	Seat	Dynamic Response Index		
			Seat Pan z	Seat Back Tangent Line	Pelvis z
5	A83-111	F-111	29.1	30.4	37.3
	A83-109	E/A	18.2	20.7	24.6
	A84-83	E/A	18.1	19.9	22.5
6	A83-113	F-111	23.4	28.1	35.1
	A83-103	E/A	17.6	21.6	24.9
	A84-81	E/A	17.0	26.1	24.5
8	A83-112	F-111	26.5	25.9	34.0
	A83-101	E/A	18.6	18.4	24.2
	A84-82	E/A	17.2	16.2	23.7

Two things should be noted while evaluating these data. First, no tare tests were conducted. Such a test would have sent the seat down the track without an occupant, and due to the inertial loading of the seat pan, the load cell readings could have been recorded. These values could then have been subtracted from the readings taken during a test with the occupant. The result would have been the load applied to the seat pan by the occupant. This would be somewhat less than the loads listed in Table 15, which were measured at the bottom of the seat pan. Secondly, as presented in Section 2.4, there was some difference in the weights of the operational F-111 and the energy-absorbing seat pans. This 3.35-lb difference will affect the loads measured at the bottom of the seat pans. Thus, if tare tests had been conducted, there would have been a difference in the seat pan inertial loads recorded for the two seats. Due to its higher weight, the operational seat would record higher inertial loads. However, since the maximum accelerations measured were on the order of 30 G, the maximum difference in the inertial loads can be estimated to be approximately 100 lb. Even using this value as an adjustment to the loads measured, the data still show that the vertical loads experienced by the occupant in the operational seat were much higher than those experienced in the energy-absorbing seat during a similar test.

The difference in the total loads recorded while simulating NASA Test Number 6 is not as great as in the other two test conditions. The loads applied to the seat pan are a function of both the test pulse and the seat orientation.

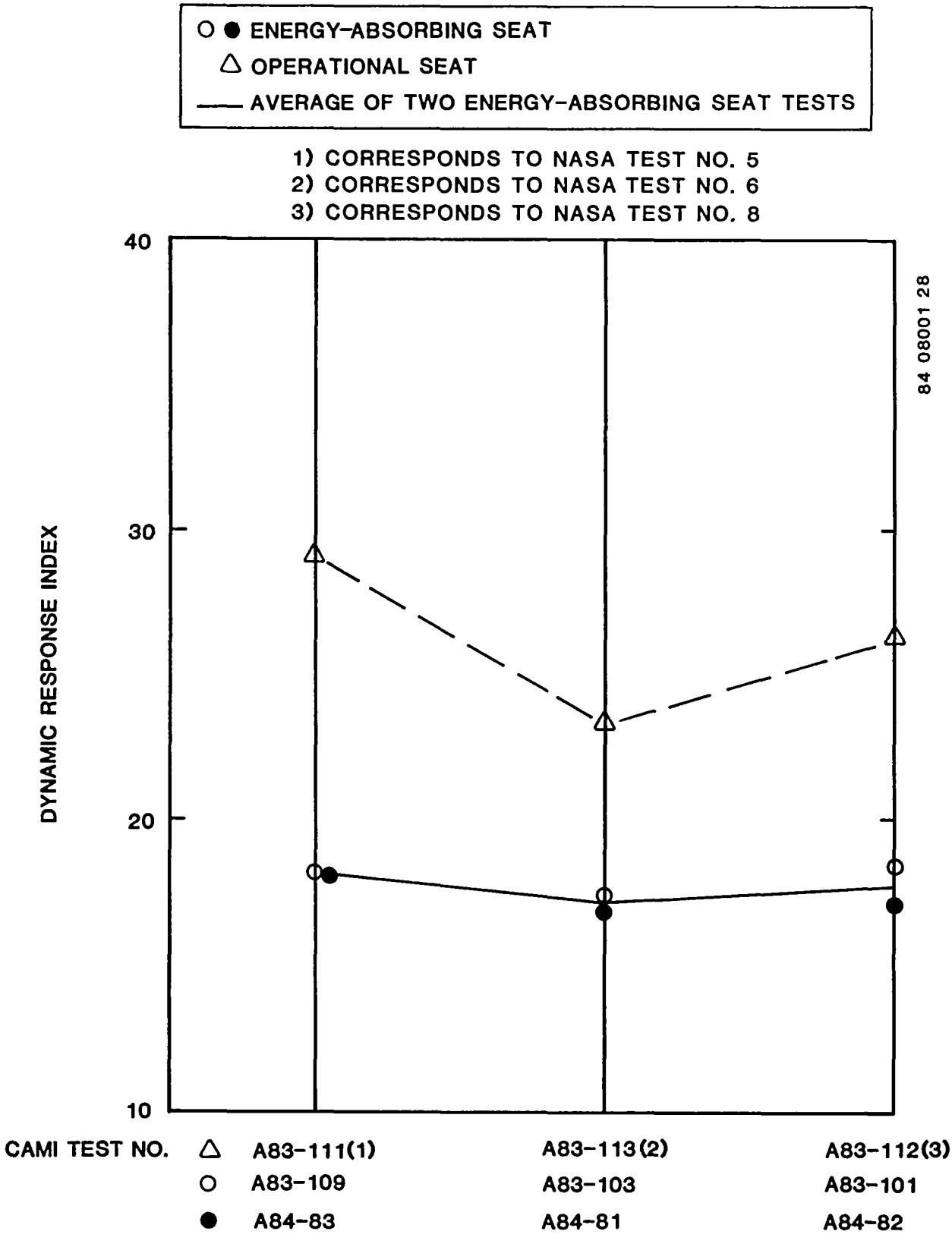

Figure 40. Dynamic Response Index determined from seat pan z-axis accelerations in CAMI tests.

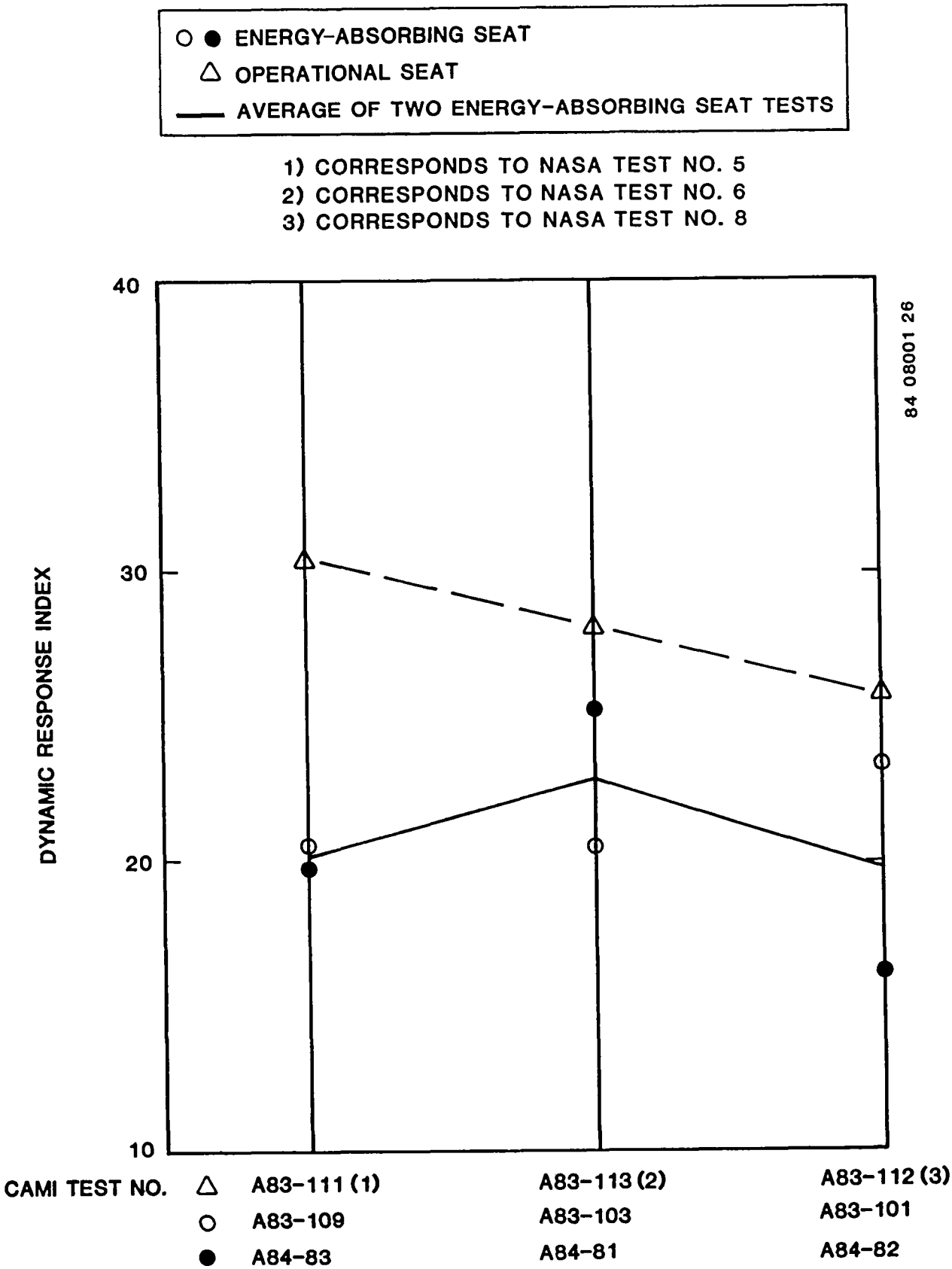

Figure 41. Dynamic Response Index determined from seat back tangent line accelerations in CAMI tests.

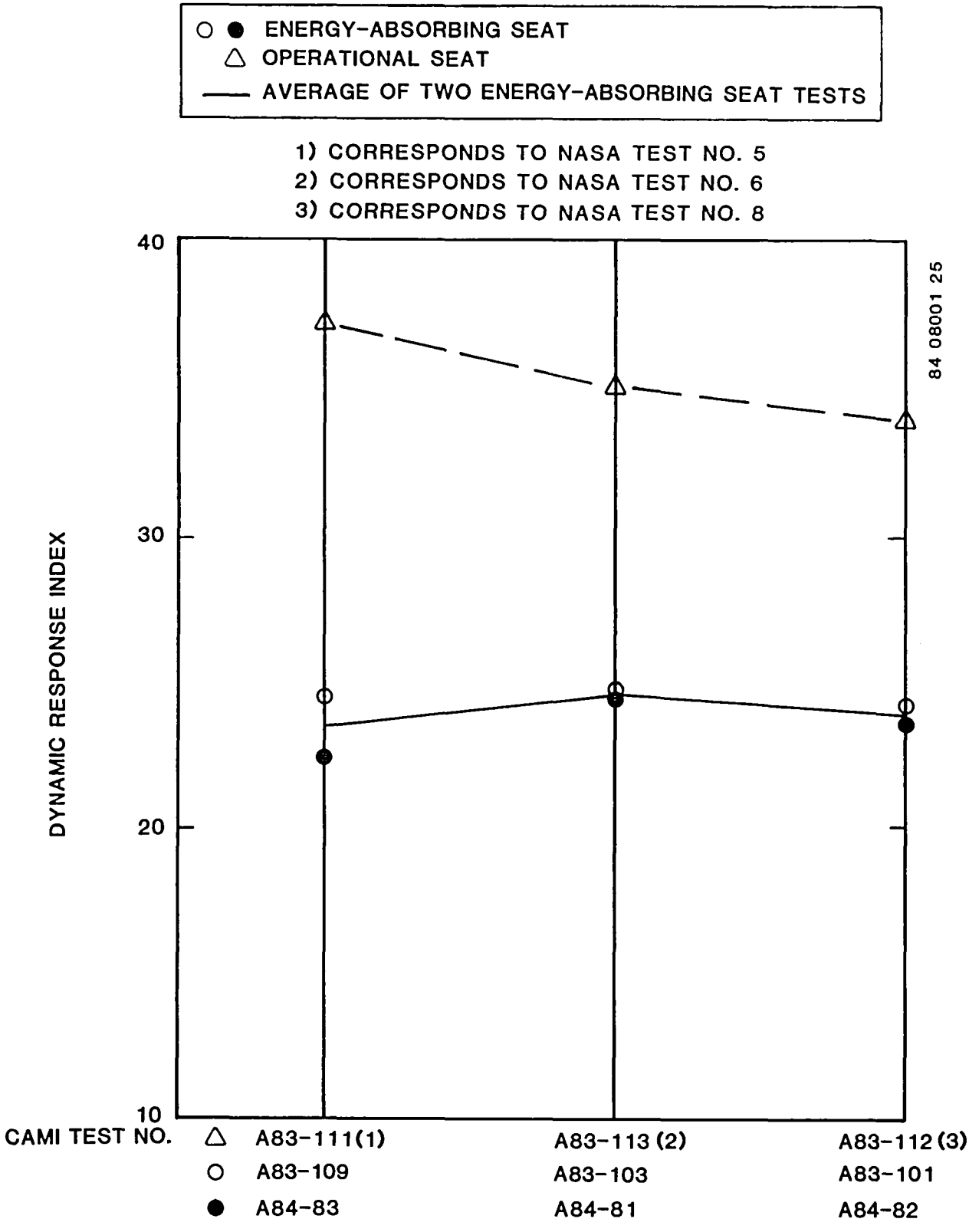

Figure 42. Dynamic Response Index determined from dummy pelvis z-axis accelerations in CAMI tests.

TABLE 13. COMPARISON OF EIBAND MEASUREMENTS FOR OPERATIONAL (F-111) AND ENERGY-ABSORBING (E/A) SEATS IN CAMI TESTS

NASA Test Number	CAMI Test Number	Seat	Duration Above 23 G (sec)	
			Seat Pan z	Seat Back Tangent Line
5	A83-111	F-111	.005(1)	.005(2)
	A83-109	E/A	0	.004
	A84-83	E/A	0	.002
6	A83-113	F-111	.002	.003(2)
	A83-103	E/A	.002	.006
	A84-81	E/A	0	.017
8	A83-112	F-111	0	0
	A83-101	E/A	0	0
	A84-82	E/A	0	0

(1) Longest duration of three spikes over 23 G.
(2) Longest duration of several spikes over 23 G.

In CAMI tests A83-113 and A84-81 that simulated NASA Test Number 6, the seat was pitched up on the sled only 40 degrees, as shown previously in Figure 22. In this orientation a significant inertial load is carried through the legs into the footrest structure. The peak footrest z-axis loads for all six tests of interest are presented in Table 16. With the energy-absorbing seat, the seat pan loads are limited independent of the footrest loads. Thus, the total inertial loads measured on the seat pan in CAMI tests that simulated NASA Test Number 6 are not very different from those measured in tests simulating NASA Test Numbers 5 and 8, where the seat was pitched 70 and 90 degrees, respectively. However, since the operational seat does not limit the loads applied to the seat pan, the seat pan loads are dependent on the proportion of the total load carried by the footrest. Therefore, under test conditions where a high percentage of the vertical load is supported by the footrest, the difference between seat pan loads measured on an energy-absorbing seat and an operational seat will not be as great as under seat orientations where the footrest carries less load. Of course, the test conditions must be severe enough to cause seat stroke for there to be any difference in the seat pan loads.

Figures 46 through 48 show plots of the center seat pan load cell force and the spinal z-axis force on the same plot. While there is some phase difference, which should be expected, the seat pan force and spinal force show the

TABLE 14. LUMBAR LOAD CELL MEASUREMENTS FOR OPERATIONAL (F-111) AND ENERGY-ABSORBING (E/A) SEATS IN CAMI TESTS

NASA Test Number	CAMI Test Number	Test Seat	Maximum Spinal Load Cell Measurements	
			Z-Axis Load (lb)	Y-Axis Moment (in.-lb)
5	A83-111	F-111	2162	979
	A83-109	E/A	1436	1000
	A84-83	E/A	1527	560
6	A83-113	F-111	1992	1870(1)
	A83-103	E/A	1476	1795(1)
	A84-81	E/A	1365	1916(1)
8	A83-112	F-111	2049	951
	A83-101	E/A	1364	631
	A84-82	E/A	1240	333

(1) Peak moment occurred significantly after peak axial load.

same characteristics. While on the operational seat the loads climb to a single high value, with the energy-absorbing seat there are two smaller peaks. The first peak occurs after the seat starts stroking and when the seat pan accelerations drop to approximately 0, the initial notch. The second peak load occurs after the secondary peak on the seat pan accelerations. During the same time, loads in the dummy and seat pan of the operational seat climb to a much higher single peak. This illustrates how an energy-absorbing seat limits the loads experienced by the occupant.

3.4.4 Conclusions

Several conclusions can be made from the presented data:

- In every case, peak acceleration levels measured for the seat pan, pelvis, and chest z-axes, as well as seat pan accelerations along the seat back tangent line, were lower on the energy-absorbing seat.
- DRI values for the energy-absorbing seat were consistently 6 to 10 points lower than for the operational seat.

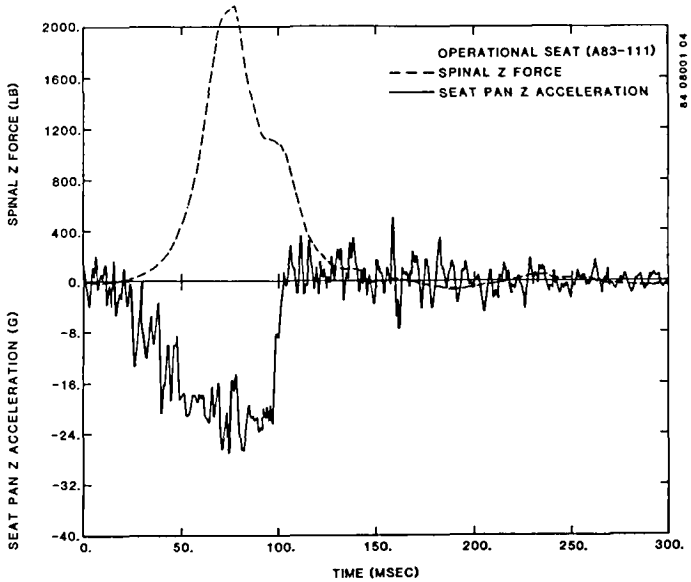

a. Operational seat

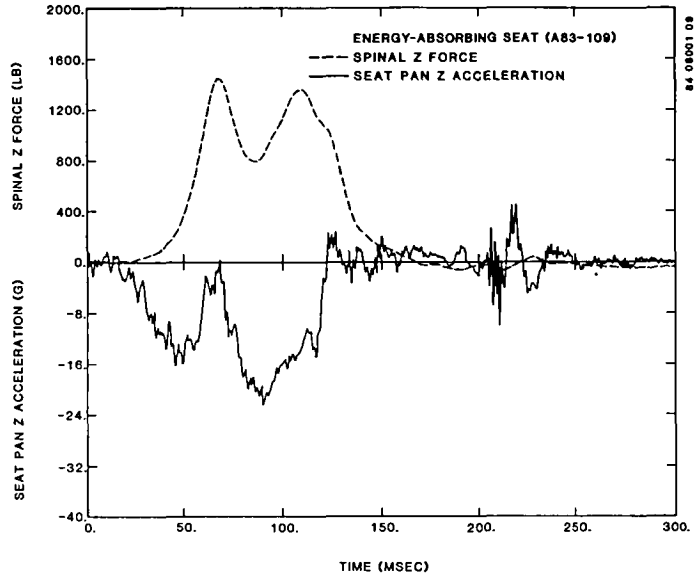

b. Energy-absorbing seat

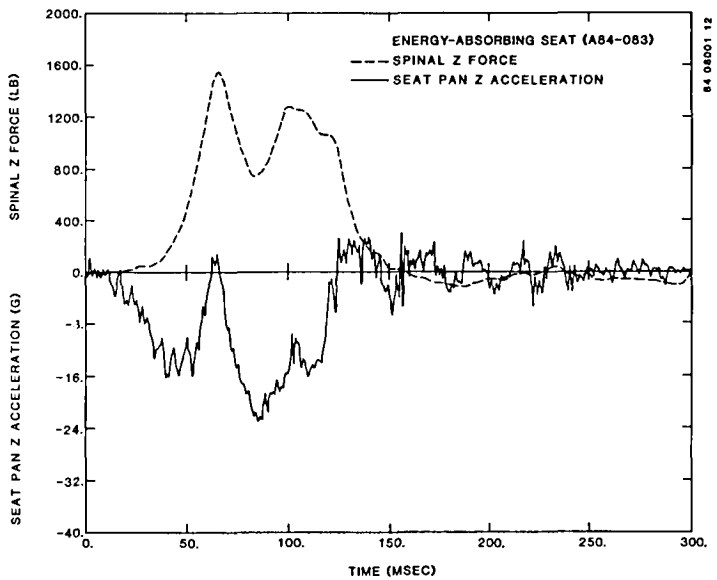

c. Energy-absorbing seat

Figure 43. Seat pan z-axis accelerations and spinal compression loads for CAMI tests corresponding to NASA Test Number 5.

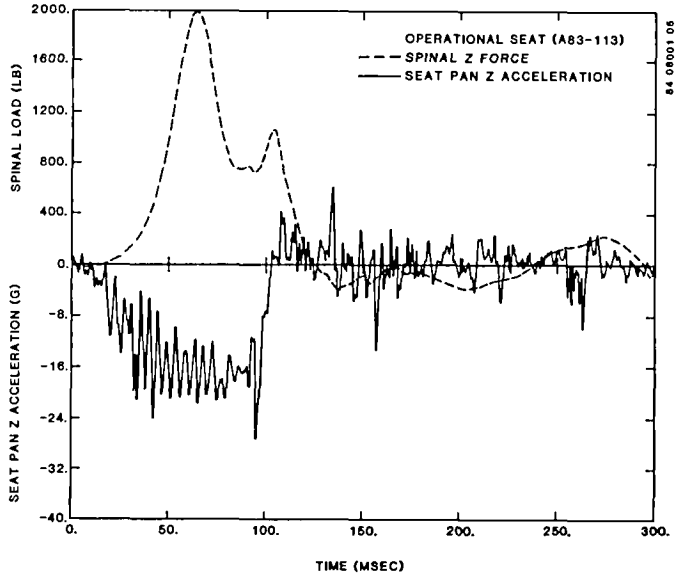

a. Operational seat

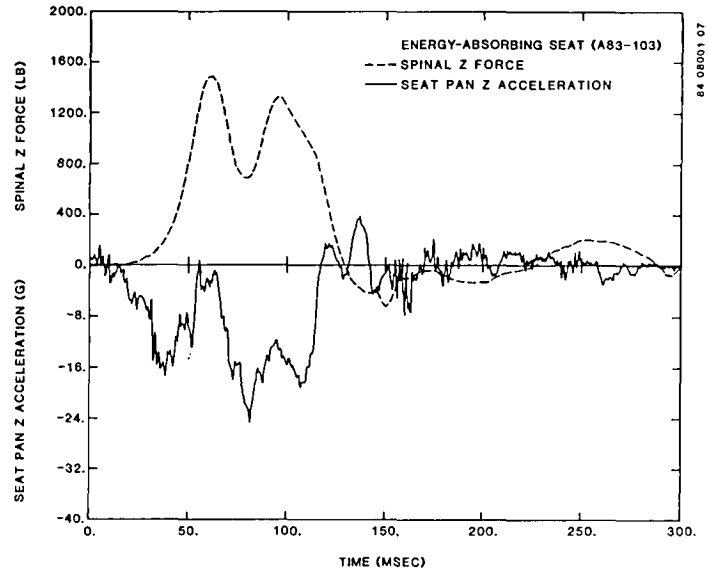

b. Energy-absorbing seat

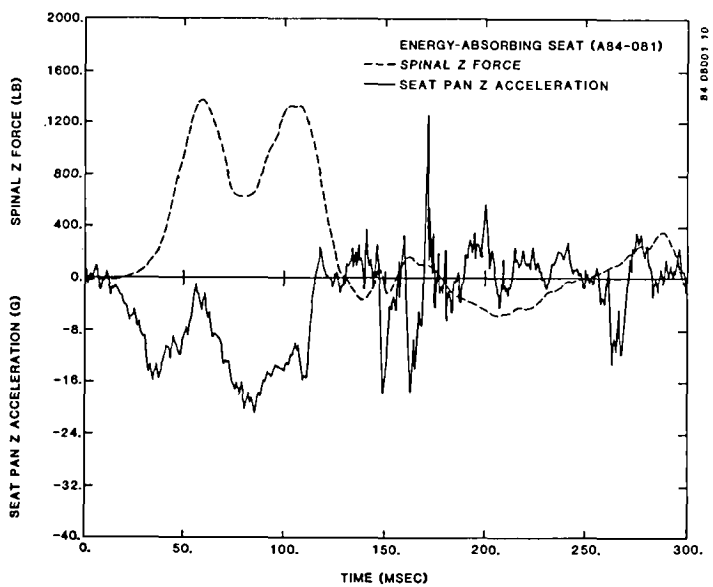

c. Energy-absorbing seat

Figure 44. Seat pan z-axis accelerations and spinal compression loads for CAMI tests corresponding to NASA Test Number 6.

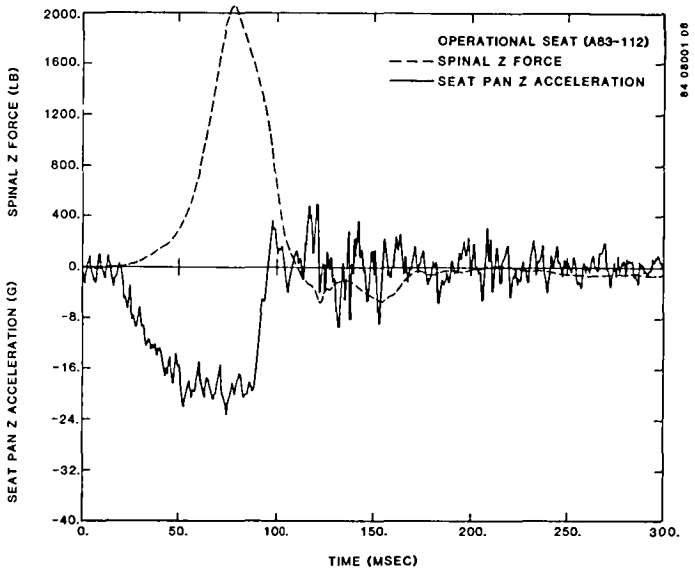

a. Operational seat

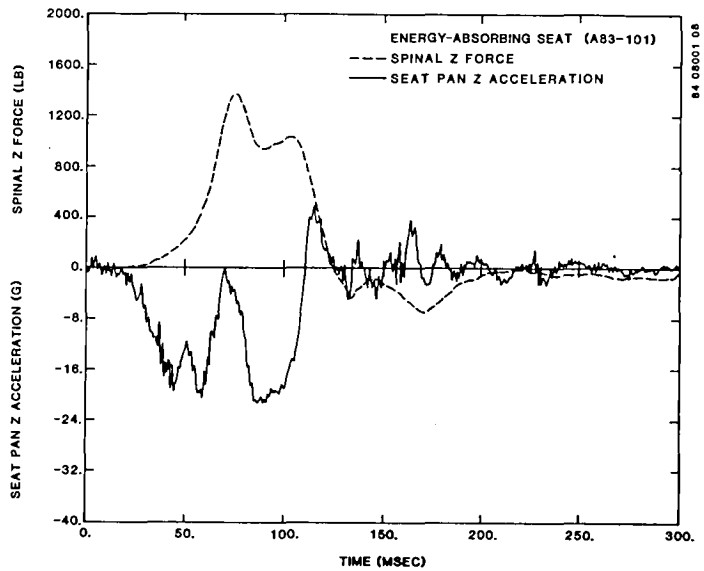

b. Energy-absorbing seat

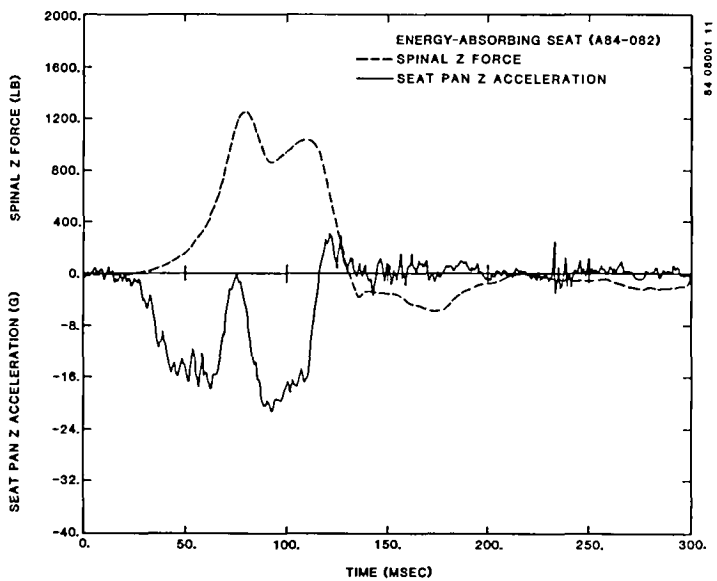

c. Energy-absorbing seat

Figure 45. Seat pan z-axis accelerations and spinal compression loads for CAMI tests corresponding to NASA Test Number 8.

TABLE 15. SEAT PAN LOAD CELL MEASUREMENTS FOR OPERATIONAL (F-111) AND E/A SEATS (E/A)

NASA Test Number	CAMI Test Number	Seat	Maximum Seat Pan Load Cell Measurements (lb)			
			Center	Left	Right	Summation
5	A83-111	F-111	2319	229	2822	4830
	A84-83	E/A	1121	320	1408	2626
6	A83-113	F-111	1600	922	1355	3650
	A84-81	E/A	1272	675	802	2611
8	A83-112	F-111	1995	1164	1647	4750
	A84-82	E/A	1229	965	1029	2892

TABLE 16. PEAK VERTICAL FOOTREST LOADS MEASURED IN CAMI TESTS

NASA Test Number	CAMI Test Number	Seat	Footrest Peak Load (lb)
5	A83-111	F-111	1573
	A83-109	E/A	1969
	A84-83	E/A	1221
6	A83-113	F-111	2647
	A83-103	E/A	2661
	A84-81	E/A	2687
8	A83-112	F-111	1020
	A83-101	E/A	1528
	A84-82	E/A	852

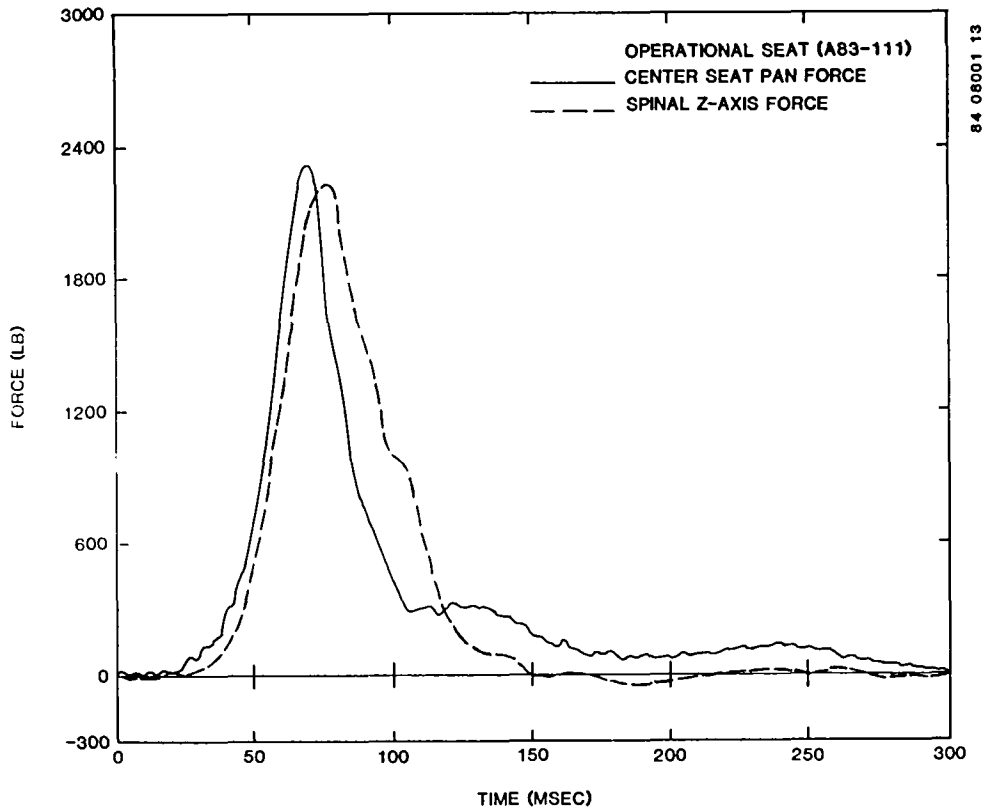

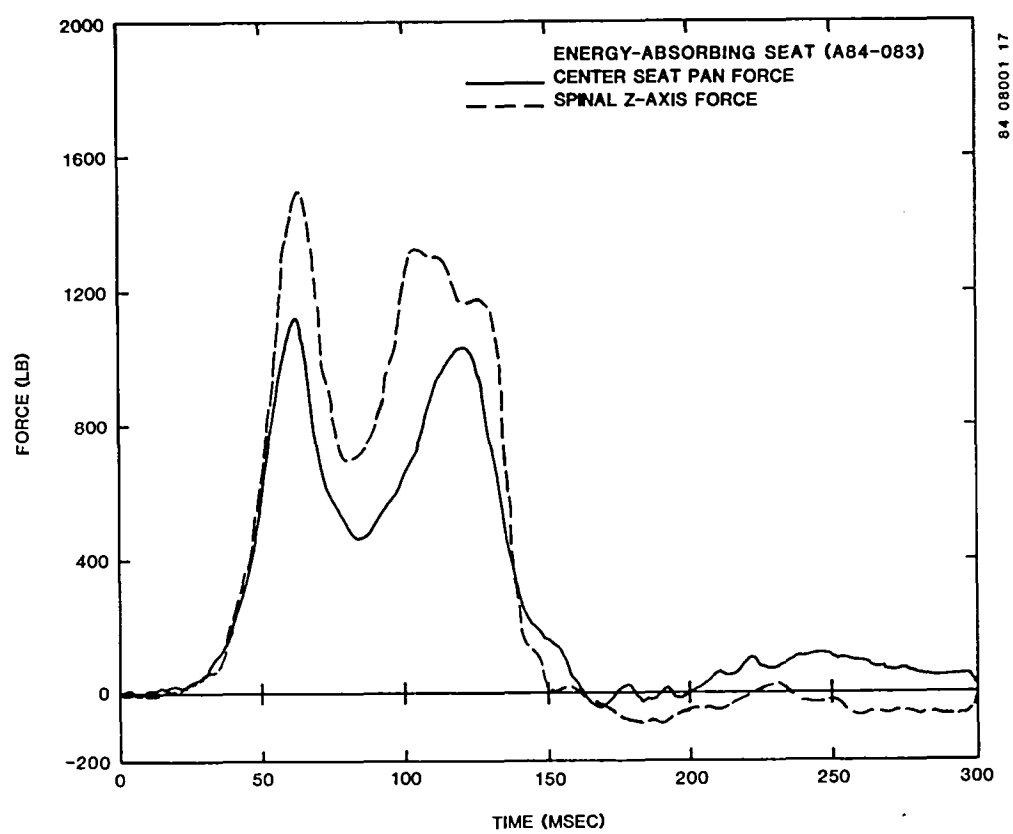

Figure 46. Dummy spinal compression and center seat pan vertical loads in CAMI tests corresponding to NASA Test Number 5.

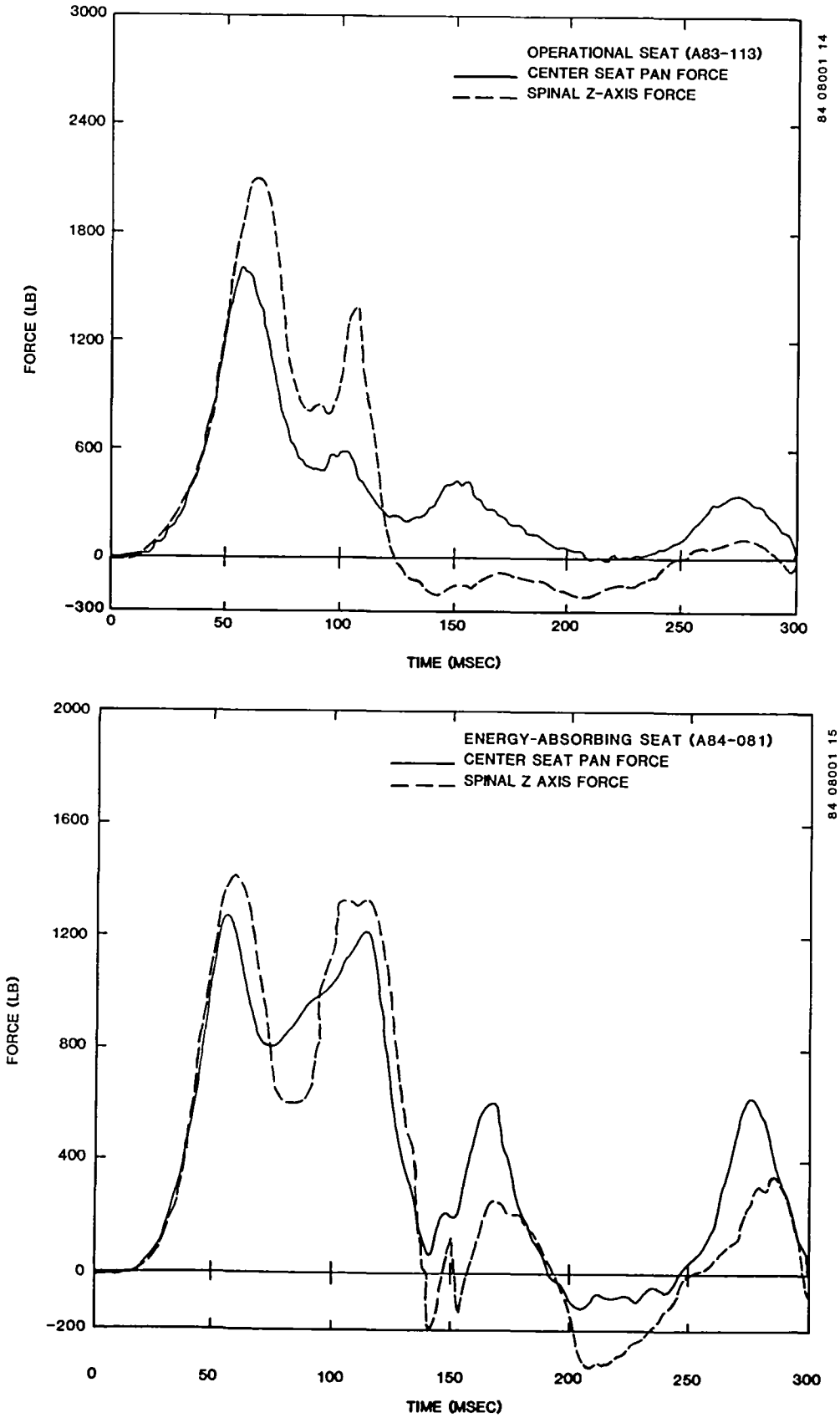

Figure 47. Dummy spinal compression loads and center seat pan vertical loads in CAMI tests corresponding to NASA Test No. 6.

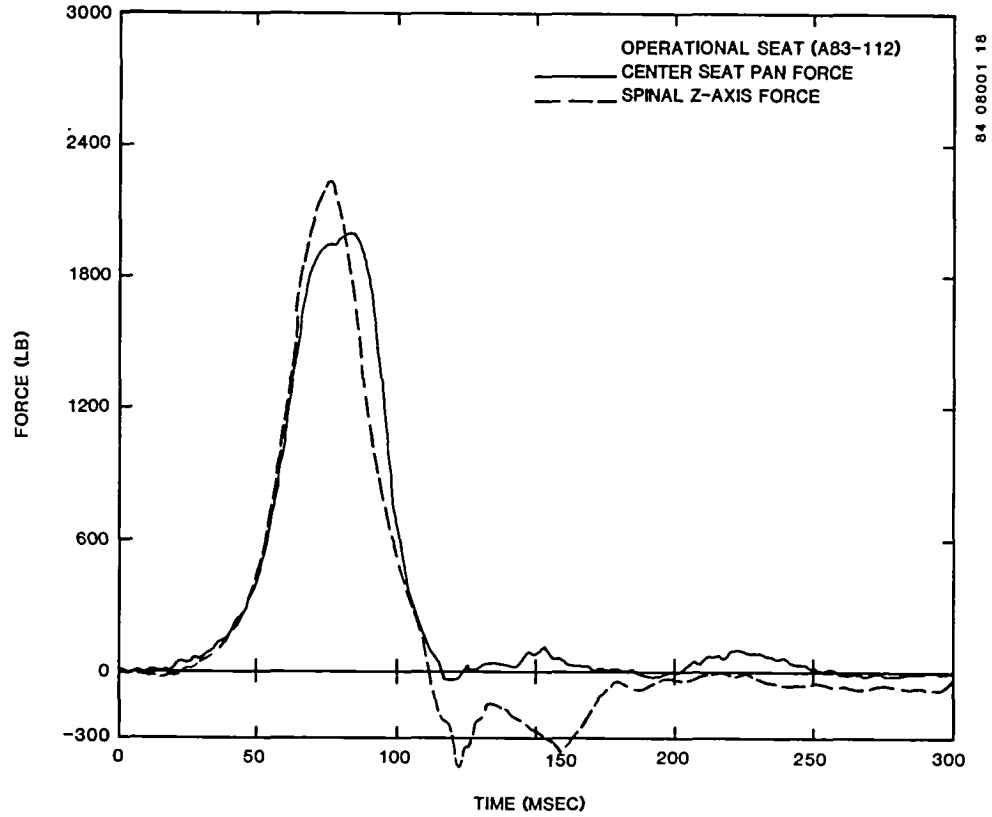

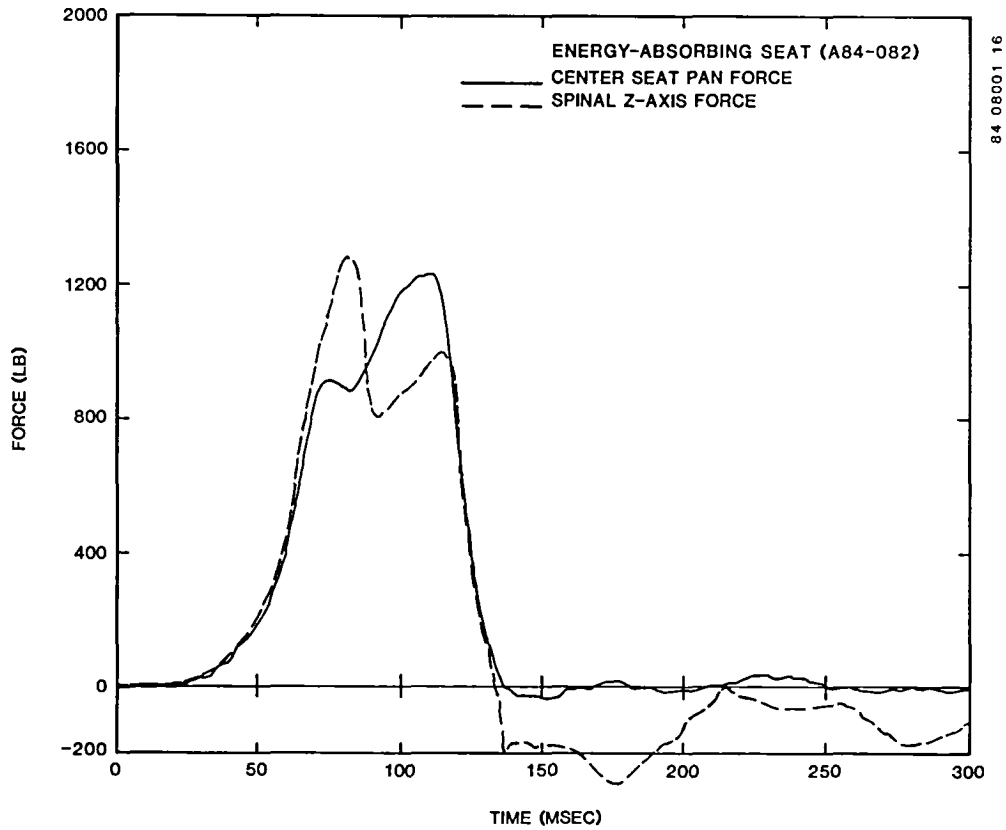

Figure 48. Dummy spinal compression loads and center seat pan vertical loads in CAMI tests corresponding to NASA Test No. 8.

- The acceleration pulses did not cause the operational seat to violate the Eiband criterion, even though the tests attempted to simulate an environment that field experience has proven to be severe.

- The average z-axis spinal load measured for the operational seat was 2070 lb; for the energy-absorbing seat it was 1400 lb (32 percent less).

- Using the equation:

$$\% = 1 - \frac{LOAD_{E/A} + 100}{LOAD_{Oper}} \times 100 \text{ percent,}$$

  The total seat pan vertical loads for the energy-absorbing seat were 25 to 44 percent lower than for the operational seat.

The 100 lb is simply a factor to take into account the difference in the seat pan weights for the operational and energy-absorbing seats. Since the 100 lb is based on the maximum values of the acceleration measured, and the loads actually peak at lower acceleration values, the actual factor is less than 100 lb. Accordingly, the differences in the energy-absorbing and operational seat pan loads would be slightly larger than calculated in the above equation, but not as large as the differences calculated if no adjustment factor were used.

4.0 CAPSULE TESTING

Dynamic testing of the Simula energy-absorbing seat and the operational F-111 seat in an F-111 capsule was conducted in April and May 1984 at NASA Langley Research Center, Hampton, Virginia.

4.1 TEST OBJECTIVES

The primary objective of this test series was to evaluate the performance of the energy-absorbing seat over the full range of ground impact conditions. Thus, it was necessary to make three main determinations:

- Determine the environment to which the occupant is subjected in the energy-absorbing seat. Accelerometers were placed at various locations on the capsule, on the seat, and in the anthropomorphic dummy.

- Determine if there was enough room for the vertical energy-absorbing stroke necessary to limit the spinal loads to non-injurious levels. For this purpose, the stroke was measured in each of the tests.

- Determine if the capsule bulkhead structure was strong enough to withstand the loads imposed by the energy-absorbing seat. Overall, the loads applied to the bulkhead by the energy-absorbing seat would be less than the loads applied by the operational seat. However, the energy-absorbing seat is attached to the bulkhead in a different location. Therefore, the bulkhead modification used to attach the test seat carried the loads to the same structure that the retrofit seat would carry the loads.

To satisfy all these objectives, testing was required over the full range of design ground impact conditions.

There were some other secondary objectives to be examined during the test series. This included gaining some additional comparative information on the operational and energy-absorbing seats. Seat pan load cell measurements, as well as the previously mentioned accelerometer measurements, were also used at NASA for this purpose. Another objective concerned reducing the severity of the ground impact environment by reducing the vertical descent rate of the capsule. The U.S. Air Force is presently considering replacing the existing parachute with one that would reduce the vertical descent rate from 32 to 25 ft/sec. In order to briefly examine the performance of the energy-absorbing seat under these conditions, some pure vertical tests were conducted at a reduced vertical velocity.

4.2 CONDUCT OF TESTING

4.2.1 Test Facility

All capsule testing in the program was conducted at the NASA Langley Impact Dynamics Research Facility. Capsule swing tests requiring both horizontal and vertical velocities were conducted under the gantry shown in Figure 49. The gantry is 240 ft high, 400 ft long, and has a movable bridge that can traverse the length of the gantry at the 217-ft height. Also visible in

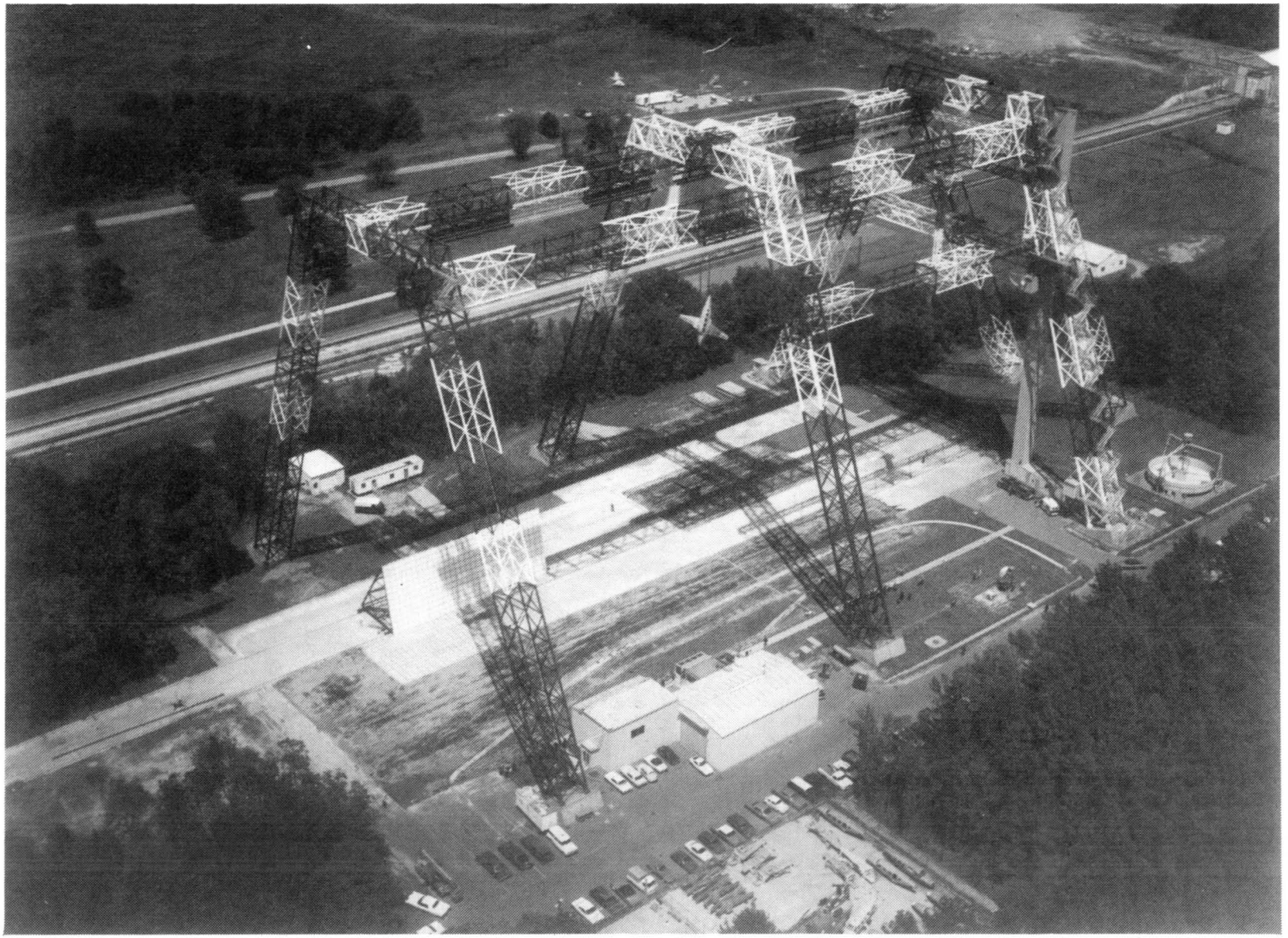

Figure 49. Impact Dynamics Research Facility at NASA Langley Research Center (Reference 17).

the figure, under the southwest quadrant of the gantry, is the control room, from which all operations are directed during tests. Along the centerline beneath the gantry is a strip of reinforced concrete. During the F-111 capsule testing the landing area on this concrete was covered with soil. Visible just north of the concrete runway is the photographic backboard that was painted with a 1-meter reference grid.

Pure vertical tests were conducted at the drop tower shown in Figure 50. This is located at the northwest corner of the gantry.

4.2.2 Test Methods

4.2.2.1 Test Procedure. All capsule testing started with proper outfitting of the capsule. This included four main items: IAB, various instrumentation devices, capsule hard points, and seats with anthropomorphic dummies.

A new IAB was used for each test. For the drops with a vertical descent rate of 32 ft/sec, the IAB that is presently installed on all F-111 aircraft was used. For the pure vertical tests at 25 ft/sec, special IAB's, modified to account for the reduced descent rate, were used.

During the capsule outfitting, certain preparations for the instrumentation were made. This included installation of a new power supply, examination of the accelerometer mounts on the bulkhead and seat, and electronic checkout of any instrumentation suspected of improper functioning. A complete list of the instrumentation used is in Section 4.2.2.2.

Relocating some structure that provided capsule hard points was necessary prior to most of the swing tests. These capsule hard points were used to support the capsule from cables that controlled the aircraft's pitch, roll, and yaw orientations during a test. Some of the hardware used is visible in Figures 51 and 52.

Prior to each test the seats were examined for any damage and prepared for the next test. This preparation included examination of the roller bearing assemblies; in some cases, bolts that had been scored and or the rollers themselves were replaced to insure that the energy-absorbing system loads were consistent for all tests. Energy absorbers that showed any stroke were replaced prior to the next test.

Four energy-absorbing seats were provided for the test series, only one of which was equipped with seat pan load cells. Both seats that had been used at CAMI were used again at NASA. The operational seat used (also equipped with seat pan load cells) was the same seat used in testing at CAMI.

After the seats were installed in the aircraft, the anthropomorphic dummies were placed in the capsule. In all tests, two 50th-percentile Part 572 dummies (the same type of dummy used in the seat tests at CAMI), were utilized. These dummies however, were not equipped with the spinal load cells.

After the capsule was fully prepared it was taken to the test area. At this time the attitude control cables were attached. The attitude control cables

Figure 50. Drop tower of Impact Dynamics Research Facility at NASA Langley Research Center.

Figure 51. Structure at front of crew module added for attachment of attitude control cables.

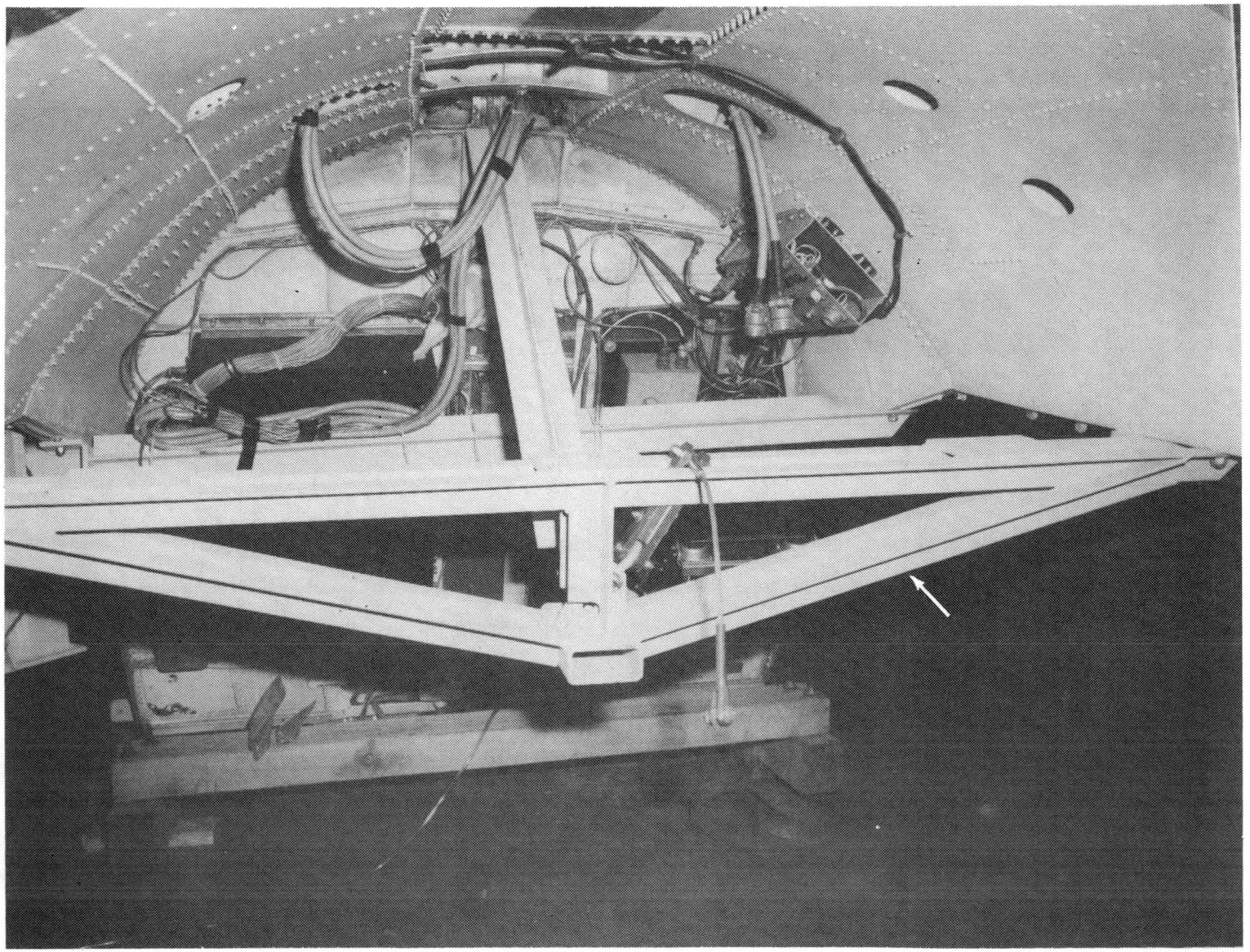

Figure 52. Structure at rear of crew module added for attachment of attitude control cables.

were adjusted prior to each test to provide the proper pitch, roll, and yaw of the capsule. A typical set-up for a swing test is shown in Figure 53. Attitude control cables for a drop test are visible in Figure 50.

Figure 54 is a diagram showing the systems used in performing a swing test. Platforms at the west end of the gantry support the winches and pulleys used to control the length of the swing cables. The length of the swing cables is adjusted to provide the proper impact angle and correct ratio of horizontal and vertical velocities. The pull-back platform is attached to the underside of the movable bridge, where the winch and pulley system controls the length of the pull-back cable. The aircraft is pulled up to the height required to obtain the proper horizontal and vertical velocities at impact.

For tests requiring only a vertical velocity, the drop tower was used. The capsule was again supported by cables attaching it to the test fixture, which was then lifted to the height required to obtain the proper vertical velocity. The fixture is guided along rails during descent.

Final preparation for either a swing test or a pure vertical drop test started after the attitude cables are properly positioned. The instrumentation umbilical cord was attached and the instrumentation was once again checked for continuity. A final inspection was made of the seats, dummies, and restraint system. The shoulder belts are given their final tightening. Although in this case belt tension was not being measured, the tightening procedure produced approximately the same amount of tautness indicated in the CAMI test series.

During preparation for a swing test, pyrotechnic wire cutters were attached to the attitude control cables. These are guillotine-type wire cutters that operate just before the capsule hits the ground. Thus, at ground impact the capsule was not being subjected to any loads from the cables. Another pyrotechnic device is attached to the umbilical cord fitting. This device released the umbilical cord but was delayed so that operation occurred after the important ground impact data was transmitted. Releasing the umbilical cord reduced the chances of damage from the capsule rolling during the ground impact sequence. In a vertical drop test, these pyrotechnic devices are not necessary.

The IAB was then inflated from a nitrogen gas bottle that remained on the ground. Pressure was regulated by the regulator inside the capsule. With the inflation of the IAB, the capsule was ready for the test. Pull-back cables lifted the capsule into the proper position, which was checked using surveying equipment. Figure 55 shows the capsule in position just prior to a swing test. For both the swing and the vertical drop tests the landing area was covered with an 18-in.-deep layer of soil.

Still photographs were also taken before and after each test. All accelerometer and load cell data from the test were recorded on tape for analysis. Several channels from each test were then displayed on oscillograph paper for immediate use. NASA filtered all channels of data per the Society of Automotive Engineers Recommended Practice J211b, and determined the DRI values required for the evaluation of the test results.

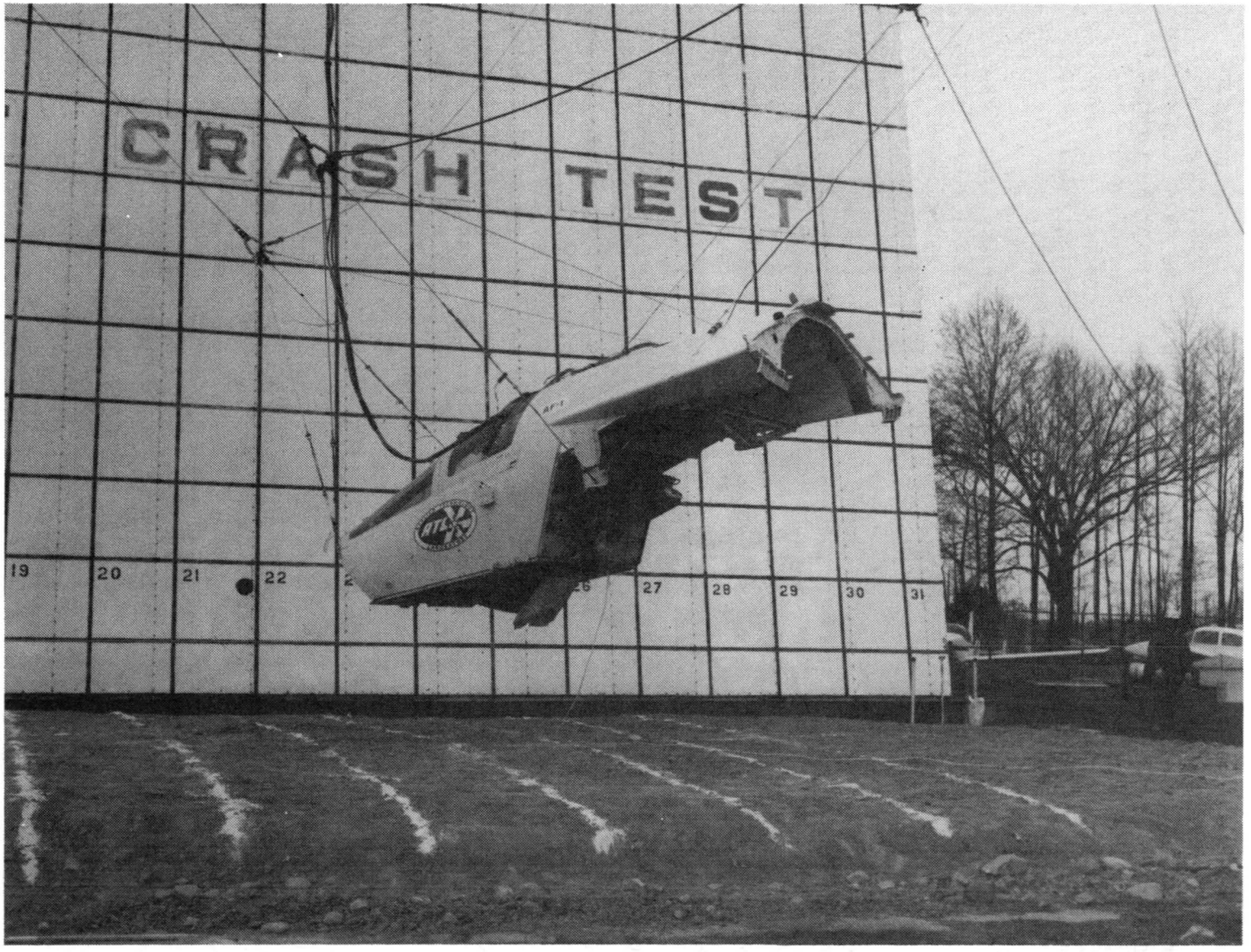

Figure 53. Swing test setup at NASA Impact Dynamics Research Facility.

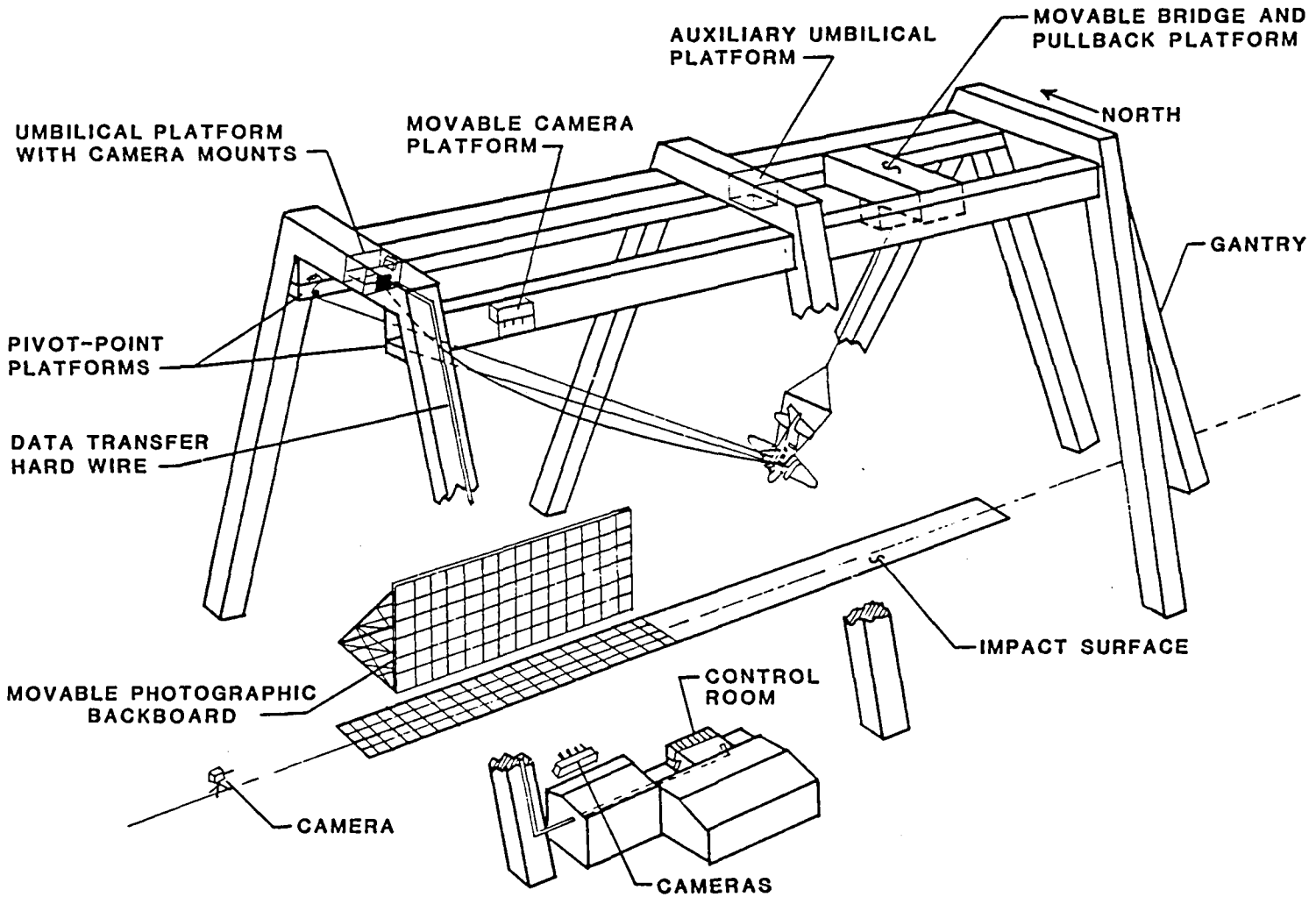

Figure 54. Diagram of NASA Impact Dynamics Research Facility (Reference 17).

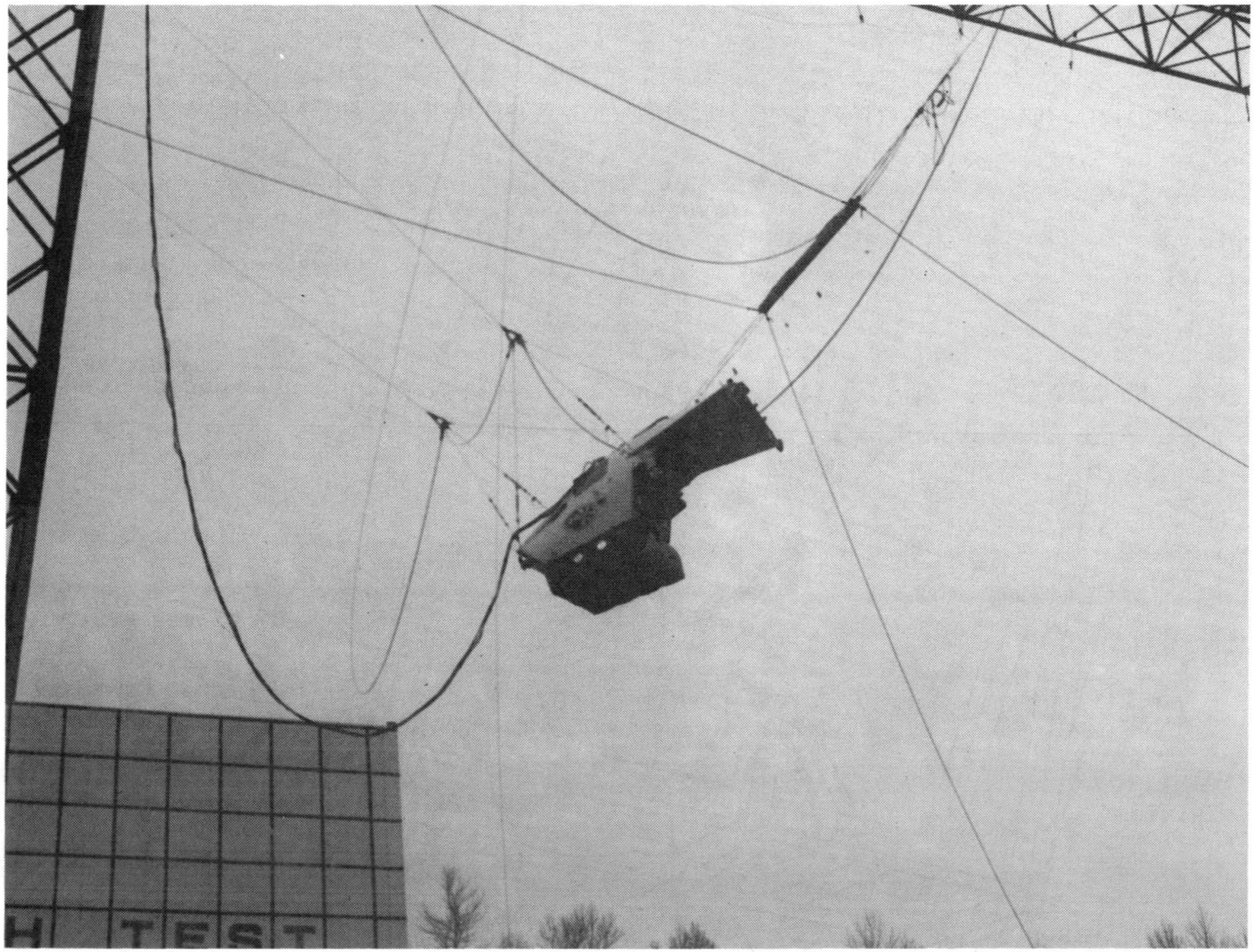

Figure 55. Crew module immediately prior to swing test at Nasa Impact Dynamics Research Facility.

4.2.2.2 Instrumentation. Camera coverage for each test was quite extensive. The following is a list of the motion picture cameras used.

- Cameras

  - Normal speed, 16-mm color, hand held, one

  - High speed, 16-mm color, 400 frames/sec, five minimum:

    1 - side view
    1 - front view
    1 - top view
    2 - in capsule (one each seat).

In most cases seven to nine cameras were used. Camera views added included a hand-held high-speed view, a close-up view from the side, and a close-up view from the top.

Accelerometers, load cells, string potentiometers, and pressure transducers occupied up to 50 channels of data during the test series. The same accelerometer measurements were taken for all tests. The load cell channels were utilized whenever seats with seat pan load cells were tested. String potentiometers were used to measure the stroke of the energy-absorbing seat. The pressure transducer channels were only used with the modified IAB during the vertical drop tests at the reduced descent rate.

- Accelerometers

  - Aircraft bulkhead, left side, triaxial, three channels

  - Aircraft bulkhead, right side, triaxial, three channels

  - Aircraft center of gravity, triaxial, three channels

  - Left seat pan, triaxial and along back tangent line, four channels

  - Right seat pan, triaxial and along back tangent line, four channels

  - Left dummy
    -- pelvis, triaxial, three channels
    -- chest, triaxial, three channels
    -- head, triaxial, three channels

  - Right dummy
    -- pelvis, triaxial, three channels
    -- chest, triaxial, three channels
    -- head, triaxial, three channels

The bulkhead accelerometers for the right side are visible in Figure 56. A similar location was used on the left side. The accelerometers mounted at the capsule center of gravity are visible in Figure 57. Typical seat pan accelerometer mountings are shown in Figures 58 and 59.

Figure 56. Bulkhead accelerometer mountings for crew module tests.

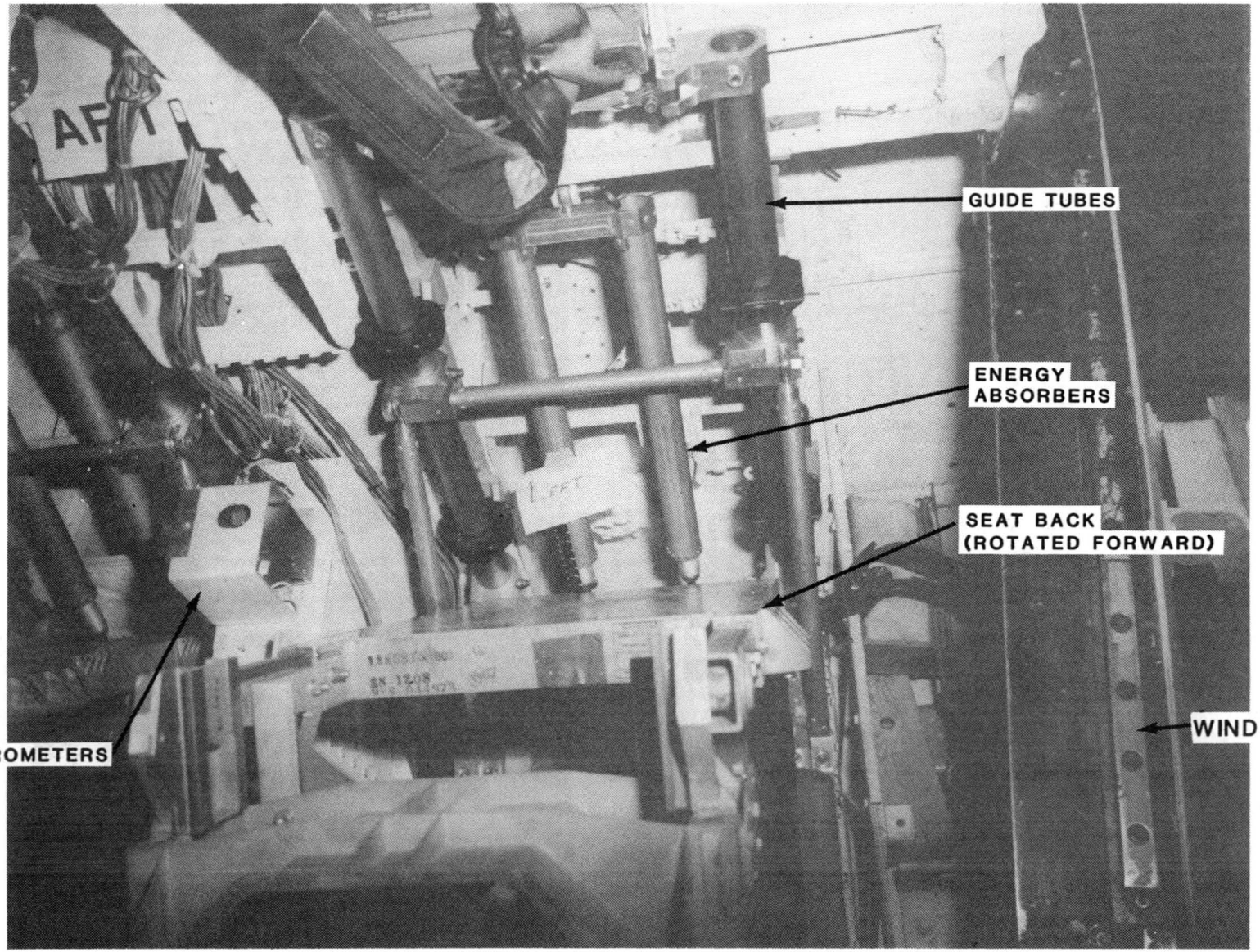

Figure 57. Capsule center of gravity accelerometer mounting for crew module tests.

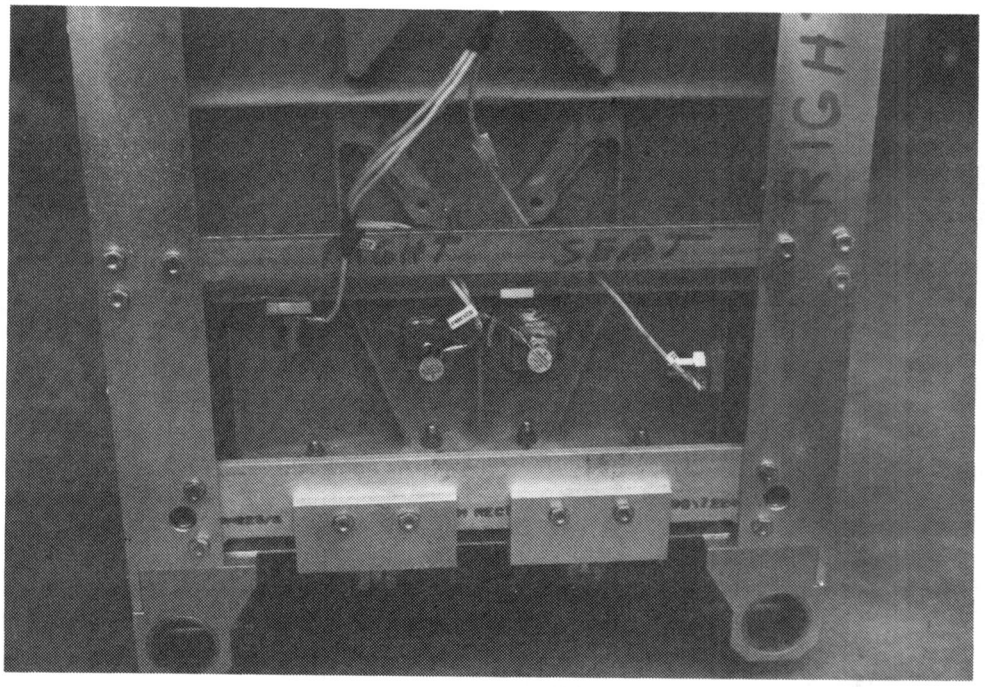

Figure 58. Seat pan accelerometer attachment on energy-absorbing seat in crew module tests.

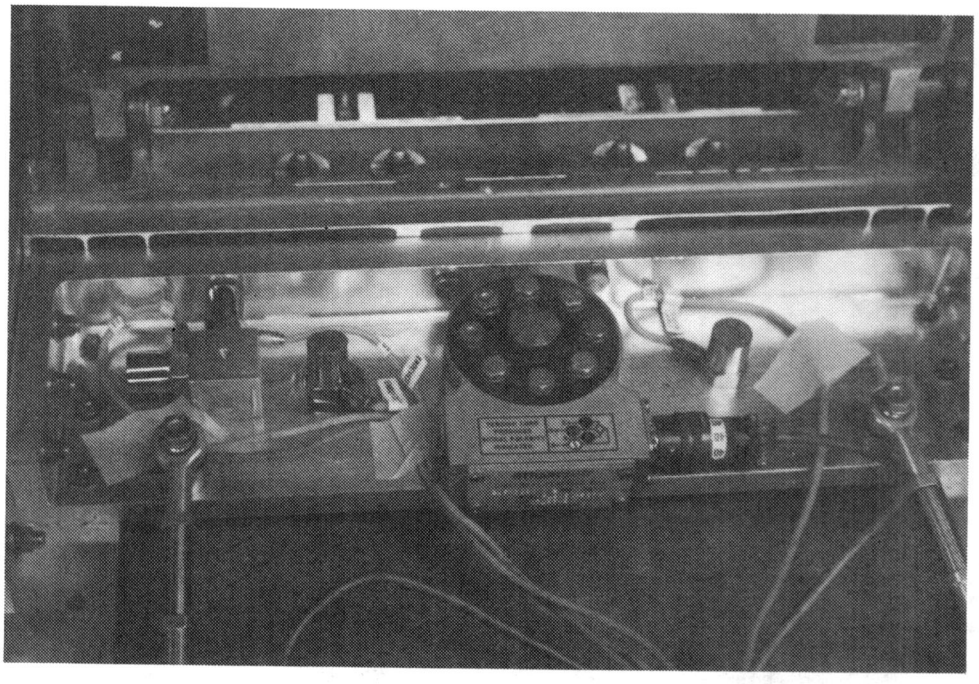

Figure 59. Seat pan accelerometer mounting on energy-absorbing seat with seat pan load cells used in crew module tests.

- Load Cells
  - Left seat pan, vertical, three channels
  - Right seat pan, vertical, three channels

The load-cell-equipped seats were only used in certain tests. Mounting of these load cells was described in Section 2.4.

- String Potentiometers
  - Left seat, along guide tubes, one channel
  - Right seat, along guide tubes, one channel

The string potentiometer for the right seat is visible in Figure 56. These were only used in tests requiring measurement of energy-absorbing stroke.

- Pressure Transducers
  - Modified IAB, exit holes, six channels

These transducers were only used in the drop tests at a reduced descent rate.

- Radar Gun
  - Horizontal orientation along flight path, one channel

The radar gun was mounted to measure the horizontal velocity of the capsule at impact. The data was analyzed immediately after the test and recorded as a velocity.

4.2.2.3 Seat Installation. Some modifications to the aircraft bulkhead were necessary to mount the energy-absorbing seat. Figure 60 is a view of the modification to the pilot side of the aircraft, which is similar to the modification on the weapons system officer (WSO) side of the aircraft.

The upper and lower bearing assemblies are attached by bolts to the appropriate fittings (labeled in Figure 60). The top of the energy absorber assembly is a rod end bearing that is also attached by a bolt to the vertical adjustment clevis. These five points are the only seat attachments to the bulkhead.

The modification used in the test series is not the same modification that would be used in a retrofit application. The bulkhead modification used does carry the loads to the same aircraft structure that would carry the loads from a retrofit seat. The bulkhead modification also positions the seat reference point within the presently defined adjustment envelope.

Figure 61 shows the doubler placed in the bottom of the air ventilation duct. In order to maintain access to the storage areas behind the crew, stringers running across to connect the main vertical members were not used. Thus, torsional loads must be carried up to stronger structure. This doubler helps transfer torsional loads from the main vertical member to the strong structure running across the capsule.

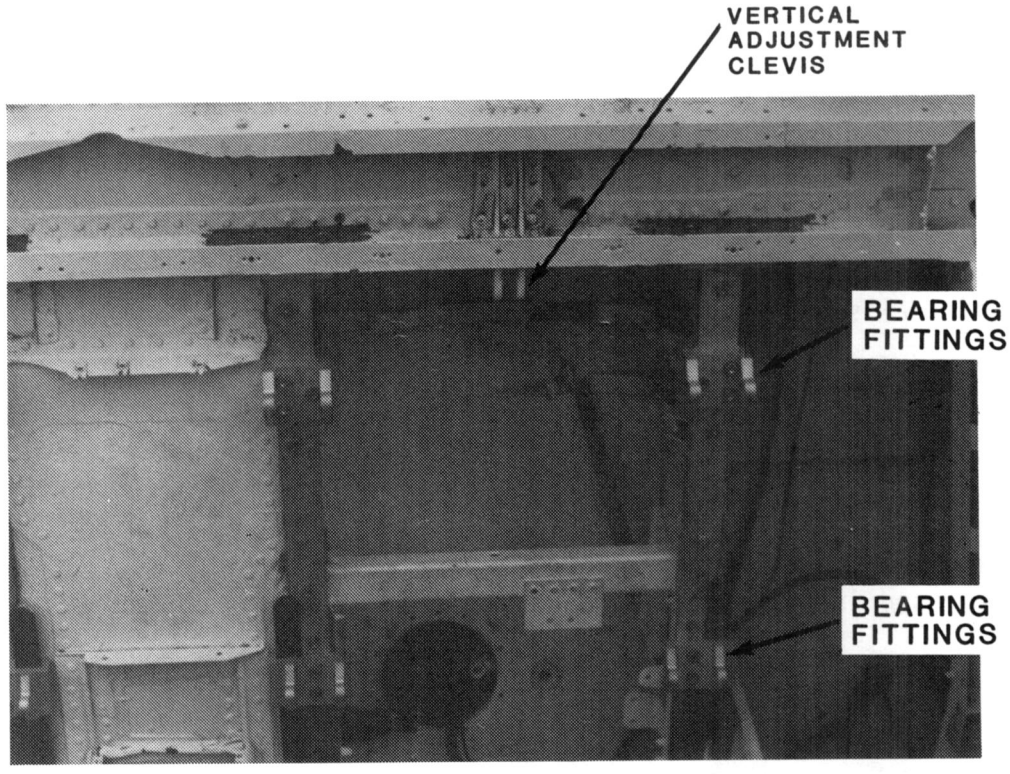

Figure 60. Modification used to mount energy-absorbing seat in crewseat module tests.

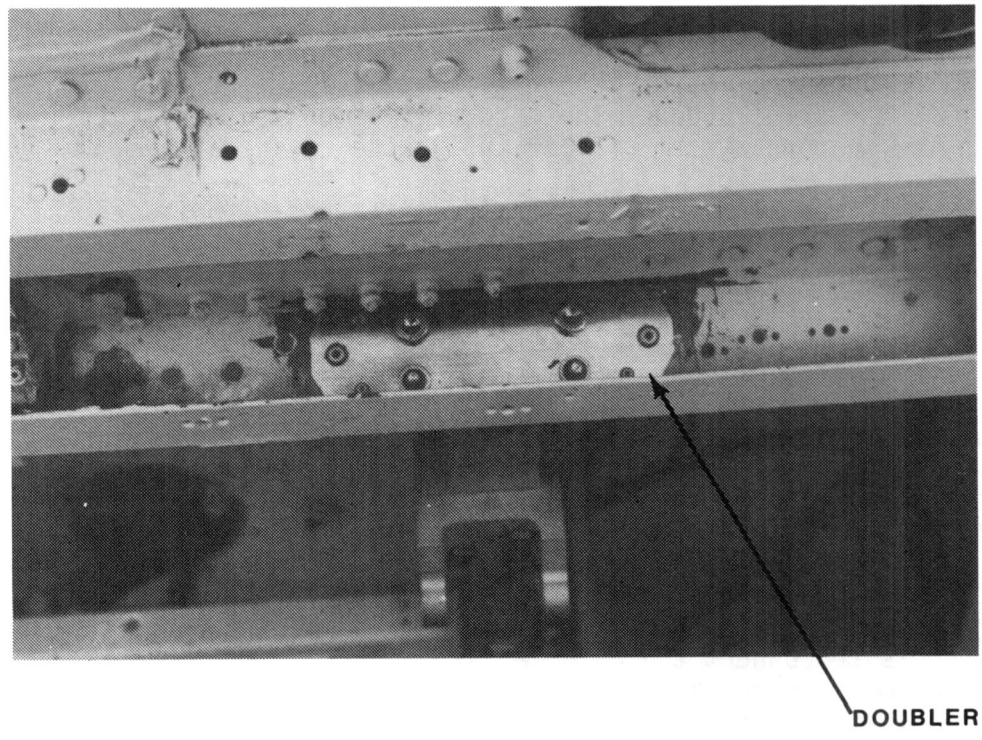

Figure 61. Doubler placed in air ventilation duct.

Figure 62 is a side view showing the added main vertical member. It is attached to the existing bulkhead structure, an L-section running up and down the bulkhead. Doublers prevent this L-section from opening up when forward loads are applied.

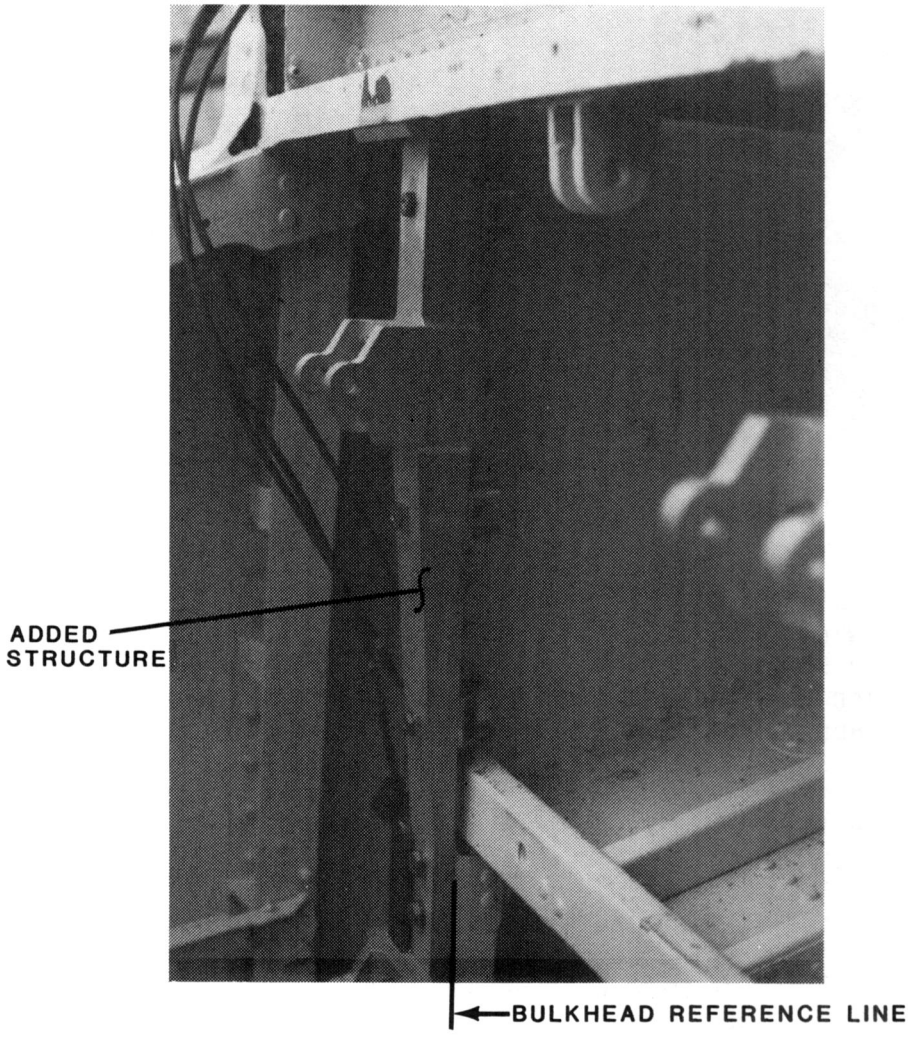

Figure 62. Modification to capsule bulkhead.

A closer view of the lower bearing fitting is shown in Figure 63. In the F-111 capsule, two sets of tracks are used to guide the operational seat. The lower bearing attachment fittings use the upper set of existing tracks to carry some of the load.

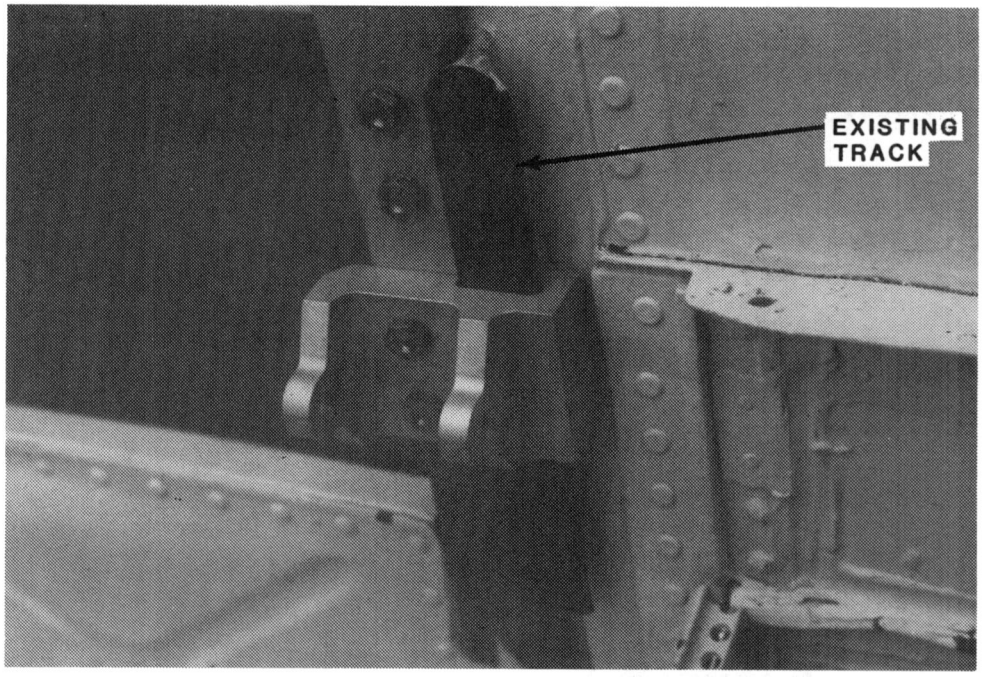

Figure 63. Lower bearing fitting for energy-absorbing seat.

Figure 64 is a side view showing the outline of a 50th-percentile occupant in the test seat when installed in the aircraft. No cushion is shown since the occupant compressed it during the impact. The seat is in approximately the full-up position to provide the maximum room for seat stroke. The seat reference point is approximately 4 in. forward of the full-back position. This is forward of neutral, but it allowed the seat to stroke to the floor without hitting the bottom set of tracks. The foot pedals are in the full-back position, and remained in this location because no adjustment was possible in the capsule used.

Figure 65 is a side view of the operational seat installed in the aircraft. The height is about 3/4 in. below the midpoint of the vertical adjustment range. The seat pan is 3 in. forward of the full-back position. Again, the foot pedals are in the full-back position.

The difference in these two positions will have some effect on various data measured during the test series. The thigh angle differences in the two figures show that the operational seat will transfer more load to the foot pedals, and the energy-absorbing seat will transfer more load to the seat pan through the thighs. This will change in cases where the energy-absorbing seat strokes downward towards the floor. However, in cases where there is little or no stroke the effects on the data will be noticeable.

4.2.3 Test Matrix

The capsule tests conducted consisted of two groups. The first group was the swing tests that were conducted under the large gantry. These were NASA Test

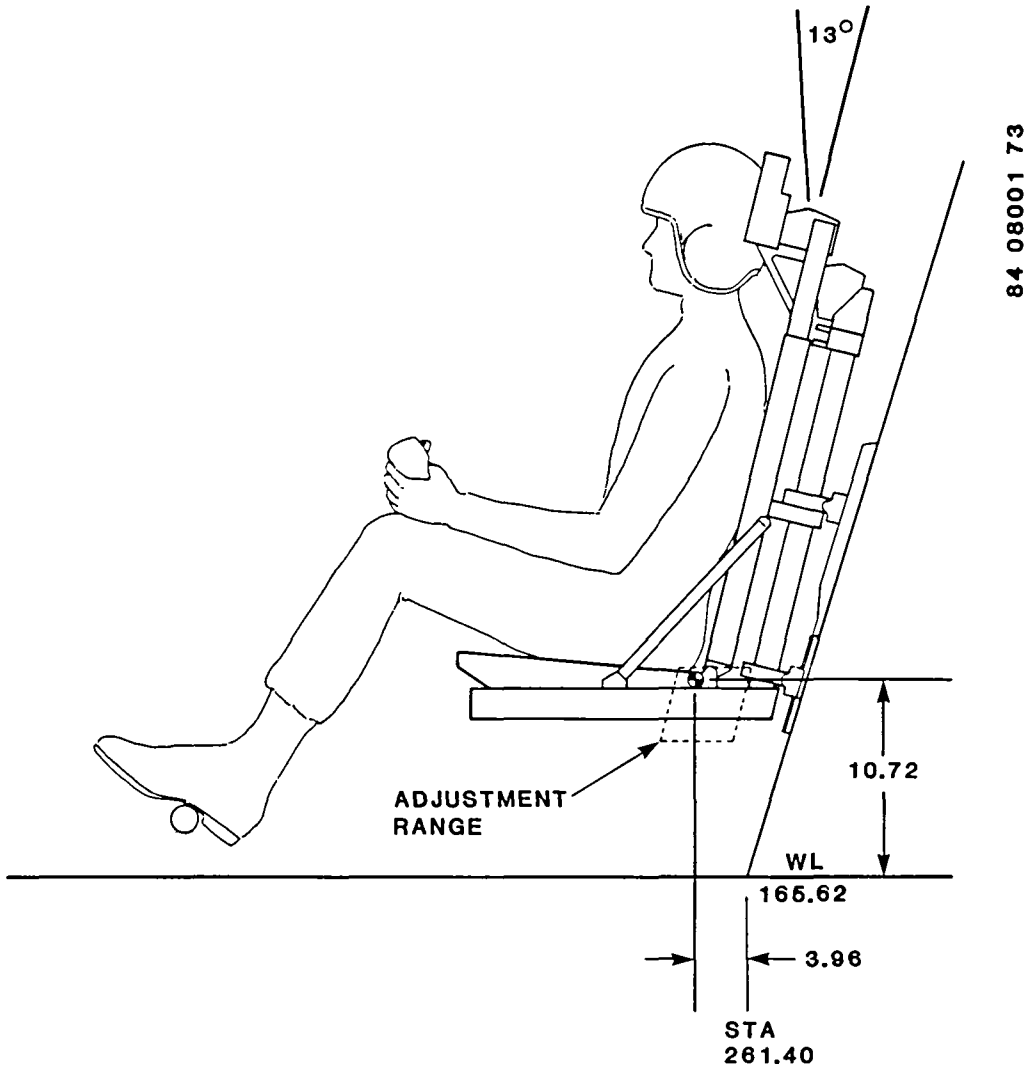

Figure 64. Occupant position in energy-absorbing seat during crew module tests.

Numbers 1 through 7; the tests included large horizontal velocities. The primary objective of this test series was to determine the performance of the energy-absorbing seat over the full range of ground impact conditions defined by the original design envelope of the capsule. The swing tests examined conditions at the edges of the design envelope. The second group of tests was the pure vertical tests conducted using the drop tower. These tests examined the ideal ground impact conditions with the capsule descending in the designed 2-degree nose-up attitude under the parachute and landing on a flat surface. Multiple tests were conducted to examine the differences in ground impacts at 32 and 25 ft/sec for the energy-absorbing and the operational F-111 seats. The CAMI test series did not examine the pure vertical 25 ft/sec ground impact because the decision to include this condition in the analysis was made after the CAMI tests were concluded.

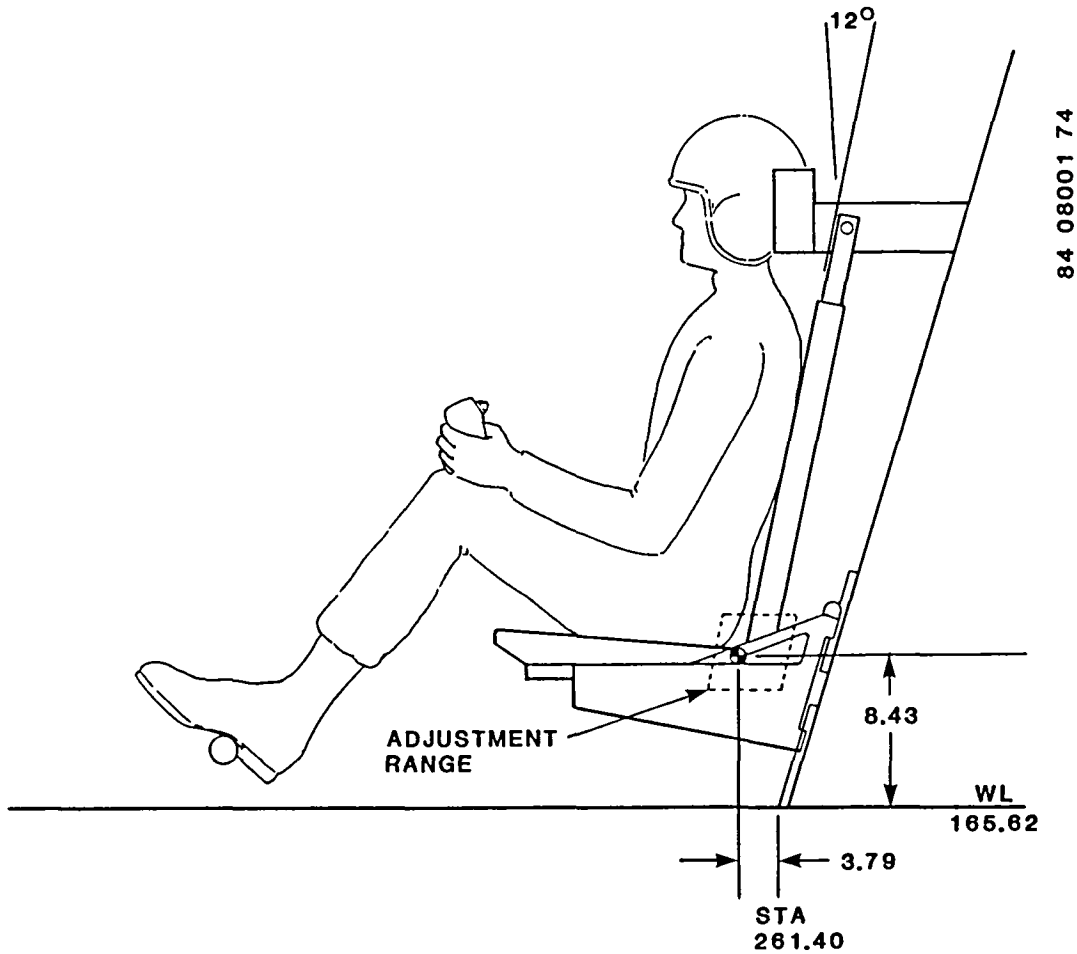

Figure 65. Occupant position in operational seat during crew module tests.

The test matrix was supplied by the Air Force and is shown in Table 17. The tests considered the following variables for the capsule impact conditions:

- Wind velocity (0-34 ft/sec)
- Wind direction (±180 degrees)
- Parachute oscillations (±10 degrees)
- Landing surface slope (±5 degrees)
- Vertical descent rate (32 or 25 ft/sec).

The effect of wind velocity on the ground impact is obvious. The capsule, descending under the support of a parachute, will be carried along by the existing wind. This both increases the magnitude of the impact velocity and changes the direction of the velocity vector. Since the primary objective of this test series was to examine the performance of the energy-absorbing seat over the

TABLE 17. CREW MODULE TEST MATRIX

NASA Test Number	Horizontal Velocity (ft/sec)	Vertical Velocity (ft/sec)	Pitch(1) (degrees)	Roll(2) (degrees)	Yaw(3) (degrees)	Left Seat	Right Seat
1	34	32	-13	0	45	E/A	E/A
2	34	32	0	15	90	E/A	E/A
3	34	32	17	0	90	E/A	E/A
4	34	32	-13	0	75	E/A	E/A
5	34	32	17	0	45	E/A	E/A
6	43	32	2	0	0	E/A	E/A
7	43	32	7	0	180	E/A	E/A
8	0	32	2	0	0	F-111	E/A
9	0	25	2	0	0	F-111	E/A
10	0	25	2	0	0	F-111	E/A
11	0	25	2	0	0	F-111	E/A
12	0	32	2	0	0	F-111	E/A

(1) Positive pitch is nose up.
(2) Positive roll is right wing down.
(3) Positive yaw is nose right.

full design envelope of the capsule, all the swing tests used conditions simulating the maximum wind velocity of 32 ft/sec. For the vertical tests the simulated wind velocity was 0.

The effect of wind direction was taken into account by yawing the capsule. Various yaw angles between 0 and 180 degrees were used.

The effect of the parachute oscillations is shown in Figure 66. In all swing tests (Test Numbers 1 through 7) maximum parachute oscillations of 10 degrees were used as test conditions. In Test Numbers 1 through 5 the capsule was modeled as being at the outer edges of a 10-degree swing. Therefore, the pitch or roll attitude was changed 10 degrees from the normal capsule descent position, which is a nose-up pitch of 2 degrees. In Test Numbers 6 and 7 the capsule condition simulated was the bottom of the pendulum swinging action under the parachute. Thus no adjustments in aircraft attitude were made; however, the horizontal velocity was increased from 32 to 43 ft/sec. The vertical drops in Tests 8 through 12 simulated conditions under which no parachute oscillations occurred.

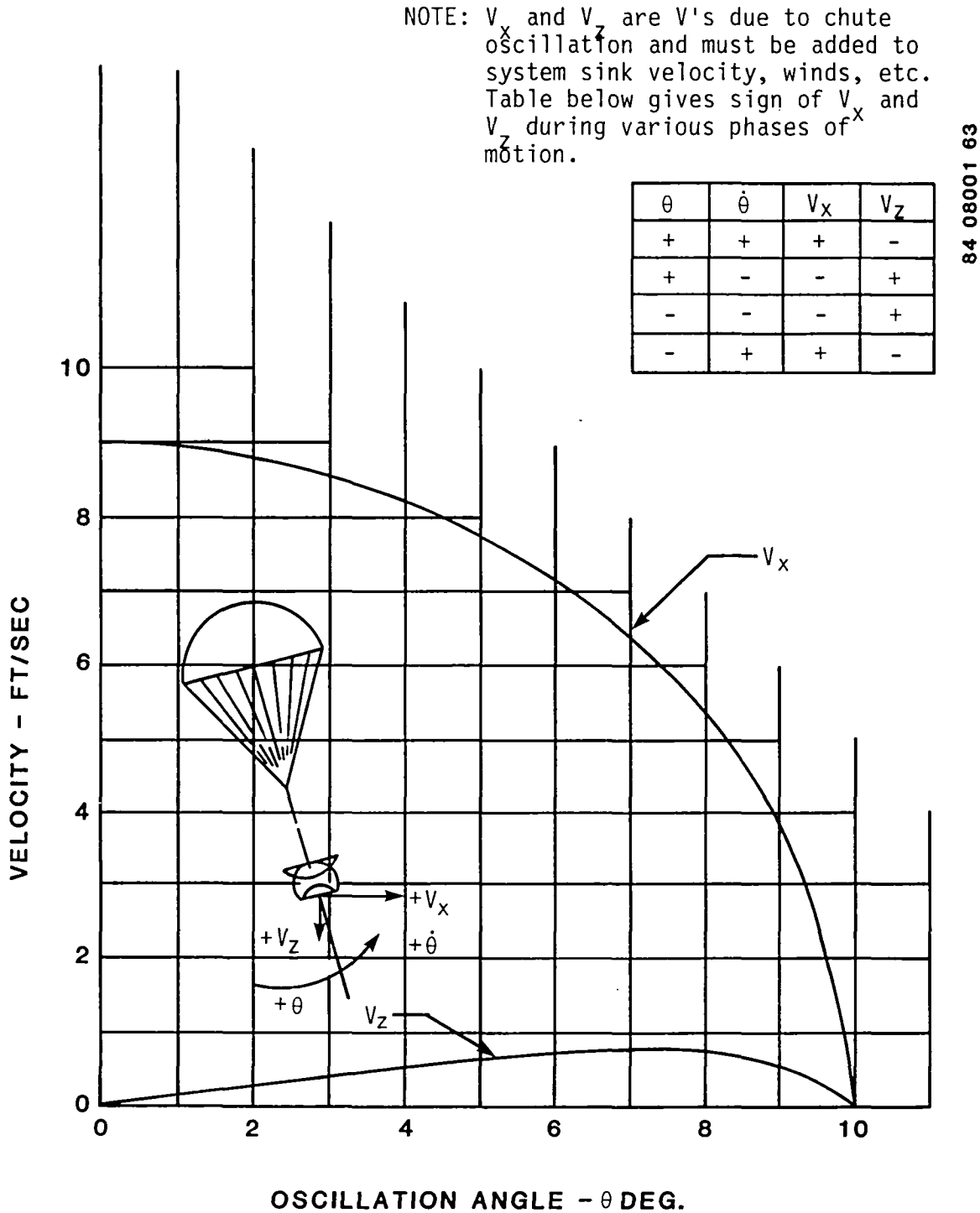

θ	$\dot{\theta}$	V_x	V_z
+	+	+	-
+	-	-	+
-	-	-	+
-	+	+	-

Figure 66. Effect of parachute oscillations on crew module horizontal and vertical velocities (courtesy U.S. Air Force).

Design parameters of the capsule were configured under the consideration that the landing slope could vary by 5 degrees. Impact conditions in Test Numbers 1 through 5, and 7 simulate a 5-degree slope on the landing surface by varying the capsule pitch or roll by 5 degrees. Test Number 6, and all the vertical tests, simulate a level landing area.

Two vertical descent rates were used. Thirty-two ft/sec is the descent velocity of the operational escape system and was used in all the swing tests and some of the vertical tests. The vertical descent rate of 25 ft/sec, based on an estimate of a new parachute system presently under consideration, was used in only some of the vertical tests.

In all swing tests, the energy-absorbing seat was used on both sides of the aircraft. In the vertical tests it was expected that the environment on both sides of the aircraft would be similar. Therefore, it was possible to use the energy-absorbing seat in the right seat and the operational F-111 seat in the left seat to obtain comparative data.

4.3 RESULTS OF CAPSULE TESTING

Test results from the capsule test series will be evaluated with respect to three major concerns:

- The acceleration levels to which the capsule and the occupant are subjected
- The seat pan loads measured mainly as a comparative tool between the operational and energy-absorbing seats
- The vertical stroking distance used by the energy-absorbing seat under various conditions.

4.3.1 Test Conditions

The test conditions measured during the swing tests are presented in Table 18. The vertical velocity was calculated from the measured horizontal velocity and the angle of the capsule flight path at impact, which was measured from the high-speed films. Pitch, roll, and yaw measurements were also taken from the high-speed film data.

The roll in NASA Test Number 2 is defined as a 15-degree, right-wing-down configuration. Inadvertantly, this roll direction was opposite to that used in CAMI Test Number A83-106. However, the test conditions in NASA Test Number 2 still represent a data point at the edge of the design envelope for the capsule.

For the vertical tests, a direct measurement of the velocity was not made. Analysis of the film data showed the drops to be within 2 ft/sec of the ideal conditions listed in Table 17. Although normal camera angles for the measurement of pitch and yaw at ground impact were not possible on the drop tower, the camera angles used did not show a noticeable difference from the planned test conditions.

Accelerometers mounted on the bulkhead behind both the left and right seats gave the best indication of the environment to which each seat had been subjected. Table 19 presents both the velocity change determined by integrating the bulkhead z-axis acceleration measured on each side of the aircraft and the peak value of the acceleration curve.

TABLE 18. CREW MODULE SWING TEST CONDITIONS

NASA Test Number	Ideal Test Conditions					Measured Test Conditions				
	Horizontal Velocity (ft/sec)	Vertical Velocity (ft/sec)	Pitch(1) (degrees)	Roll(2) (degrees)	Yaw(3) (degrees)	Horizontal Velocity (ft/sec)	Vertical(5) Velocity (ft/sec)	Pitch(1) (degrees)	Roll(2) (degrees)	Yaw(3) (degrees)
1	34	32	-13	0	45	33.3	32.7	-12	4	35
2	34	32	0	15	90	34.3	35.5	-10	21	85
3	34	32	17	0	90	33.5	31.2	8	2	82
4	34	32	-13	0	75	35(4)	35	-18	8	67
5	34	32	17	0	45	32.9	31.8	11	9	36
6	43	32	2	0	0	42.2	33.0	3	-3	2
7	43	32	7	0	180	40.6	32.9	7	-1	176

(1) Positive pitch is nose up.
(2) Positive roll is right wing down.
(3) Positive yaw is nose right.
(4) Cable interference with radar gun, estimated to be within 2.2 ft/sec.
(5) Calculated from radar gun analysis of horizontal velocity and impact angle from films.

TABLE 19. VELOCITY CHANGE AND PEAK ACCELERATION MEASURED ALONG A VERTICAL AXIS ON CAPSULE BULKHEAD

NASA Test Number	Left Seat(1) Velocity Change (ft/sec)	Left Seat(1) Peak(3) Acceleration (G)	Right Seat(2) Velocity Change (ft/sec)	Right Seat(2) Peak(3) Acceleration (G)
1	29.0	15.5	37.0	21.8
2	19.5	14.9	44.5	35.3
3	36.0	15.5	48.0	25.8
4	22.0	18.2	32.0	27.4
5	29.0	18.6	51.5	33.4
6	40.5	19.1	41.0	21.1
7	35.0	21.3	33.5	16.0
8	31.5	15.7	29.5	15.5
9	24.0	10.7	26.5	11.0
10	23.5	11.6	23.0	10.9
11	24.5	10.8	26.0	10.5
12	30.5	16.6	29.5	16.2

(1) Pilot seat.
(2) Weapons system officer seat.
(3) All peak values measured from plots of data reduced with a class 60 filter per SAE Recommended Practice J211b.

Effects of the aircraft attitude in swing Test Numbers 1 through 7 are evident. The yaw present in Test Numbers 1 through 5 created very different acceleration traces on the left and right sides of the aircraft. Figure 67 shows the bulkhead z-axis acceleration plots for Test Number 5; while the basic shapes of the curves are similar, there is a large difference in magnitude. The orientations for Test Numbers 6 and 7 could be expected to create similar environments on the left and right sides of the aircraft. Table 19 shows that this is indeed the case, as the velocity changes and peak acceleration measurements are much closer than those measured in earlier swing tests.

Overall, the capsule swing test conditions at NASA were more severe than those at CAMI. At CAMI, the seat was simply oriented properly with respect to the velocity vector and subjected to the impact velocity and a designated peak acceleration. This was done based on previous test data that showed mild impacts

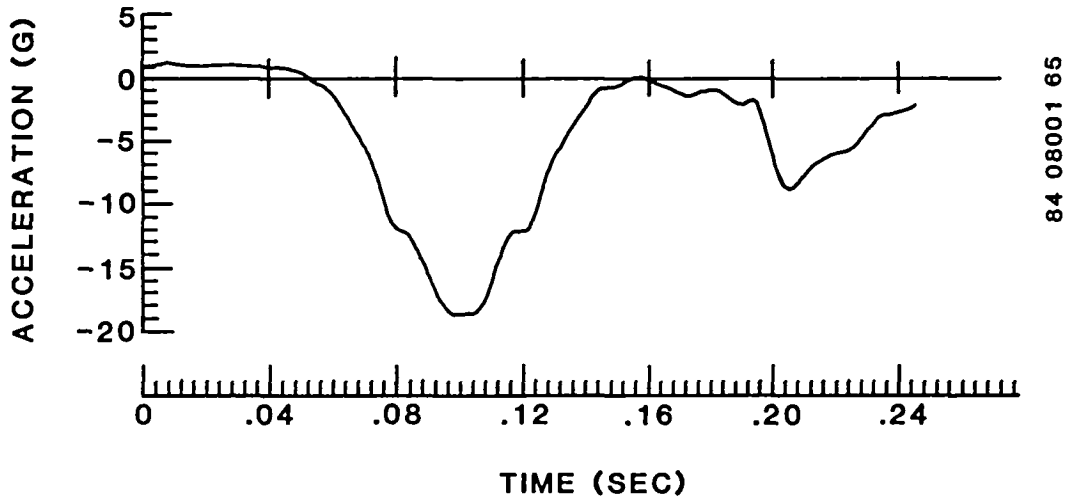

a. Left side

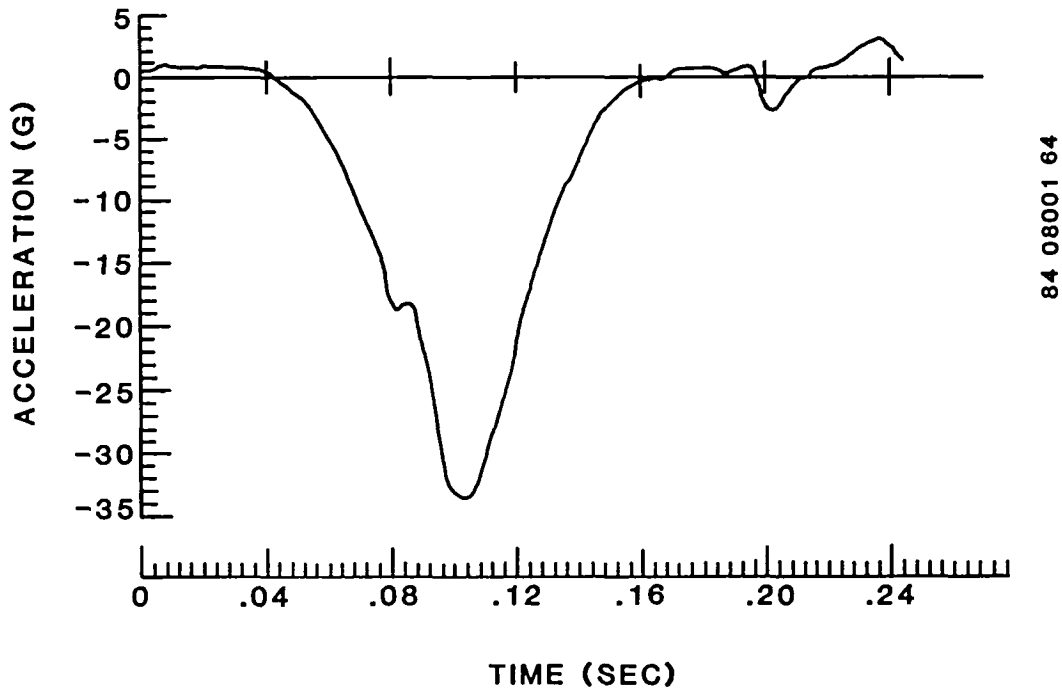

b. Right side

Figure 67. Bulkhead z-axis acceleration from NASA Test Number 5.

under which there was little rebound of the capsule. During the tests at NASA the capsule impacted with various amounts of pitch, roll, and yaw. Under these conditions the capsule does not uniformly load the IAB, and thus the efficiency of the IAB can be severely reduced. When the capsule impacts with an orientation which is yawed with respect to the velocity vector, occupants on opposite sides of the capsule are subjected to different environments with different amounts of rebound. Even when the capsule is not yawed or rolled, a significant horizontal velocity will increase the severity of the impact for both occupants. In most of the swing tests conducted there was a certain amount of yaw, and the capsule rolled between 90 and 360 degrees after the initial ground impact. Thus, the NASA tests were more severe for two reasons. The capsule attitudes at impact reduced the efficiency of the IAB and the energy of the ground impact was not evenly distributed between the two seats. While these problems were anticipated prior to the CAMI test series, the data needed to make suitable adjustments in the CAMI test pulses were not available.

As would be expected for the drop tests, Table 19 shows similar velocity and acceleration values for the left and right sides in Test Numbers 8 through 12.

4.3.2 Occupant Acceleration Levels

This section includes the evaluation of the acceleration measurements taken in the dummies and on the seat pan during all of the tests. Analysis centers on the vertical accelerations, since they are most directly related to the spinal injury potential. The peak vertical accelerations measured in all of the tests are listed in Table 20.

Looking at the performance of the energy-absorbing seat, one can see that in the swing tests the accelerations measured on the seat pan, both pure vertical and along the back tangent line, varied from 17.2 to 22.1 G, excluding Test Number 2. In Test Number 2 the seat used all of the available stroking distance and bottomed out for approximately .010 seconds. The vertical seat pan acceleration measured in this case is shown in Figure 68. Even though the seat bottomed for a short time, the acceleration levels did not climb to extremely high values; measurements of 26 to 27 G were recorded on the seat pan.

Seat pan accelerations for the energy-absorbing seat in the vertical tests were lower than those measured in the swing tests. Measurements at the 32-ft/sec descent rate ranged from 15 to 19 G, while at the 25-ft/sec descent rate the seat pan accelerations were all between 12 and 13 G.

Dynamic amplification resulted in pelvis and chest accelerations slightly higher than the seat pan accelerations. In the swing tests the values measured ranged mostly from 20 to 25 G. One data point, the chest z-axis acceleration in Test Number 5, was not in accordance with any other test data from either that test or any other test. Pelvis and chest accelerations in the vertical tests were also slightly higher than the corresponding seat pan accelerations. Peaks of 19 to 21 G for drops at 32 ft/sec, and 15 through 17 G for drops at 25 ft/sec were recorded. These values are all in accordance with proper operation of the energy-absorbing seat.

Peak acceleration values can also be used to compare the operational and energy-absorbing seats during the vertical tests. Figures 69 through 71 show plots

TABLE 20. PEAK VERTICAL ACCELERATIONS MEASURED IN CREW MODULE TESTS (1)

NASA Test Number	Left Seat (2)				Right Seat			
	Seat Pan z (G)	Seat Back Tangent Line	Pelvis z (G)	Chest z (G)	Seat Pan z (G)	Seat Back Tangent Line	Pelvis z (G)	Chest z (G)
1	17.2	18.7	22.6	22.1	18.0	19.2	21.3	21.8
2	19.6	19.9	24.6	23.6	26.6	26.4	25.6	23.2
3	21.2	17.8	19.8	20.2	20.1	19.8	21.6	20.9
4	21.1	20.7	25.6	24.8	19.2	21.9	25.5	24.9
5	19.5	19.5	23.8	22.6	20.4	22.1	21.1	43.3
6	19.3	19.5	21.2	22.4	19.2	19.7	24.1	23.7
7	18.1	16.1	16.8	18.8	18.3	16.8	18.6	18.9
8	23.1	21.8	25.0	19.4	15.0	18.6	19.4	19.6
9	12.6	11.6	17.7	16.3	13.0	12.7	15.0	15.8
10	12.8	12.7	17.6	16.9	12.5	12.3	15.6	16.5
11	11.9	12.2	17.4	16.7	12.5	12.4	14.9	15.7
12	22.1	21.1	26.4	25.7	16.5	16.0	21.0	20.7

(1) All peak values measured from plots of data reduced with a class 180 filter per SAE recommended practise J211b.
(2) Operational F-111 seat used for left seat in test numbers 8 through 12.

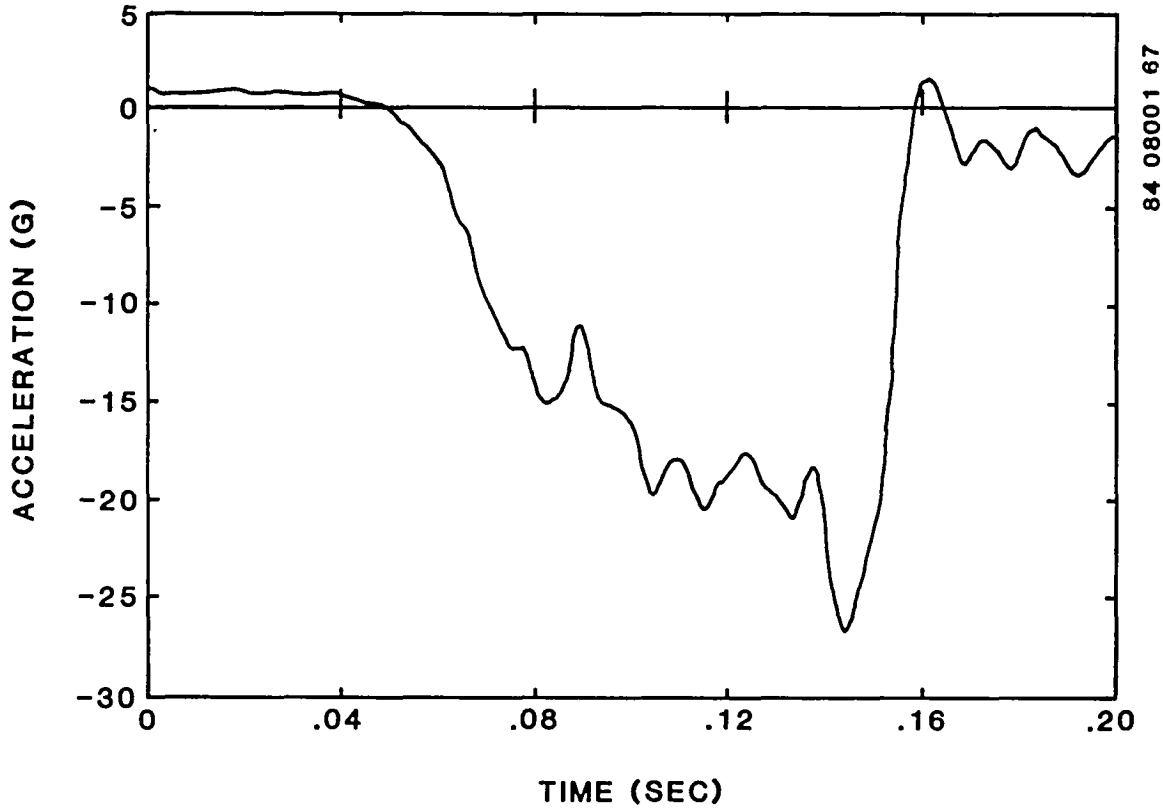

Figure 68. Seat pan vertical acceleration from right seat in NASA Test Number 2 (data filtered with Class 180 filter).

of the peak acceleration levels measured on the seat pan and in the dummy pelvis for both the operational and energy-absorbing seats. All three plots show an improvement with the energy-absorbing seat in Test Numbers 8 and 12, conducted at 32 ft/sec. There is no significant difference in the seat pan peak accelerations measured in the 25 ft/sec tests. In Figure 71, there is a significant difference in pelvis z-axis acceleration peaks. However, this is believed to be due to the slightly different positions of the occupants in the two seats rather than any difference in seat performance.

Another criterion used in evaluating seat pan acceleration data is the Eiband criterion, previously explained in Section 3.3.1. Table 21 shows that in only one case was the Eiband criterion violated; in the second test, the right seat bottomed out and the acceleration levels on the seat pan, both vertical and along the seat back tangent line, were above 23 G for more than .006 sec. In other cases, the seat pan accelerations did not exceed 23 G.

The acceleration durations above 23 G contain no information useful in comparing the energy-absorbing seat to the operational seat in the drop tests. The fact that some differences were visible in the earlier plots but neither seat produced pan accelerations above 23 G, shows the mild nature of these tests.

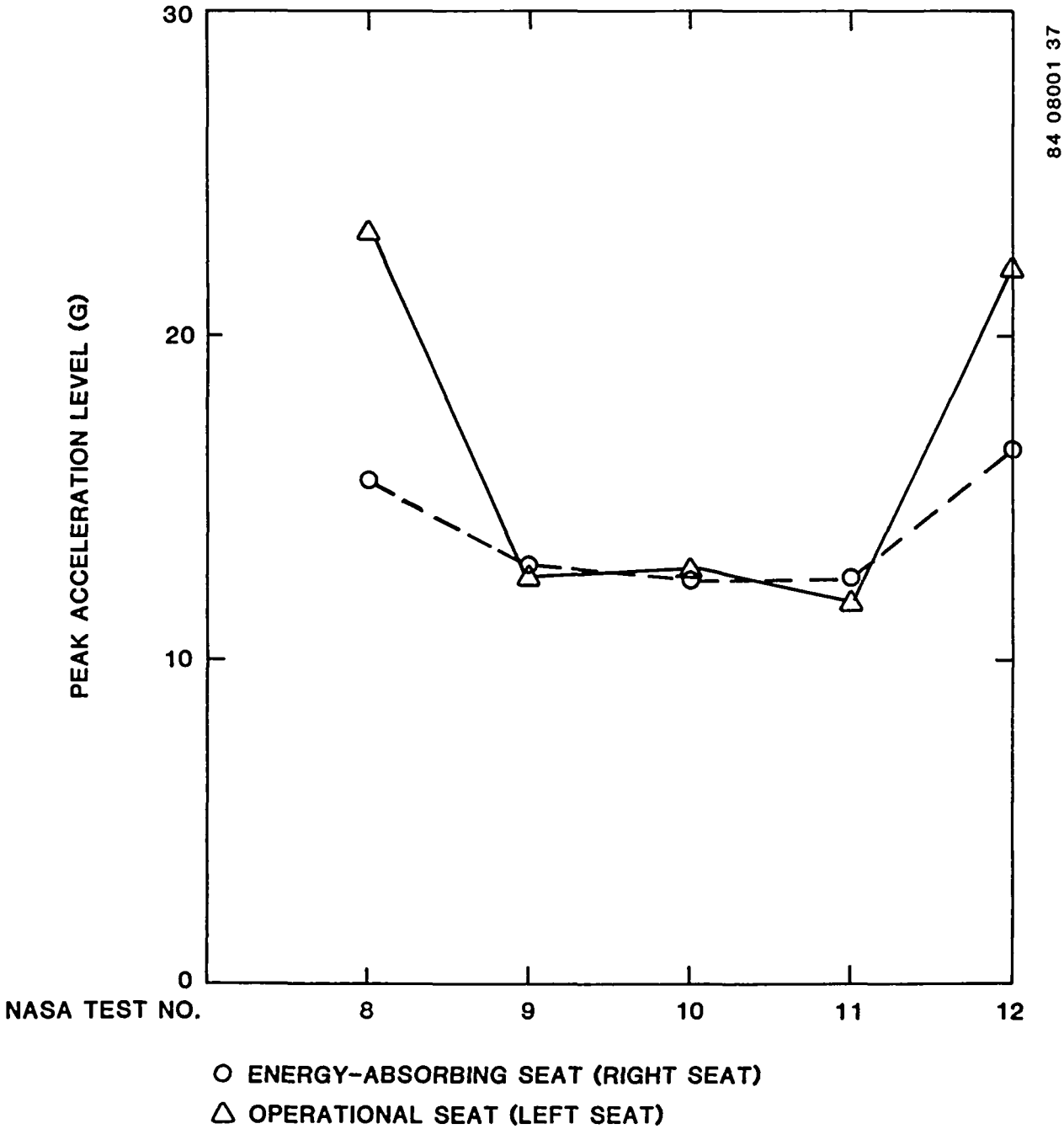

Figure 69. Peak seat pan vertical accelerations in crew module drop tests.

Three acceleration plots (seat pan z-axis, seat pan along the back tangent line, and pelvis z-axis) were evaluated to determine the Dynamic Response Index (DRI), and the results are presented in Table 22. In the swing tests, the seat pan DRI's ranged from 19 to 23, with the average being around 21. This excludes the one test where the seat bottomed out and the DRI climbed to between 24 and 25. Overall, the DRI's in the swing tests are higher than the DRI's measured in previous testing at CAMI. The main reason for this is that the NASA

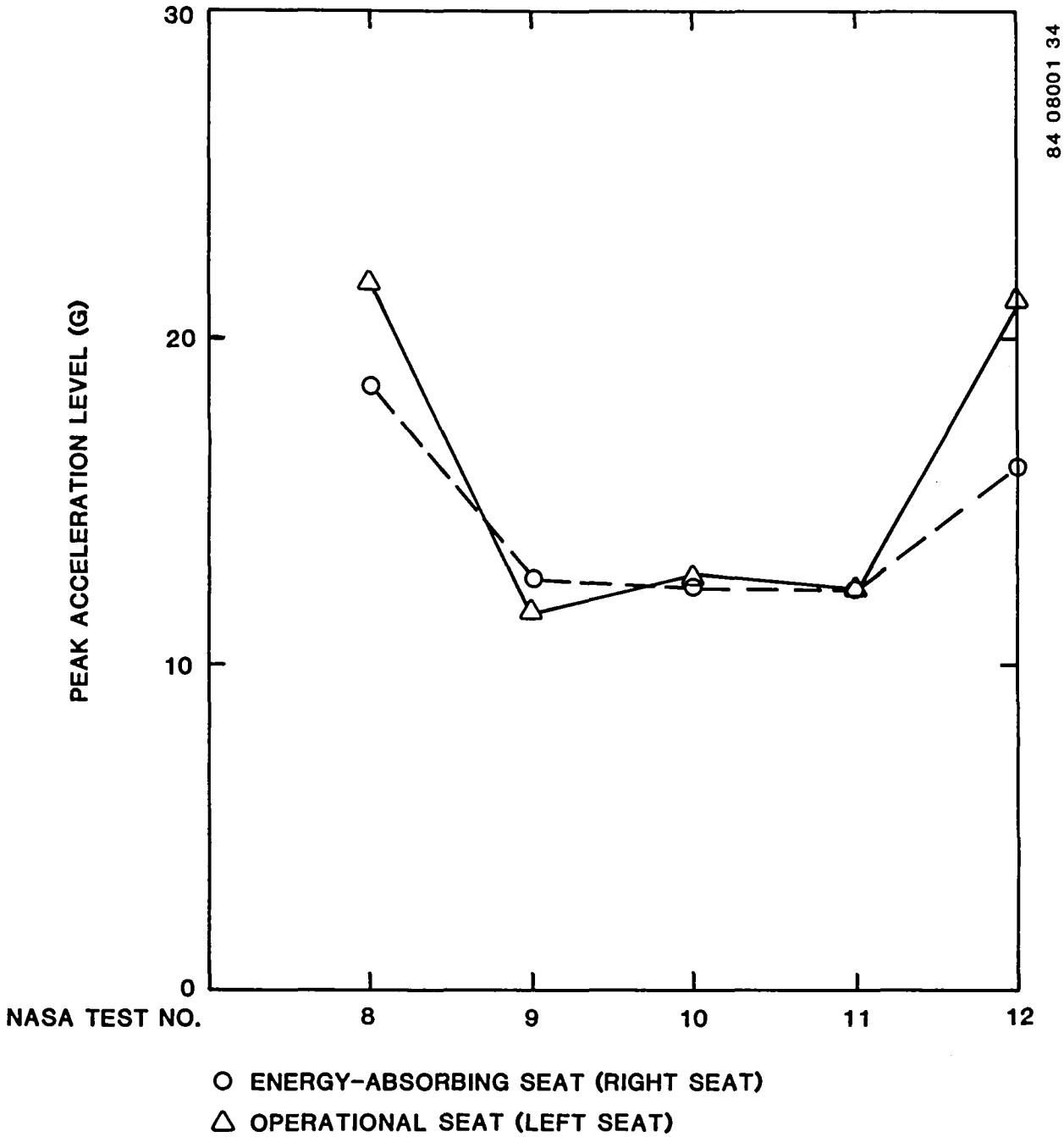

Figure 70. Peak acceleration levels along the seat back tangent line in crew module drop tests.

test conditions were on the average more severe than those at CAMI. The vertical velocity changes and peak accelerations measured on one side of the bulkhead in the NASA tests were sometimes as large as the total velocity change and peak acceleration in the corresponding CAMI test. However, DRI values in the range of 21 to 22 are still within the range that should be expected for an energy-absorbing seat with energy absorber limit loads of 14.5 G. Also, the test conditions swing the capsule in a way that closely simulates a free

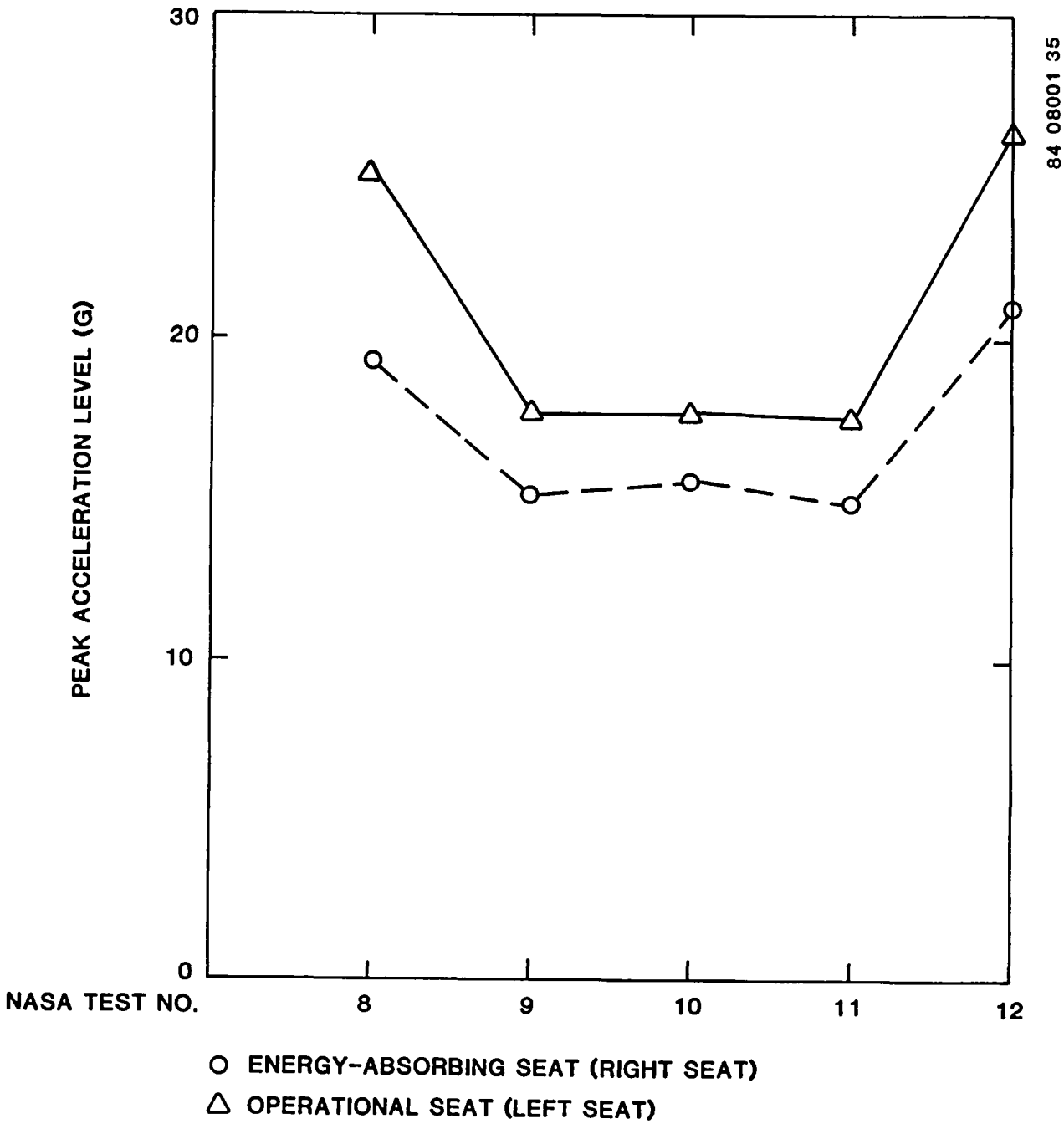

Figure 71. Peak dummy pelvis z-axis acceleration levels in crew module drop tests.

fall. Under actual capsule descent, the body would be under a 1-G preload. With such a preload, the dynamic amplification effects are reduced and the accelerations measured on the seat pan and in the pelvis can be expected to be slightly lower than in a free fall. The DRI values measured would also be lower. Sled test conditions such as those at CAMI may provide some gravity preload to the vertical axis of the seat system, depending on the orientation of the seat on the sled.

TABLE 21. DURATION ABOVE 23 G OF SEAT PAN ACCELERATIONS MEASURED IN CREW MODULE TESTS

NASA Test Number	Left Seat(2)		Right Seat	
	Seat Pan (sec)	Seat Back (sec)	Seat Pan (sec)	Seat Back (sec)
1	0	0	0	0
2	0	0	0.008(1)	0.010(1)
3	0	0	0	0
4	0	0	0	0
5	0	0	0	0
6	0	0	0	0
7	0	0	0	0
8	0.001	0	0	0
9	0	0	0	0
10	0	0	0	0
11	0	0	0	0
12	0	0	0	0

(1) Seat used all available vertical stroke and bottomed out.
(2) Operational F-111 seat used for left seat in Test Numbers 8 through 12.

The DRI's for the vertical tests are shown in Figures 72 through 74, as well as in Table 22. Basically, the energy-absorbing seat shows a slight improvement over the operational seat at 32 ft/sec, but no difference at 25 ft/sec.

4.3.3 Seat Pan Loads

The energy-absorbing seat equipped with seat pan load cells was used in some of the capsule swing tests and in all of the drop tests. However, some of the data channels from the swing tests were lost. The limited data from these swing tests are not meaningful, and are therefore not presented. Individual channels that were recorded are presented in Volume III. In the vertical tests, both the operational seat and the energy-absorbing seat were equipped with seat pan load cells. The peak values recorded are presented as a comparative tool in Table 23 and Figure 75.

TABLE 22. DYNAMIC RESPONSE INDEX (DRI) MEASUREMENTS FROM CREW MODULE TESTS

NASA Test Number	Left Seat(1)			Right Seat		
	Seat Pan	Seat Back Tangent Line	Pelvis	Seat Pan	Seat Back Tangent Line	Pelvis
1	19.1	20.2	23.4	21.0	22.7	23.9
2	23.3	22.0	24.2	24.9	24.6	24.5
3	20.7	18.7	21.8	22.5	21.6	22.4
4	20.5	20.7	23.2	21.7	21.9	23.8
5	22.5	21.5	26.9	22.9	24.5	23.4
6	21.0	20.2	21.8	21.4	21.8	22.4
7	22.3	18.5	19.0	21.6	19.0	21.1
8	23.9	22.8	24.6	18.7	23.6	22.4
9	14.6	13.6	18.3	14.3	13.9	16.3
10	15.3	14.7	18.9	15.6	15.4	17.5
11	14.2	14.0	18.0	14.7	14.4	15.6
12	24.9	23.9	29.6	20.9	20.4	19.8

(1) Operational F-111 seat used for left seat in test numbers 8 through 12.

One can see that in the 25-ft/sec tests (Test Numbers 10 and 11), the total loads on the operational seat were less than those for the energy-absorbing seat. This is related to the difference in occupant position in the two seats.

The energy-absorbing seat was in the full-up position for all testing, while the operational seat was in a more neutral position. As explained in Section 4.2.2.3, the thigh loads for the energy-absorbing seat will be higher than for the operational seat. Tests 9 through 11 demonstrate this, as the difference in the total seat pan load is due to the load under the dummy's thigh. The center load cells, more in line with the spine, show little difference between the two seats.

In the 32-ft/sec tests, the energy-absorbing seat shows some improvement over the operational seat. Despite the difference in seat positions, the total load on the seat pan is noticeably less on the energy-absorbing seat. Figures 76 and 77 show the center seat pan load cells plotted along with the seat

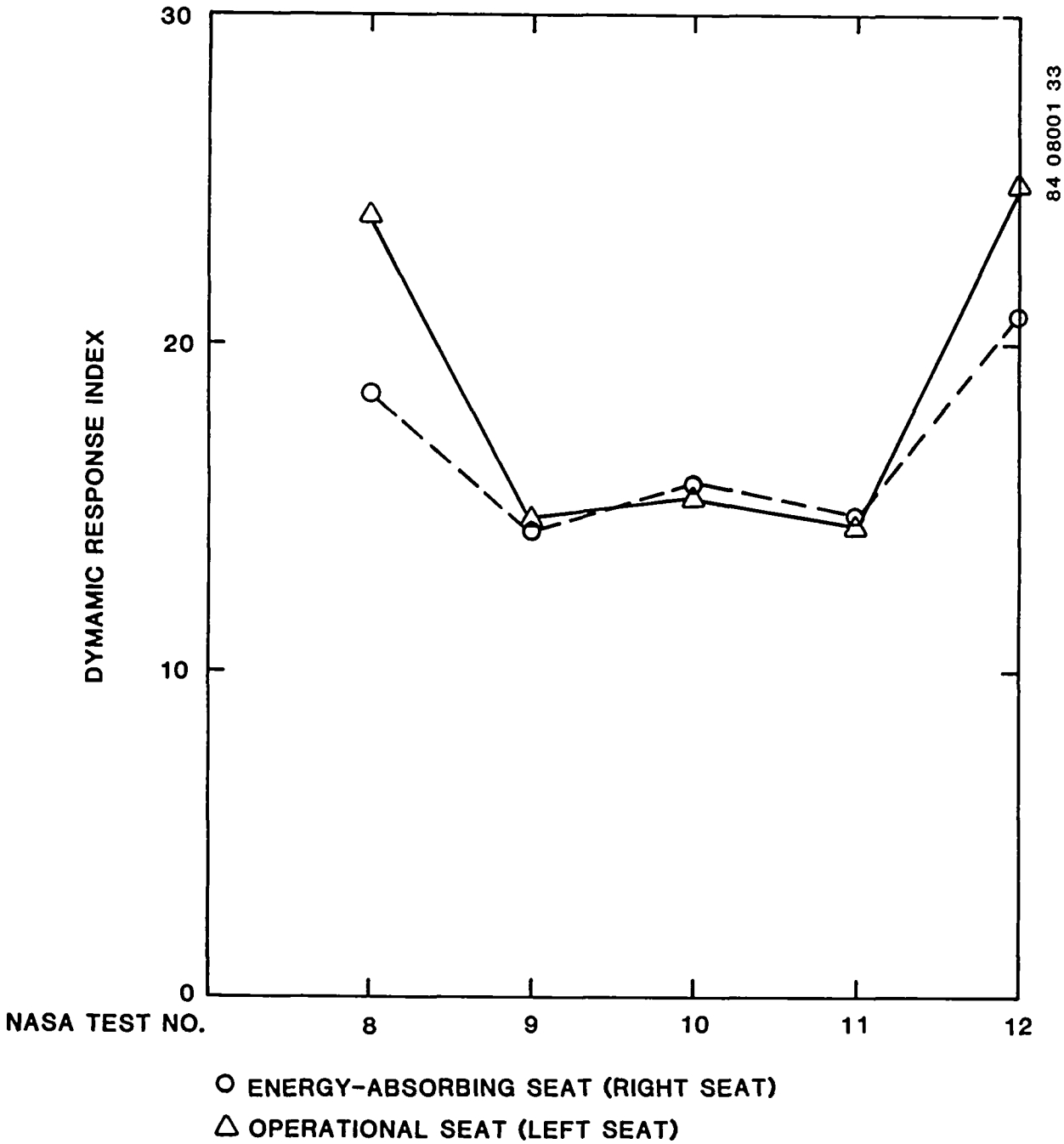

Figure 72. Seat pan z-axis Dynamic Response Index (DRI) measurements from module drop tests.

pan z-axis accelerations. The center load cells show performance improvement in the energy-absorbing seat at 32 ft/sec, but no difference in performance at 25 ft/sec.

The values presented in Table 23 have not been adjusted for the slight weight difference in the seat pans on the two seats. This weight difference is discussed in Section 3.4.3. The weight difference would have only a slight effect on the numbers presented, and no effect on the conclusions reached using these numbers.

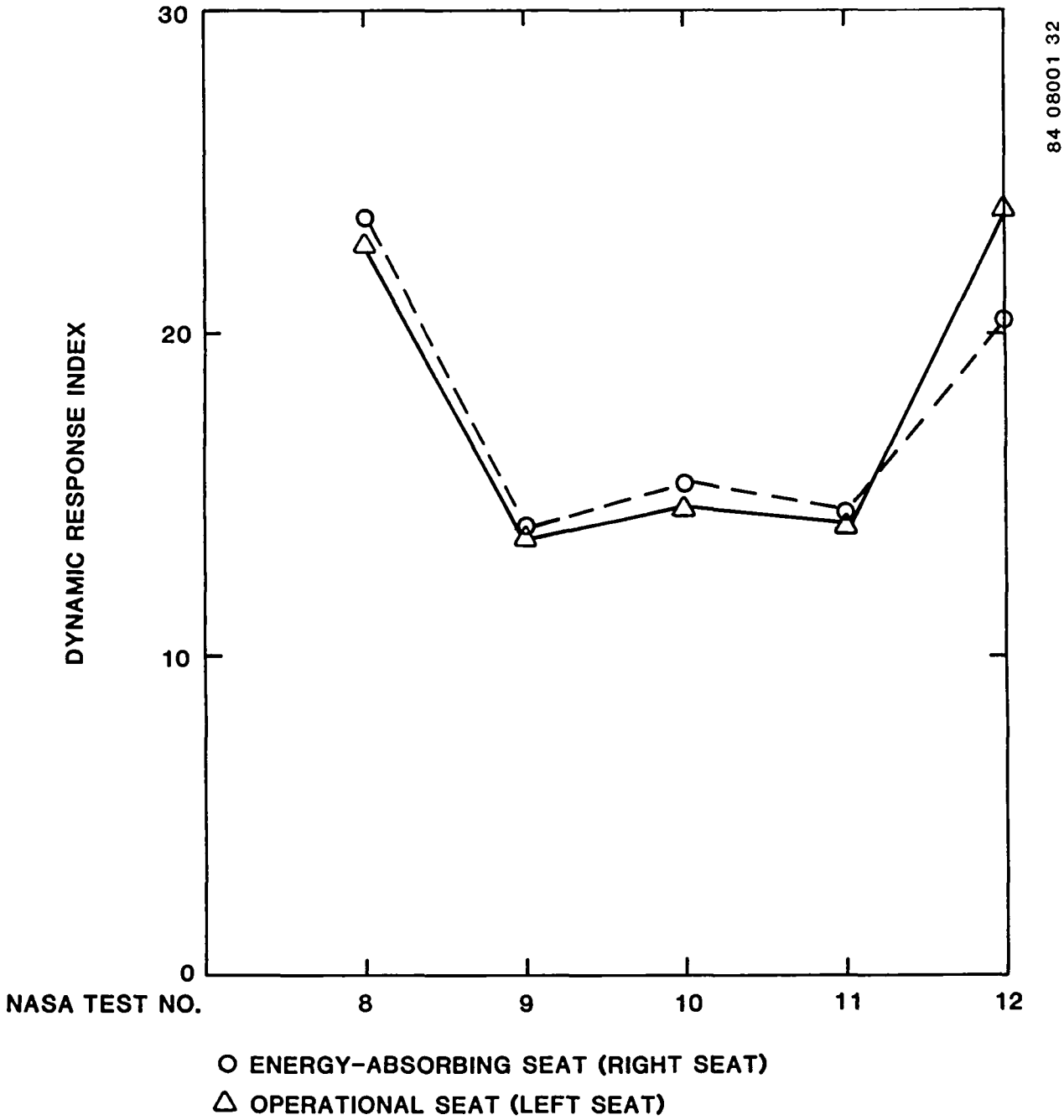

Figure 73. Seat back tangent line Dynamic Response Index (DRI) measurements in module drop tests.

4.3.4 Vertical Stroking

The vertical stroke measured in each of the 12 tests is listed in Table 24. As would be expected, the higher stroking distances were recorded in the more severe swing tests. The maximum stroke was recorded in Test Number 2, where the right seat bottomed out after 7.75 in. of stroke. Depending on the seat position, 6 to 11 in. of vertical stroke would be available with a retrofit

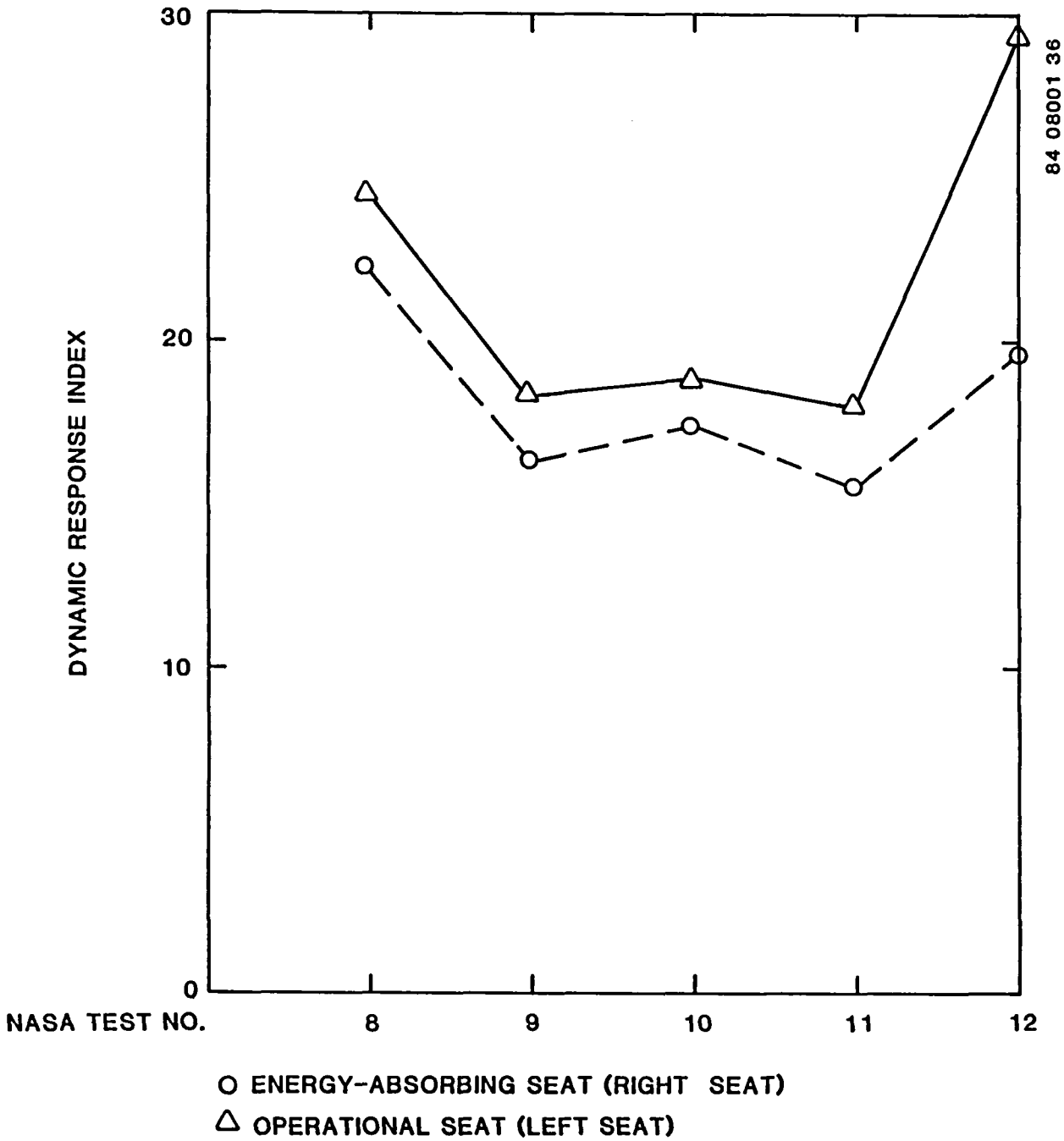

Figure 74. Dynamic Response Index (DRI) measurements from pelvis z-axis accelerations in module drop tests.

seat. Because of the test seat pan configuration, less stroke was available with the test seat in the full-up position than would be available with a retrofit seat in the full-up position. The retrofit seat would need to have been in the top half of the adjustment range to provide room enough to prevent bottoming out in Test Number 2. Other tests where the seat would need to have been above the minimum position are Test Number 5 (the right seat) and Test

TABLE 23. PEAK SEAT PAN LOADS RECORDED DURING MODULE TESTS

NASA Test Number	Operational F-111 Seat (Left Side)				Energy-Absorbing Test Seat (Right Side)			
	Left (lb)	Center (lb)	Right (lb)	Total(1) (lb)	Left (lb)	Center (lb)	Right (lb)	Total(1) (lb)
8	400	2481	213(2)	3079	339	1578	326	2239
9	270	1357	85	1708	(3)	1334(2)	397	-
10	265	1413	131	1790	533	1194	322	2031
11	242	1319	111	1665	282	1334	342	1950
12	386	2166	211	2750	333	1595	411	2339

(1) Total is maximum summation of all load cells at one time.
(2) Raw data used to obtain load.
(3) Lost data channel.

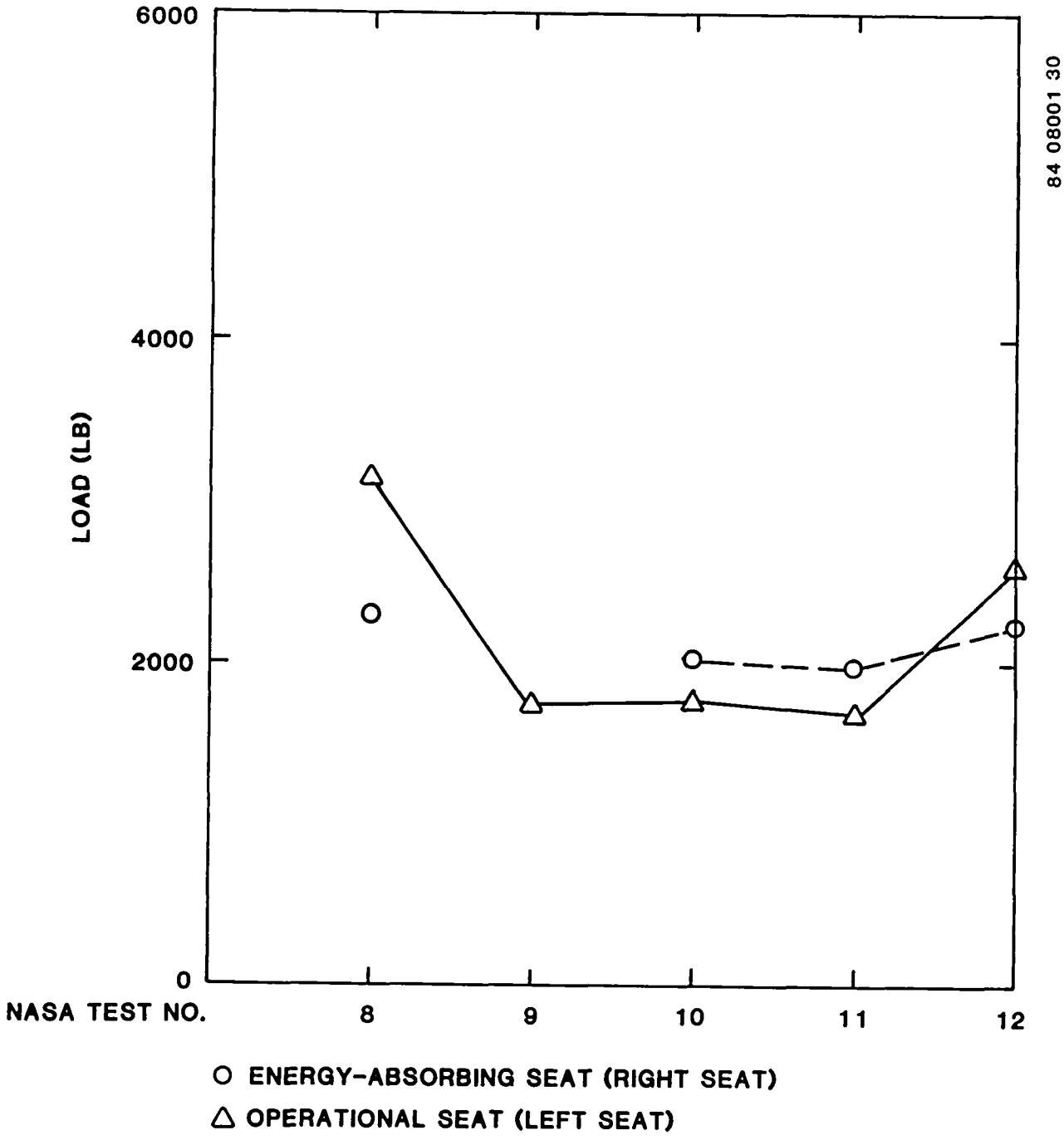

Figure 75. Comparison of total seat pan loads in module drop tests.

Number 6 (both seats), measuring 7.72, 6.45, and 6.00 in. of stroke, respectively. However, it must be remembered that these swing test conditions represent the outer edges of the design envelope. Even in these cases, the majority of occupants required between 1 and 6 in. of stroke. Under typical capsule operation, enough stroke would most likely be provided even at the lowest seat adjustment position.

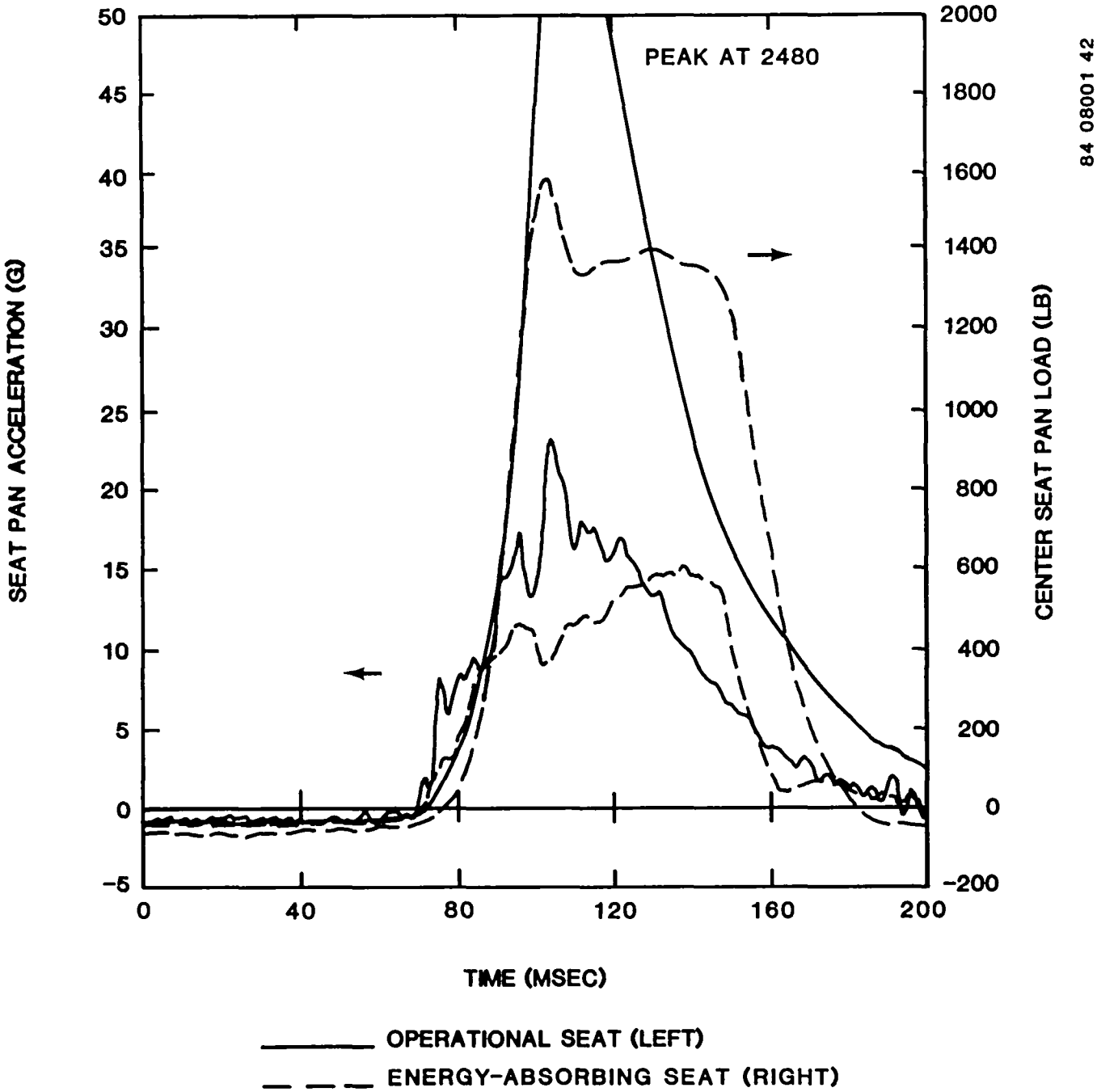

Figure 76. Seat pan z-axis acceleration and center seat pan vertical load for NASA Test Number 8 (32-ft/sec drop test).

Stroking distances for the vertical tests are also shown in Table 24. The high-velocity drops required about 2 in. of stroke, while the low-velocity drops required little or no stroke. This is consistent with the previous acceleration and seat pan load data that has already been presented. In the low-velocity drops, the energy-absorbing capability of the test seat was not required. Thus, there is not a noticeable difference in the performance of the

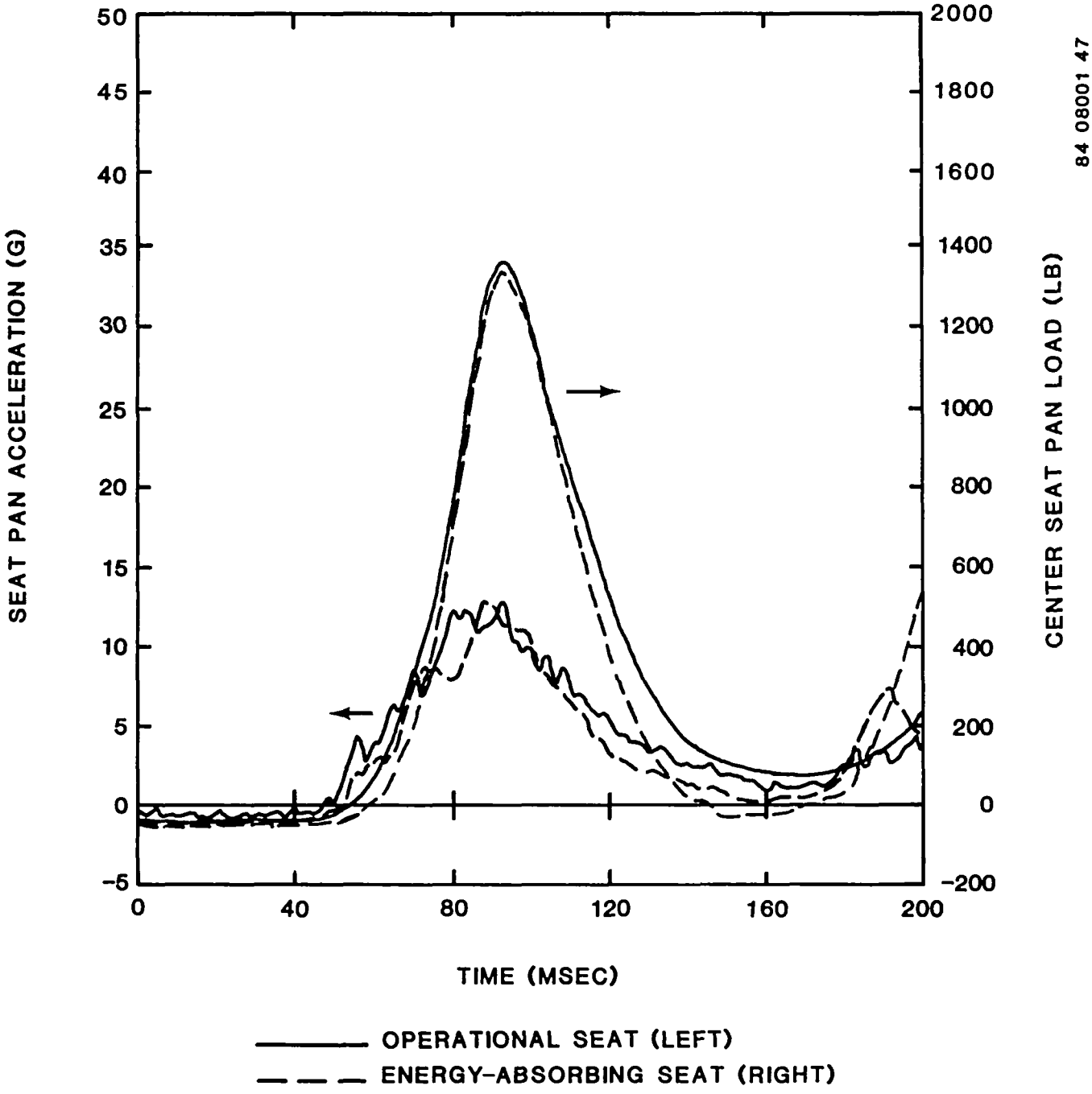

Figure 77. Seat pan z-axis acceleration and center seat pan vertical load for NASA Test Number 9 (25-ft/sec drop test).

energy-absorbing and operational seats. When the descent velocity is increased, the energy-absorbing characteristic of the test seat is needed. At this time, the differences in the two seats become apparent. Acceleration levels and seat pan loads both show the performance of the energy-absorbing seat to be an improvement over that of the operational seat.

TABLE 24. VERTICAL STROKE MEASURED DURING CREW MODULE TESTS

NASA Test Number	Left Seat Vertical Stroke (in.)	Right Seat Vertical Stroke (in.)
1	1.5	2.25
2	3.1	7.75(1)
3	1.25	5.25
4	3.15	5.30
5	3.15	7.70
6	6.00	6.45
7	0.75	1.25
8	-(2)	1.75
9	-(2)	0
10	-(2)	0.15
11	-(2)	0.05
12	-(2)	2.30

(1) Seat bottomed out.
(2) Operational F-111 seat.

The ideal descent of the capsule, pure vertical with no wind, required 2 in. of energy-absorbing stroke. Ground impacts under conditions on the edges of the design envelope required from 1 to 8 in. of stroke. The very low stroke was required when the capsule landed at an attitude yawed 180 degrees to the velocity vector. Thus, the energy-absorbing seat would be beneficial in the large majority, if not all, of the ground impacts. The chances of an occupant having his seat below the mid-height position and landing in an impact severe enough to require more than the available stroke, appear to be small. A study of the recorded impacts would have to be made to determine actual statistical relationships.

4.3.5 Structural Integrity

Maintenance of the seat during the capsule test series consisted of the planned replacement of stroked energy absorbers, and the replacement when necessary of rollers and bolts from the bearing assemblies. None of the four energy-absorbing test seats used suffered any structural damage during the test series.

The bulkhead modification used to mount the test seat is not the same modification that would be used for a retrofit seat. However, this modification carried loads up into the sill stiffener that runs across the capsule behind the seat. In a retrofit seat this same sill stiffener would be required to carry loads from the retrofit seat. Neither the sill stiffener, nor any of the bulkhead mounting points for the roller bearings, showed signs of deformation or any loss of structural integrity during the test series.

4.4 CONCLUSIONS

The NASA data provide justifications for the following conclusions:

- On the average, module test conditions at NASA resulted in more severe bulkhead accelerations than were simulated in corresponding tests conducted at CAMI.

- The present IAB is very efficient in pure vertical drops. Under conditions simulating high-wind drift and capsule swing, the efficiency of the bag decreases significantly for one or both occupants.

- Wind drift and capsule swing can cause the ground impact deceleration pulse experienced by one occupant to be much more severe than that experienced by the other occupant.

- The Eiband criterion does not show a hazardous condition in either the 25 or 32-ft/sec pure vertical impact conditions.

- Peak acceleration levels for the energy-absorbing seat were consistent with other successful energy-absorbing seats.

- DRI measurements from seat pan accelerations for the energy-absorbing seat in the swing tests were consistently between 20 and 23. These are higher than the values recorded at CAMI, but are still consistent with proper operation of an energy-absorbing seat load limited to 14.5 G.

- Peak acceleration levels, DRI, and seat pan loads show an improvement with the energy-absorbing seat for pure vertical drops at 32 ft/sec, but no significant differences in pure vertical drops at 25 ft/sec.

- The maximum vertical stroke required was approximately 8 in. Since between 6 and 11 in. of stroke would be provided in a retrofit seat, a retrofit seat would need to have been in the top half of the vertical adjustment range to provide this much stroke.

- Neither the seat nor the module bulkhead suffered any structural damage during the testing.

5.0 RETROFIT SEAT

Before a seat was designed for the dynamic tests conducted at CAMI and NASA, various concepts were considered for a retrofit energy-absorbing seat. The concepts considered such options as:

- Whether or not the existing tracks could be used
- Where the inertia reel should be mounted
- How the vertical adjustment mechanism would be attached to allow space for the energy absorbers
- Whether the bearings should be on the seat, the bulkhead, or another structure between the seat and bulkhead
- How the headrest and seat pan adjustments would be provided.

Several ideas for how to provide the energy-absorbing stroke were also examined. These included guiding the seat vertically using round tubes, square tubes, or I-beams. Rotating links guiding the seat as it moved along an arc were also examined.

After a thorough examination of these and other factors, a concept for a retrofit seat was chosen. Based on this concept, the test seat described in Section 2.3 was designed and built. The guidelines for the design of the retrofit seat are discussed in Section 5.1, while Section 5.2 presents a more detailed description of the concept for a retrofit seat.

The design described in Section 5.2 is not a carefully refined design. It does present the best concept for a retrofit seat based on the space and weight limitations of the existing seat and the requirement to provide some of the same characteristics that exist in the present operational seat. If a retrofit seat were to be developed, a specification for this seat would be required. Then the conceptual design could be examined and changed when necessary, various parts could be sized, and a proposal for a retrofit seat could be initiated.

5.1 DESIGN GUIDELINES

Three seats are discussed in this report: the operational seat, the energy-absorbing test seat, and an energy-absorbing retrofit seat conceptual design. Although the design guidelines for both the test and retrofit seats were based on the operational seat, there are some differences between the requirements for the two seats. Therefore, the design guidelines for the retrofit seat are discussed before the conceptual design is presented.

As mentioned earlier, there is no specification for the design of an energy-absorbing seat for the F-111 aircraft. The design guidelines presented here come from evaluations of both the hardware and specifications currently used. The operational seat was examined for characteristics that have proven worthwhile and should be maintained in a retrofit seat. The F-111 crew module was thoroughly scrutinized to define the space limitations inherent in the design of a retrofit seat. Specifications for ejection seats (MIL-S-9479, Reference

18) and escape modules (MIL-C-25969) were also inspected for requirements that might be imposed on a new seat.

The requirements considered were of a general nature: anthropometric requirements for the seat back angle, headrest, etc. Knowledge of these facts was necessary to analyze the space available in the crew module. Strength requirements of the seat under specific loading conditions were not rigorously defined.

The resulting design guidelines for a retrofit seat include the following requirements for the seat adjustment system:

- Five inches of vertical (along the bulkhead reference line) adjustment
- Five inches of fore and aft adjustment of the seat pan
- A power screw vertical adjustment mechanism.

The 5 in. of vertical adjustment is necessary to allow pilots to properly position the seat with respect to the design eye point. Since the rudder pedal adjustment is limited, the horizontal adjustment in the seat pan is necessary to properly position the rudder pedals for pilots.

In the present configuration of the operational seat in the F-111 capsule, the headrest remains at a constant height, and is adjustable in the fore and aft directions. As discussed in Section 2.1, moving the headrest also adjusts the seat back angle. Behind the headrest, the power haul-back inertia reel is mounted to the bulkhead. Since these design features did not have any inherent advantages, the design guidelines for the retrofit seat did not require them. Rather, the design guidelines required that:

- The headrest be attached to the bulkhead or the seat; however, proper head suppport at all adjustment locations and throughout any vertical energy-absorbing stroke must be provided.
- The inertia reel may be mounted on the bulkhead or the seat; however, proper restraint at all adjustment locations and throughout any vertical energy-absorbing stroke must be provided.
- The seat back should provide a 13-degree back angle, either as a fixed back or as one of the adjustment positions.

Other design guidelines concerned the entire escape system:

- The seat design must allow access to survival gear stored behind it.
- Aircraft modifications are to be kept to a minimum.

If access to the survival gear was not required, the overall performance of the escape system would be degraded, and the retrofit seat design would be unacceptable. Any other modifications to the aircraft that are necessary to install the seat but degrade overall capsule performance would also be unacceptable. Keeping the aircraft modifications to a minimum also keeps retrofit costs to a minimum.

5.2 SEAT DESCRIPTION

5.2.1 Overall Description

A layout of the conceptual design for the retrofit seat is presented in Figure 78. The same seat would be used in both the pilot and weapons system officer positions. The seat consists of four major subassemblies:

- Linear bearings
- Energy absorbers
- Carriage and guide tubes
- Seat pan and back.

The linear bearings provide an interface between the seat and bulkhead. The energy absorbers would be attached to the vertical adjustment mechanism and support the seat in the vertical direction during normal flight. The carriage and guide tubes would provide both the basic load-carrying structure in the seat and the means for horizontal adjustment of the seat pan and headrest. The guide tubes slide inside the linear bearings during vertical adjustment and energy-absorbing stroke. The seat pan and back assembly would provide the structure that comfortably supports the occupant during flight. One can see that the retrofit seat would use the same guided stroke concept and would interface with the bulkhead in the same way as the test seat.

The linear bearings that would be used on a retrofit seat are not the roller bearings that were used on the test seat and described in Section 2.3. The retrofit bearings would have a Teflon-impregnated liner mounted in an aluminum housing. The liner provides a smooth sliding surface for the guide tube during vertical seat adjustment and energy-absorbing stroke. These bearings require much less room and are lighter than the roller bearings used on the test seat. The small size of these bearings allows the retrofit seat to be mounted much closer to the bulkhead than the test seat.

The linear bearing assemblies would be attached to the bulkhead in the same four locations used by the test seat. Prior to seat installation, fittings would be bolted to the bulkhead at each attachment point. The linear bearings would already be on the seat, so that when the seat was placed in the aircraft a single pin would attach the bearing to the fitting on the bulkhead. Hardware mounted on the bulkhead is discussed further in Section 5.2.2.

The back view of the seat in Figure 78 shows the variable-load energy absorber system supported by the vertical adjustment mechanism. The power screw mechanism shown attached to the bulkhead is the one presently used on the seat, but the energy absorber subassembly could be designed to incorporate a different mechanism.

In order to provide the best protection in the most severe ground impacts, the criterion for determining the load at which the vertical energy-absorbing system should stroke was established as the maximum load tolerable by the occupant. The maximum load was selected so that the system could absorb the maximum amount of energy within the limited stroke distance. Based on experience

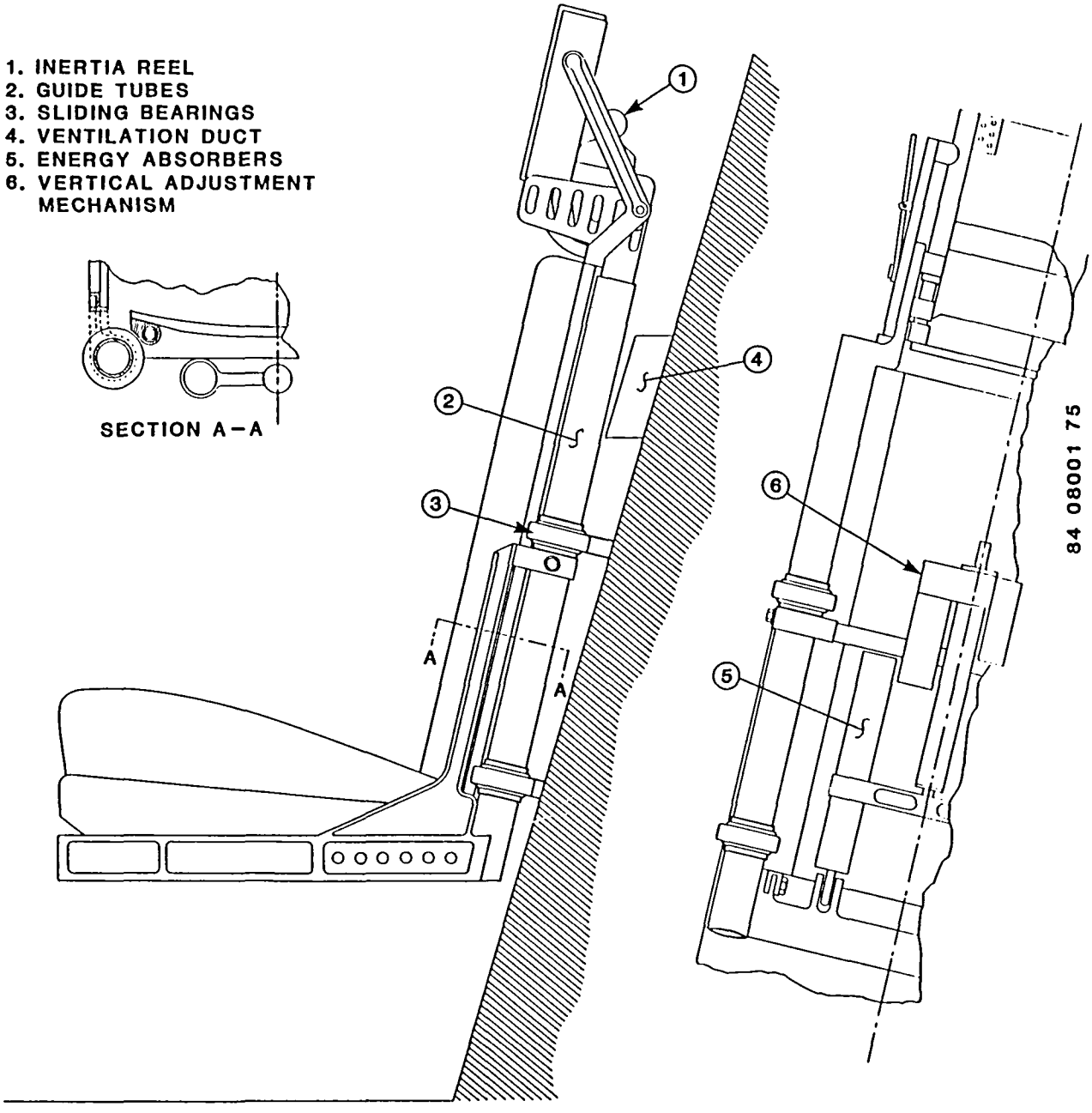

Figure 78. Conceptual design of energy-absorbing retrofit seat for F-111 crew module.

with seats for several military helicopters, including Sikorsky's UH-60A Black Hawk, a 14.5-G load factor was used in the test seat. In the retrofit seat, the variable-load adjustment mechanism would enable all occupants from the 5th- to the 95th-weight percentile to adjust the system to provide the 14.5-G load factor.

In the retrofit seat for the F-111 aircraft, the variable-load inverted-tube-type energy absorbers are installed between the vertical adjustment mechanism and the guided seat pan carriage. These energy absorbers function in the same manner as on the test seat: the tubes elongate when the inertial loads from the movable part of the seat and the effective mass of the occupant reach the load factor of the energy absorbers. The seat strokes until the inertial loads decrease or the seat hits the floor. Deceleration spikes will exceed 14.5 G because of the dynamic response of the occupant/seat system. Unlike the test seat, a pin would be incorporated into the bottom end of each energy absorber of the retrofit seat. The pin would remain in place, preventing seat stroke during the first phase of the escape sequence, when the rockets carry the capsule away from the aircraft. The pin would then be removed before ground impact. Thus, the energy-absorbing stroke would be available to protect the occupant during the ground impact phase. The pin could be removed pyrotechnically or manually. A pin puller could be connected to the existing pyrotechnic system on the aircraft, enabling the pin to be removed automatically. Manual removal of the pin could be used either as the primary method of removal, or as a secondary safety measure. Since no final decision on these requirements has been made, the pin is not shown in the layout.

The seat carriage and guide tube assembly provide most of the major load-carrying structure of the seat. The carriage would consist of identical aluminum forgings for the left and right side, joined by sheet metal along the bottom to form a "pan", and heavier structure including hard points for the mounting of the energy absorbers along the back of this pan. Holes in each side of the carriage will be provided for horizontal adjustment of the seat pan. Each of the left- and right-side forgings attaches to a guide tube in two places: at the bottom and at a point almost midway up the tube.

The guide tubes will be heat-treated steel. The tubes are plated for protection from corrosion and coated to provide a smooth surface for the bearings. The tubular shape is needed to support the high bending loads from the inertia reel and the carriage. At the top of each guide tube an aluminum fitting would be provided for mounting the power haul-back inertia reel. The inertia reel presently used with the operational seat is shown in the layout; however, the upper guide tube fittings could be modified to use a different reel. These fittings also have slots for horizontal adjustment of the headrest. Slots are necessary instead of holes because the headrest is adjusted independently of the seat pan.

The mounting points for the reflected straps could be on the upper guide tube fittings or the top of the seat back. The guide tube mounting provides a more direct load path; if the straps were connected to the top of the seat back, the loads would go through the headrest adjustment mechanism. However, mounting the straps to the seat back may provide better restraint over the full range of seat positions. Some layouts, with the seat in various positions, would be done to determine the best attachment point for the reflected straps. In either case, the inertia reel loads and the headrest loads would be carried to the guide tubes through the upper guide tube fittings.

The seat pan and back assembly provides the interface between the occupant and the seat. This assembly would consist of the seat pan and seat back, hinged together by two pins, with the headrest mounted on top of the seat back.

The seat pan could be either aluminum, a fabric-reinforced laminate, or a combination of the two types of materials. Horizontal adjustment and attachment of the tiedown strap would be similar to the operational seat. There are two options for the top of the seat pan. It could be flat and covered with strips of Velcro tape. In this case, the contour required to provide maximum comfort to the pilots would be formed in a hard foam in the bottom of the seat pan cushion. The alternate option could have a comfort contour molded into foam and bonded to the top of the seat pan, as is done on the operational seat. In either case, the seat pan cushion would be designed for both maximum comfort and protection during ground impact.

The seat back would be hinged to the seat pan in the same manner as the operational seat. Aluminum tubes would be supported above each of the hinge points, and a contoured aluminum sheet would join the tubes to form the seat back. The seat back cushion would be similar to that in the operational seat, but the cushion shape would be contoured to match the seat back. Support along the seat back will be provided to the maximum height possible. Layouts will have to be made to determine the optimum height of the inertia reel, positions and of the reflected straps, and support height of the seat back for the wide range of seat positions and occupant sizes. Improvements over the operational system, which has low reflected-strap attachment and seat back support heights, would be made.

The headrest would be attached to the top of the seat back at a fixed height above the seat reference point. To provide maximum visibility, the shape of the support surface on the operational seat would be retained. The length of the headrest would be that necessary to provide support for the specified range of occupant sizes. Cushioning such as that on the operational seat should be provided. Headrest adjustment would be accomplished by a lever beside the headrest; movement of the headrest is on an arc around the hinge point between the seat back and pan.

Position of the headrest contact surface would be approximately 1-1/2 in. in front of the seat back tangent line. This is further forward than the requirements of References 9 and 18, which place the headrest contact surface 1 in. aft of the seat back tangent line. However, further movement aft of the headrest is prevented by the inertia reel. If a smaller inertia reel could be used, the headrest could be moved back to a preferred position. However, this headrest position is not unlike the position in the operational seat.

In comparing the operational seat to the retrofit seat, one can see that the operational seat pan carriage has been replaced by a lighter version; the same applies to the seat back and headrest assemblies. The structure on the bulkhead supporting the headrest and inertia reel has been completely removed. On the other hand, the retrofit seat adds guide tubes with fittings, energy absorbers, and linear bearings. If the inertia reel and power screw mechanism were replaced by lighter versions, then the retrofit seat could use steel guide tubes and be built at approximately the same weight as the present operational system. If the present inertia reel and power screw mechanisms are to be used, the guide tubes would be made out of aluminum with internal stiffening structure. This is a lighter albeit more expensive method of producing the guide tubes.

This section has presented an interpretation of the retrofit seat, and has presented improvements that would be made to the operational seat's restraint system and general occupant interface. The configuration shown in Figure 78 satisfies the design guidelines and provides the vertical energy-absorbing feature for ground impacts. Obviously, the prototype design process would examine the system in more detail. A new seat pan cushion could provide better protection at ground impact with no sacrifice in comfort. Further layouts would be needed to define the inertia reel/seat back interface, the headrest adjustment mechanism, and the energy absorber release mechanism, as well as many other items. These layouts would show where further improvements could be made. If possible, the inertia reel and power screw mechanism should be replaced by newer versions.

5.2.2 Bulkhead Attachment

Obviously, implementation of the retrofit seat would require some modifications to the capsule bulkhead. The modifications would be made to the same portions of the bulkhead that were modified for the capsule test series. However, the modifications necessary for a retrofit seat would be considerably different than those made for the test series. The modifications for the test series were conservatively designed for several reasons. There was not enough time in the program to rigorously analyze the load-carrying abilities of the capsule bulkhead. Also, the modification hardware was manufactured with cost in mind. Extra machining operations that could have reduced the weight were eliminated in favor of keeping costs to a minimum. Finally, the guide tubes on the test seat were farther from the bulkhead than they would be on the retrofit seat. The guide tubes were positioned in this manner for two reasons. Firstly, the configuration of the test seat, using the operational seat back and large roller bearing assemblies, required the bearings to be further from the bulkhead. The retrofit seat would use a contoured seat back and sliding bearings. Secondly, the test series at NASA required that the modifications to the aircraft not destroy the capability of mounting the operational seat in the capsule. Thus, the tracks could not be removed. In order to allow the seat to stroke to the floor without hitting the seat tracks, the guide tubes were pushed out slightly further from the bulkhead. The retrofit seat is not limited by these requirements; thus, the guide tubes will be mounted much closer to the bulkhead.

Moving the guide tubes closer to the bulkhead requires the removal of some structure. First, the lower sets of tracks need to be removed in each seat location. These tracks interfere with the seat stroking fully to the floor. Also, with a retrofit seat, the tracks serve no function; they are therefore unnecessary weight. Second, the front portion of the air vent behind each seat position must be removed, as they were for the capsule test series. The parts are formed sheet metal held in place by screws, and could easily be replaced by a flat piece of sheet metal, with a minimal effect on the efficiency of the system.

The four lower bearings would be mounted in the same positions as the test seat bearings were mounted. A large part of the material in the upper set of tracks could be removed, leaving only enough track to assist in attaching the fitting. The structure around the upper track supports a large portion of the loads from the operational seat. Thus, it is strong enough to support the lower bearing loads on the retrofit seat with no additional stiffening structure.

The upper bearings would be more difficult to mount because of the pyrotechnic tubes, wire bundles, and other items that are mounted on the bulkhead in this area. Each of the four upper bearing attachments is discussed separately.

Figure 79 shows a sketch of some of the typical hardware behind the pilot's seat in an F-111 aircraft. Obviously, in order to mount the bearings on the bulkhead, some changes will need to be made. Item 1 in Figure 79 is the chaff dispenser. At the present time this is not being used; it may be possible to remove it. If not, a small change in tubing could move the switch slightly down on the bulkhead to clear the area for mounting the bearing, and slightly inboard to allow the pilot access to the switch by reaching around the guide tube. The plate running across the opening (Item 2 in Figure 79) serves as a support for both pyrotechnic tubing and a box-shaped clamp (Item 6). It would be necessary to redesign this support so that the clamp could be moved to allow for mounting of the bearing fitting and to interface with additional structure added behind the bulkhead extrusions (Items 3 and 4). The same support now given the pyrotechnic tubes could be provided. The large tube (Item 5) visible on the inboard side would need to be rerouted slightly so that it passes either above or below the bearing fitting.

Figure 80 is a view of the outboard upper bearing attachment that was used in the test series on the pilot side. For the retrofit seat, the bearing position would be much closer to the bulkhead. The stiffener would be a square aluminum tube traveling from the bearing up to the stiff structure at the bottom of the lateral vent. Some grinding at the ends of the channels that support the nitrogen bottles would be necessary, but the function of the channels would not be impaired. The existing rivets would be removed and replaced with blind rivets, joining the existing bulkhead extrusion and the bottle supports to the added stiffening structure. The area below the vent is free of pyrotechnic tubing. Thus, a fitting could be added in the area just below the vent and in front of the bulkhead reference line to join the added tubing and the bulkhead extrusion to the strong vent structure.

It is more awkward to add structure to support the upper inboard bearing on the pilot side; fortunately, less structure is needed. Figure 60 shows a front view of the pilot-side modifications for the test series. The bulkhead extrusion on the inboard side is already tied in to the box structure in the middle of the capsule. Thus, the inboard structure is already stiffer than the outboard structure. The triangular stiffeners used in the test series, shown in Figure 80, would be suitable for adding to this bulkhead extrusion. Several of these would provide the stiffness necessary to carry the loads. At the point where the bulkhead extrusion and the vent structure meet, some pyrotechnic tubes pass in front of the bulkhead reference line. Therefore, it is best to keep in mind two possible methods of adding a fitting that strengthens the attachment between the bulkhead extrusion and the vent. One option would be a fitting in front of the bulkhead reference line in the crotch formed between the two parts. If this is not possible, the fitting could sit behind the bulkhead reference line (at Item 3 in Figure 79) and extend towards the clevis (Item 7 in Figure 79) at the seat centerline. Where appropriate, it would extend in front of the bulkhead reference line and be attached to the vent structure.

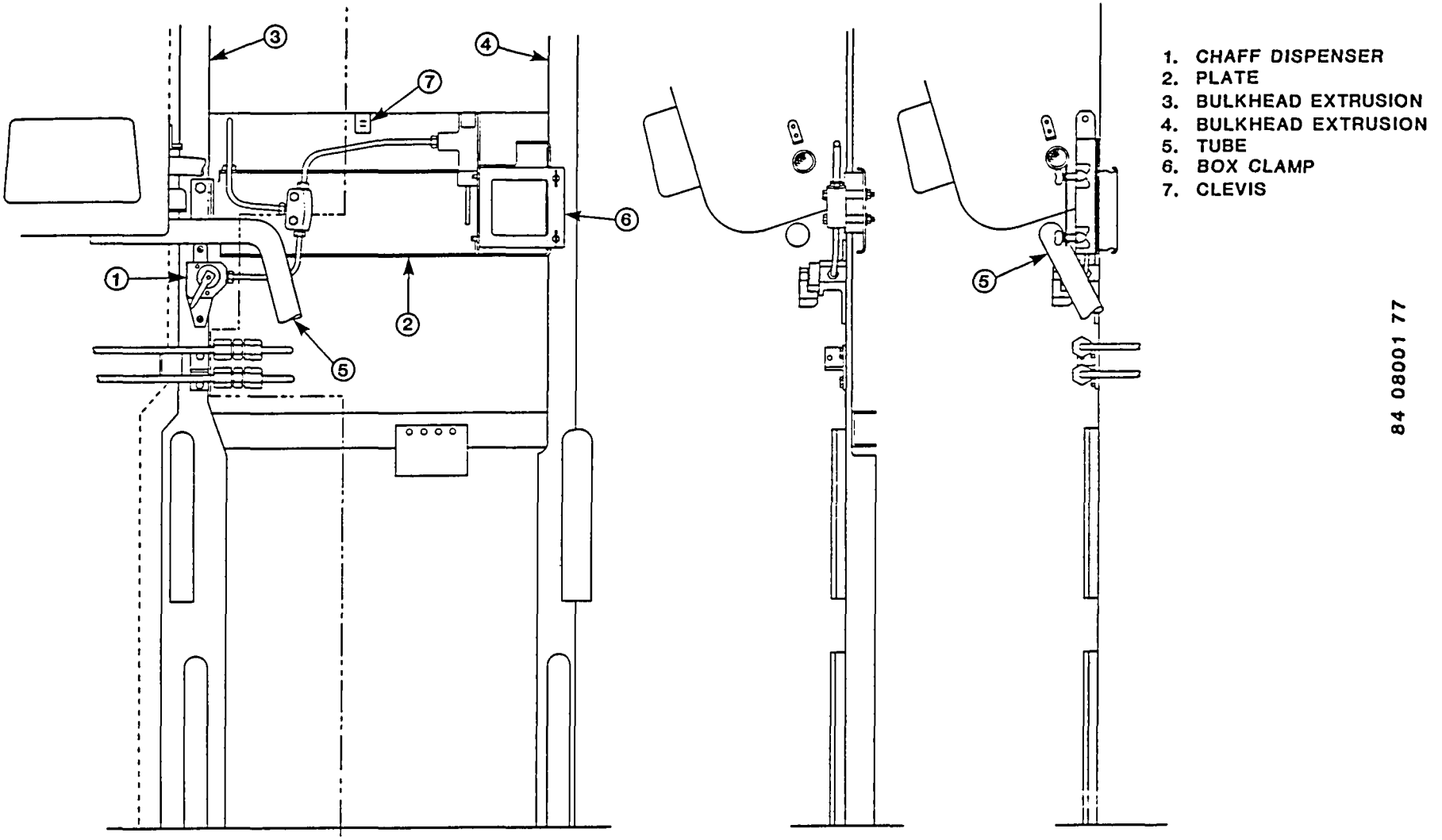

Figure 79. Hardware behind pilot's seat in some F-111 aircraft.

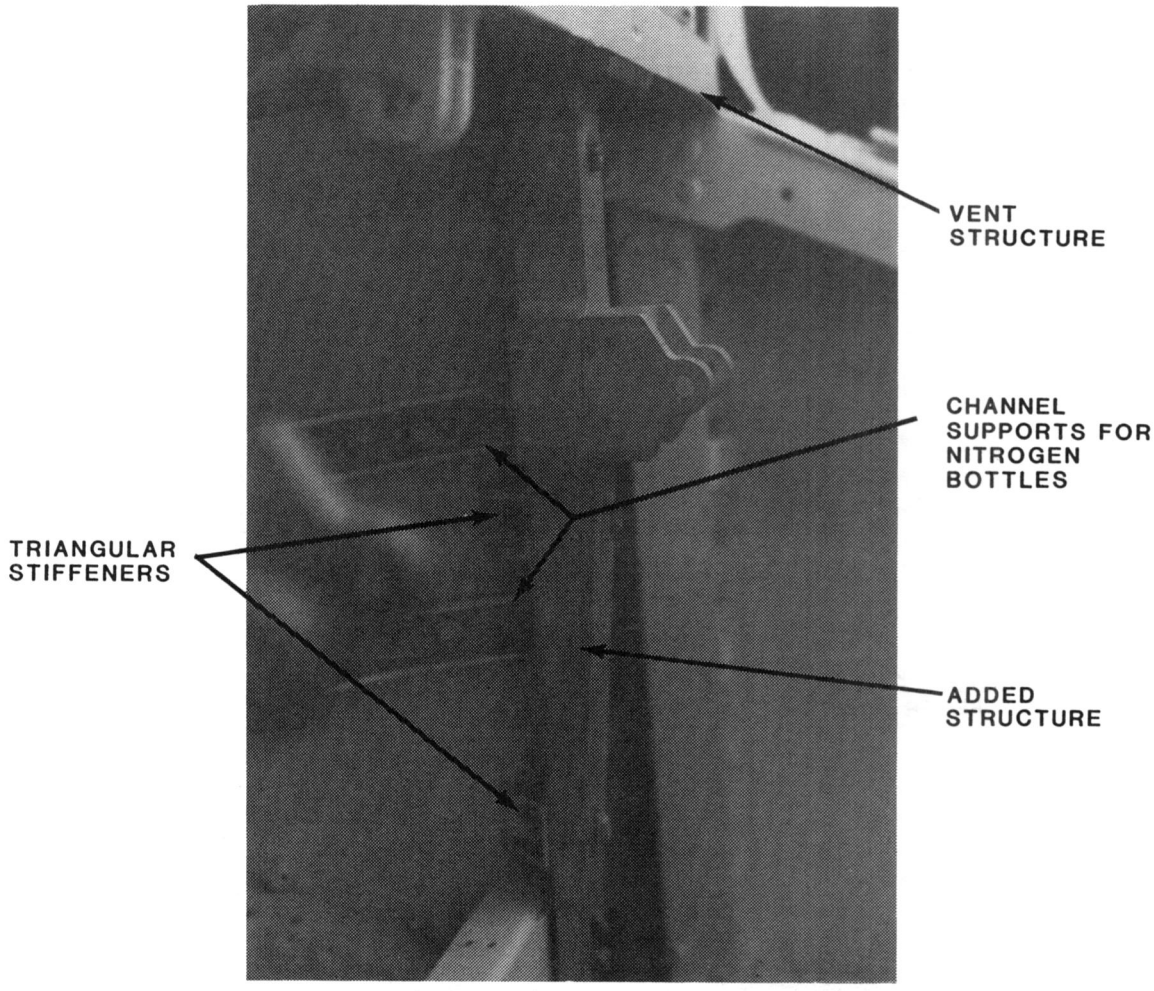

Figure 80. Upper bearing attachment on pilot outboard side during crew module tests.

Figure 62 shows a view of the outboard structure used on the weapons system officer (WSO) side of the aircraft during the capsule tests. The stiffener placed behind the bulkhead extrusion in this position would be similar to that used on the pilot outboard side. If necessary, a channel stiffener running from the bulkhead extrusion to structure at the back of the compartment could also be added. This would carry loads in the same manner as the already existing bottle supports on the pilot side. A tube runs across the area in the crotch of the bulkhead extrusion and the vent. Therefore, the top fitting must be behind the bulkhead reference line. However, on this side of the aircraft, the top of the compartment behind the seat is open. Thus, the fitting can remain behind the bulkhead reference line and still attach to the lower vent structure.

The inboard stiffener on the WSO side used for the capsule test is shown in Figure 81. This would be replaced by the diagonal stiffeners also used on the pilot side. One can see that there is already a stiffening structure running to the back bulkhead of the capsule. At the top, the fitting would also need to remain behind the bulkhead reference line, similar to the outboard fitting.

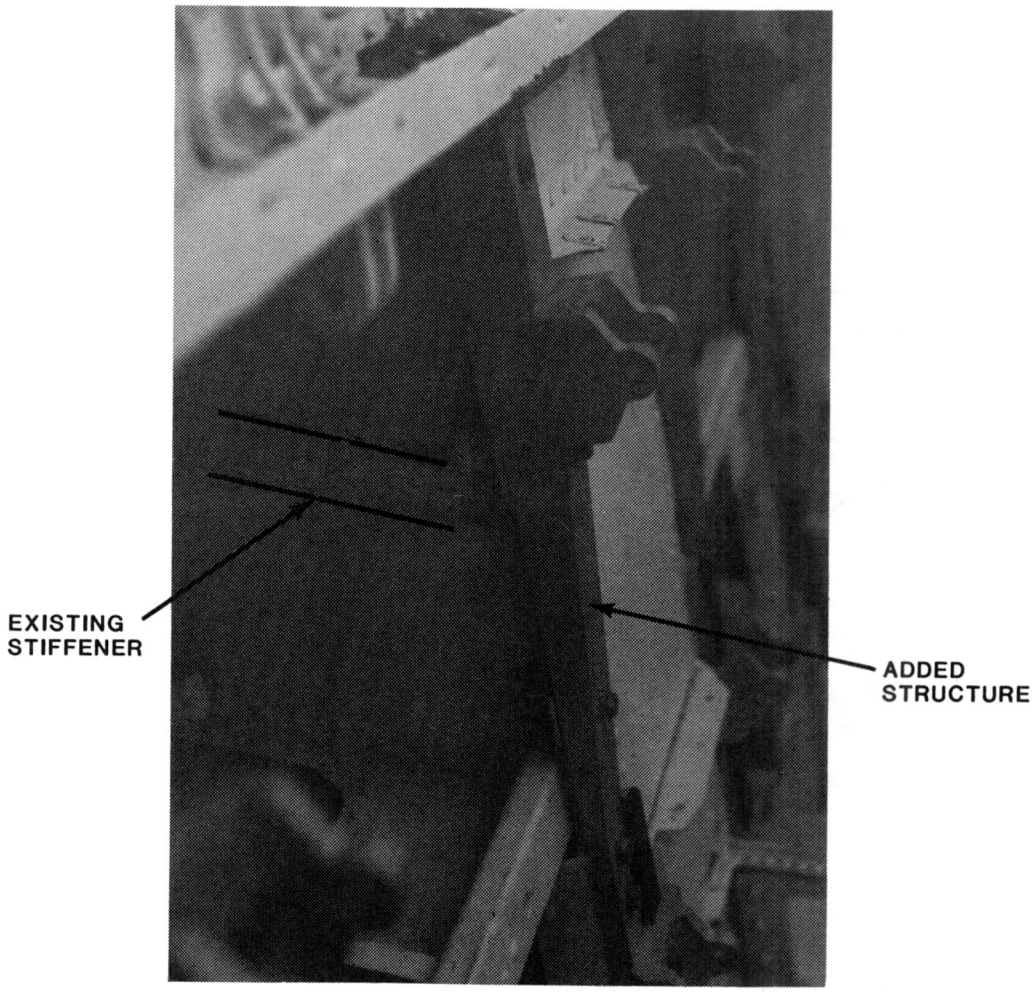

Figure 81. Upper bearing attachment on WSO inboard side during crew module tests.

In the area needed for mounting the upper inboard bearing on the WSO side, several pyrotechnic tubes run in front of the bulkhead reference line. Couplings exist in these lines very close to the bearing attachment point. It would be necessary to modify these tubes to provide room for the bearing fitting.

The two compartments behind the weapons system officer are used to store survival gear. The modifications described here would occur only in the corners of the compartments, and would not restrict access to, or noticeably change the volume of, the storage space. However, the upper compartment cover would have to be redesigned to allow clearance for the bearing fittings. Modification to the lower compartment cover may or may not be necessary.

The modifications discussed are concepts based on preliminary evaluation of the aircraft and experience gained in the test series. The estimated weight

of these modifications is approximately 2 lb. A more detailed definition of the modifications could be made after the following:

- Detailed structural analysis of the capsule
- Static tests on actual bulkheads to verify strengths
- Discussions with the Air Force to determine what modifications are the most cost effective and practical.

6.0 CONCLUSIONS

6.1 DISCUSSION

The majority of the effort put forth in this program was to conduct extensive testing. The seat tests at CAMI used estimates of the ground impact conditions to demonstrate:

- The proper operation of the energy-absorbing seat both in limiting loads and maintaining structural integrity
- Superior performance of the energy-absorbing seat when compared to the operational seat
- Adequate room for the required energy-absorbing stroke.

Even though the actual pulses at NASA were more severe than expected, the CAMI tests are still very important: they served as preparation for the NASA tests and provide excellent comparative data on the performance of the two seats. The NASA tests provided more information supporting conclusions that the seat was operating properly and that there was enough room for the needed energy-absorbing stroke in even the more severe conditions.

The severity of the present ground impact conditions was demonstrated throughout the NASA tests. With the current parachute and IAB and under the ideal impact conditions of the pure vertical drop tests, the energy-absorbing seat stroked 2 in. Under the swing test conditions, up to 8 in. of stroke was required by one of the occupants. Therefore, it is reasonable to assume that the large majority of the current ground impacts have capsule environments severe enough to require stroking of an energy-absorbing seat with 14.5-G energy absorbers. Conditions that might not require stroke are those where the capsule has a nose-up attitude and is facing aftward of any horizontal velocity vector. Both of these orientation factors would reduce the vertical component of the ground impact pulse.

The testing at NASA demonstrated that under conditions not severe enough to cause the energy-absorbing seat to stroke, the performance of the energy-absorbing and operational seats was approximately the same. However, when the conditions did require seat stroke, the improved performance of the energy-absorbing seat was evident in all cases. The CAMI tests showed lower seat pan and dummy acceleration levels, DRI values, seat pan loads, and dummy lumbar spinal loads with the energy-absorbing seat. The 32-ft/sec vertical drop tests at NASA showed similar results. In the NASA swing tests, the more severe environment resulted in slightly higher DRI measurements for the energy-absorbing seat than were recorded at CAMI. However, based on the pattern established in the other tests, one would expect that the DRI values for the operational seat under swing test conditions at NASA would be higher than those measured for the energy-absorbing seat.

Since the completion of the testing required for this program, additional swing tests were conducted at NASA to evaluate an inflatable body and head restraint system (IBAHRS). A drawing of one of the configurations of the IBAHRS system is show in Figure 82. Four swing tests featuring essentially the same test procedure used in the F-111 program were conducted. The results of one test,

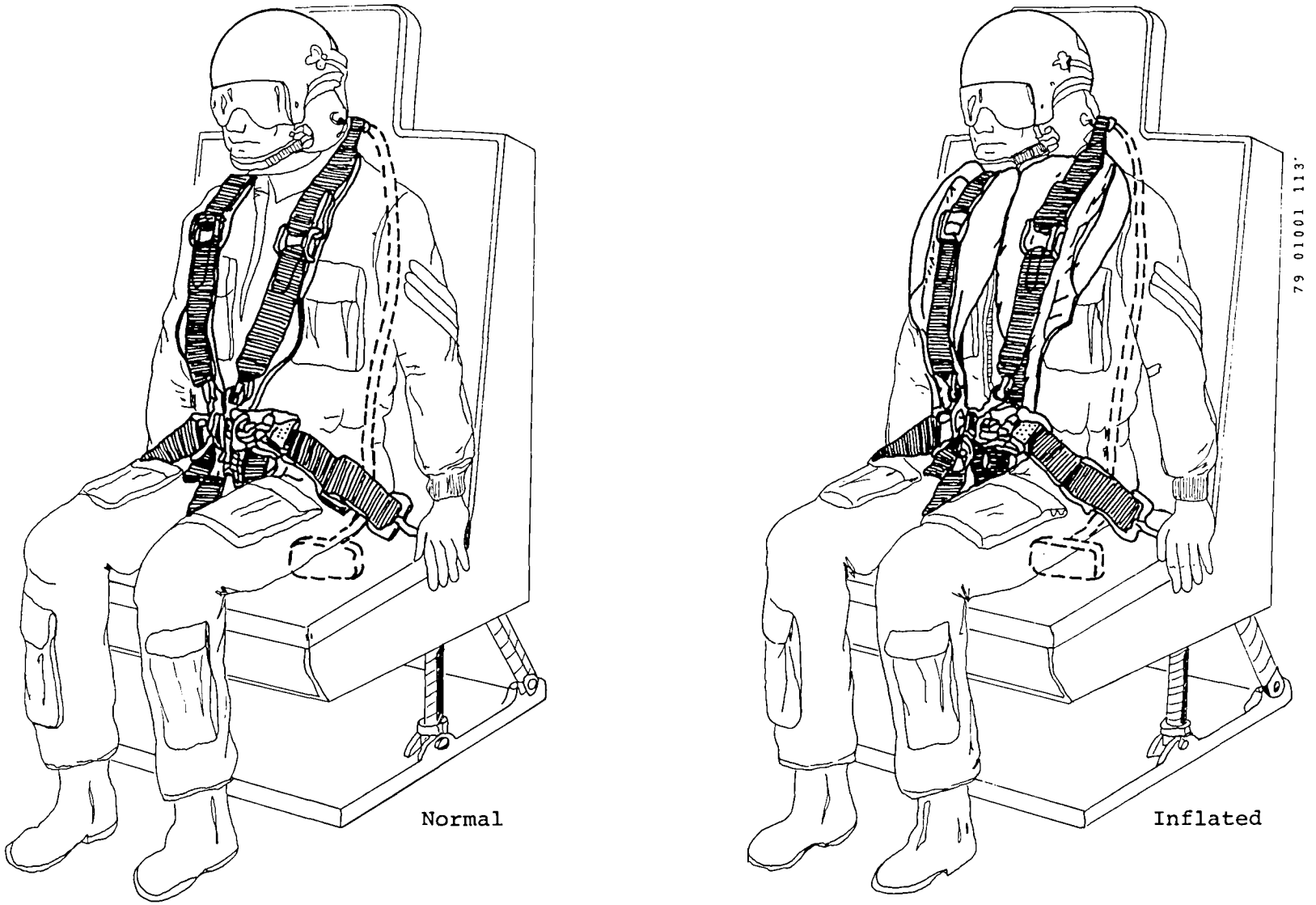

Figure 82. Inflatable body and head restraint (Reference 11).

conducted with one operational seat and one energy-absorbing seat in the capsule, are presented in Volume III. The test was conducted with the following conditions:

- Horizontal velocity: 34 ft/sec
- Vertical velocity: 32 ft/sec
- Capsule attitude

  Pitch: nose up 2 degrees
  Roll: 0 degrees
  Yaw: 0 degrees.

Under these conditions, the input pulse for both seats was essentially the same. However, the energy-absorbing seat again showed lower seat pan and dummy acceleration levels. The DRI values for the energy-absorbing seat were also much lower, with a value of 22.3 measured along the seat pan z-axis, compared to 29.6 for the operational seat.

Thus, the energy-absorbing seat featuring energy absorbers with 14.5-G load capability has shown improved performance over the operational seat under all conditions that require the seat to stroke. Also, with this energy-absorbing load there is enough space under the seat to provide the stroke required over the full design envelope of the F-111 escape system ground impact conditions. Yet a maximum DRI of 18 is required in MIL-C-25969 and could conceivably be imposed on an energy-absorbing retrofit seat as part of the specification. There are two reasons that this should not be done. First, there is no correlation of injury potential to DRI for an energy-absorbing seat that justifies a particular DRI value. For energy-absorbing seats the DRI is presently useful as a comparative tool, not an absolute measure. Second, in order to lower the DRI value for an energy-absorbing seat, the limit load of the energy absorbers would have to be reduced (see Figure 29). This increases the stroke required to absorb the energy in any particular ground impact pulse (as shown in Figure 83), and this raises the chances of bottoming out in the more severe impacts. If the seat strokes to the floor and bottoms out, there will be a deceleration spike applied to the seat. The severity of the effect of this spike will depend on the velocity of the seat relative to the floor when it makes contact. The velocity will vary with the severity of the ground impact and the amount of energy absorbed by the IAB.

Some effort was also made to evaluate the effects of a parachute replacement that would reduce the vertical descent rate from 32 to 25 ft/sec. Obviously, this would reduce the severity of the ground impact environment. However, the decrease in the efficiency of the IAB at some aircraft attitudes and horizontal velocities would still occur. In order to evaluate the benefits of an energy-absorbing seat in this system, one would have to examine the ground impact conditions over the full design envelope of the escape system. The original design envelope may be used, or perhaps more recent information on the actual conditions during previous ejections from the aircraft would be used to define a new design envelope. Caution must be exercised in not placing too much importance on previous ejection experience, gathered mainly during peacetime, to evaluate a system that must perform in wartime.

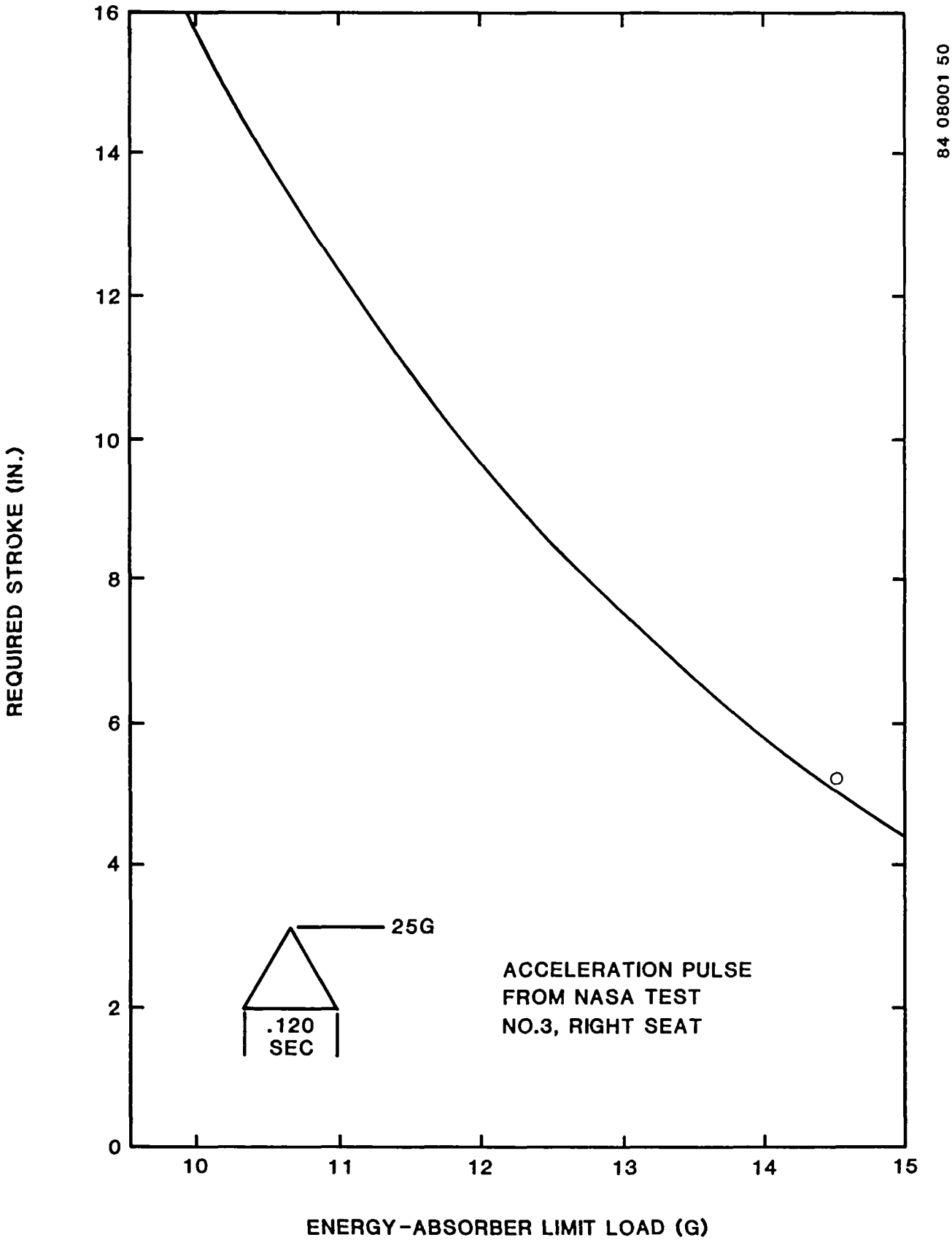

Figure 83. Vertical stroke versus energy absorber limit load (as calculated by method presented in Reference 11).

With this new and less severe environment defined, the benefits of an energy-absorbing seat could be evaluated. In this case, the possibility of reducing the energy absorber limit load and still having the required stroking distance becomes an option that could be considered. If the Air Force feels that the 14.5-G load factor is not the most efficient for the controlled ground impact of the capsule, the load factor can be easily changed in the design phase of the retrofit seat or even after seats are installed in aircraft.

6.2 CONCLUSIONS

The first conclusions concern the primary objective of the testing conducted: to determine the performance of the energy-absorbing seat over the ground impact design envelope of the F-111 escape capsule.

- The seat pan accelerations, dummy accelerations, and DRI values measured for the energy-absorbing seat are reasonable for an energy absorber limit load of 14.5 G, and therefore show the seat to be functioning properly.

- With the present escape system parachute and IAB an energy-absorbing seat, with energy absorbers limited to stroke at 14.5 G, would stroke for one or both occupants in the large majority of ground impacts.

- With a retrofit seat in the full-up position and variable-load energy absorbers set at 14.5 G, enough stroke is available to prevent bottoming out within the design envelope of ground impact conditions.

In comparing the energy-absorbing seat to the operational seat, the following conclusions can be made:

- Under conditions severe enough to cause the energy-absorbing seat to stroke, the seat pan accelerations, dummy accelerations, and DRI values show that the energy-absorbing seat with energy absorbers set for 14.5 G provides a significantly less severe environment than the operational seat.

- The seat pan loads measured at CAMI and NASA, and the dummy lumbar spinal loads measured at CAMI, all show that the energy-absorbing seat reduces the spinal loads experienced by the occupant when the ground impact is severe enough to cause seat stroke. The more severe the environment is, the greater the improvement with the energy-absorbing seat.

- Under milder conditions that would not cause seat stroke, the performance of the operational and energy-absorbing seats was approximately the same.

- The results of evaluating the data using the Eiband criterion are inconclusive. They do not show differences in performance between the operational and energy-absorbing seats that are shown by DRI, seat pan loads, and lumbar spinal loads.

Reducing the vertical descent rate to 25 ft/sec by using a new parachute will reduce the severity of the ground impact environment. However, bag efficiency will still decrease as the effects of wind velocity and direction, as well as capsule swing, become more pronounced.

6.3 RECOMMENDATIONS

Recommendations are divided into two groups, depending on whether or not the parachute is changed to a design that would reduce the descent rate. If the parachute remains the same, then the primary conclusions of this report, which illustrate the improved performance with an energy-absorbing seat, indicate that the operational seat should be replaced as quickly as possible. Therefore, the following steps should be taken:

- Prepare a specification for an energy-absorbing retrofit seat. Include the following:
  - Requirements for variable-load energy absorbers with a 14.5-G limit load
  - Requirements for a pin that fixes the position of the seat during ejection but allows energy-absorbing stroke during ground impact
  - Definition of the required static and dynamic testing of the prototype seat
  - A definition of other seat improvements where possible, such as position of headrest and reflected strap attachment points.
- Design, fabricate, and test a prototype retrofit seat.

If the parachute is modified, then the reduced descent rate will lessen the severity of the ground impact environment. However, the extent of this change is not known. Therefore, the following steps should be taken:

- Examine the history of F-111 escape capsules to obtain statistical distributions of ground impact conditions such as wind velocity, wind direction, capsule attitude, and landing surface.
- Based on escape system history (mostly during peacetime) and the performance requirements of the F-111 aircraft in a wartime situation, define the new design envelope for the improved escape system.
- Using the reduced descent rate and the varying efficiency of a new IAB, determine the ground impact environment over the new design envelope.
- Evaluate the benefits of an energy-absorbing seat over the full design envelope, considering the severity of the environment, the available stroking distance, and a suitable range of energy absorber limit loads.

One must remember that all the tests conducted in this program with the energy-absorbing seat used energy absorber limit loads of 14.5 G. Using this seat, the ground impact environment in an F-111 ejection is severe enough to cause the seat to stroke in almost every case. Also, whenever the environment is severe enough to cause the seat to stroke, the performance of the energy-absorbing seat is superior to that of the operational seat. That is, the vertical loads that the occupant experiences in the energy-absorbing seat are less than experienced in the operational seat. However, even in the most severe ground impact cases at the edge of the design envelope, if the seat starts in the top half of the vertical adjustment range, there is enough room for the seat to stroke vertically without bottoming out. Thus, an energy-absorbing seat with a 14.5-G limit load provides improved protection for the occupants of the F-111 capsule over the entire design envelope of the ground impact conditions.

If the severity of the ground impact environment is reduced, then the energy-absorbing test seat might not use all of the available stroking distance even at the edges of the design envelope. In this case, the difference in performance between the energy-absorbing seat and the operational seat could be made even greater by lowering the energy absorber limit load, since this would lower the seat pan acceleration, DRI's, seat pan loads, and dummy spinal loads measured with the energy-absorbing seat. However, the occupant must not be subjected to an injurious load from bottoming out. Care must be taken not to use all the available stroking distance and subject the occupant to an injurious load from hitting the floor before the energy in the impact has been dissipated.

7.0 REFERENCES

1. Hearon, B. F., Comparative Vertical Impact Testing of the F/FB-111 Crew Restraint System and a Proposed Modification, AFAMRL-TR-82-13, March 1982.

2. Laananen, D. H., Aircraft Crash Survival Design Guide, Volume II, Aircraft Crash Environment and Human Tolerance, Simula Inc.; USARTL-TR-79-22B, Applied Technology Laboratory, U.S. Army Research and Technology Laboratories (AVRADCOM), Fort Eustis, Virginia, January 1980.

3. Brinkley, J. W., et al, Evaluation of a Proposed, Modified F/FB-111 Crew Seat and Restraint System, AFAMRL-TR-80-52, Aerospace Medical Research Laboratory, Wright-Patterson Air Force Base, Ohio, November 1981.

4. Kazarian, L. E., et al, Spinal Injury Mechanism Assessment, AMRL-77-60, Aerospace Medical Research Laboratory, Wright-Patterson Air Force Base, Ohio, October 1977.

5. Kazarian, L. E., et al, Spinal Injuries in the F/FB-111 Crew Escape System, Aviation, Space, and Environmental Medicine, Volume 50, No. 9, September 1979, p. 948-957.

6. Ejection Experience in F/FB-111 Aircraft, 1967-1978, Proceedings of the 17th Annual SAFE Symposium, December 2 - 6, 1979.

7. Hearon, B. F., F/FB-111 Ejection Experience (1967 - 1980) Part I - Evaluation and Recommendations, AFAMRL-TR-81-113, November 1981.

8. Hearon, B. F., Mechanisms of Vertebral Fracture in the F/FB-111 Ejection Experience, Aviation, Space, and Environmental Medicine, May 1982.

9. Military Specification, Capsule Emergency Escape System, General Requirements for, MIL-C-25969 (USAF).

10. Brinkley, J. W., et al, Vertical Impact Tests of a Modified F/FB-111 Crewseat to Evaluate Headrest Position and Restraint Configuration Effects, AFAMRL-TR-82-51, Air Force Aerospace Medical Research Laboratory, Wright-Patterson Air Force Base, Ohio, August 1982.

11. Desjardins, S. P., Laananen, D. H., et al, Aircraft Crash Survival Design Guide, Volume IV, - Aircraft Seats, Restraints, Litters, and Padding, Simula, Inc., Tempe, Arizona; USARTL-TR-79-22D, Applied Technology Laboratory, U.S. Army Research and Technology Laboratories (AVRADCOM), Fort Eustis, Virginia, 1980.

12. Hearon, B. F., et al, Vertical Impact Evaluation of the F/FB-111 Crew Restraint Configuration, Headrest Position, and Upper Extremity Bracing Technique, Aviation, Space, and Environmental Medicine, Volume 54, Number 11, November 1983, p. 977 - 987.

13. Coltman, J. W., Design and Test Criteria for Increased Energy-Absorbing Seat Effectiveness, USAAVRADCOM-TR-82-D-42, Applied Technology Laboratory, U.S. Army Research and Technology Laboratories (AVRADCOM), Fort Eustis, Virginia, March 1983.

14. Military Specification, MIL-S-58095(AV), Seat System: Crashworthy, Non-Ejection, Aircrew, General Specification for, Department of Defense, Washington, D.C., August 27, 1971.

15. Eiband, A. M., Human Tolerance to Rapidly Applied Accelerations: A Summary of the Literature, NASA Memorandum 5-19-59E, Lewis Research Center, Cleveland, Ohio, June 1959.

16. Laananen, D. H., and Coltman, J. W., Measurement of Spinal Loads in Two Modified Anthropomorphic Dummies, TR-82405, Simula Inc., Tempe, Arizona; Contract DAMD17-81-C-1175, Final Report, U.S. Army Aeromedical Research Laboratory, Fort Rucker, Alabama, May 5, 1982.

17. Vaughn, V. L., and Alfaro-Bou, E., Impact Dynamics Research Facility for Full-Scale Aircraft Crash Testing, NASA Technical Note D-8179, Langley Research Center, Hampton, Virginia, April 1976.

18. Military Specification, MIL-S-9479, Seat System, Upward Ejection, Aircraft, General Specification for, Department of Defense, Washington, D.C.

Technical Report Document Page

1. Report No. NASA CR-3916	2. Government Accession No.	3. Recipient's Catalog No.
4. Title and Subtitle Design and Testing of an Energy-Absorbing Crewseat for the F/FB-111 Aircraft. Volume I—Final Report		5. Report Date August 1985
		6. Performing Organization Code
7. Author(s) S. Joseph Shane		8. Performing Organization Report No. TR-84428
9. Performing Organization Name and Address Simula Inc. 10016 S. 51st Street Phoenix, Arizona 85044		10. Work Unit No. (TRAIS)
		11. Contract or Grant No. NAS1-17387
12. Sponsoring Agency Name and Address National Aeronautics and Space Administration Washington, D.C. 20546		13. Type of Report and Period Covered Final Report May 1983 - May 1985
		14. Sponsoring Agency Code

15. Supplementary Notes

Langley Technical Monitor: Claude B. Castle
NASA CR-3917 - Volume II—Data From Seat Testing
NASA CR-3918 - Volume III—Data From Crew Module Testing

16. Abstract

Over the past years, several papers and reports have documented the unacceptably high injury rate during the escape sequence (including the ejection and ground impact) of the crew module for F/FB-111 aircraft. This report documents a program to determine if the injury potential could be reduced by replacing the existing crewseats with energy-absorbing crewseats. An energy-absorbing test seat was designed using much of the existing seat hardware. An extensive dynamic seat test series, designed to duplicate various crew module ground impact conditions, was conducted at a sled test facility. Comparative tests with operational F-111 crewseats were also conducted. After successful dynamic testing of the seat, more testing was conducted with the seats mounted in an F-111 crew module. Both swing tests and vertical drop tests were conducted. The vertical drop tests were used to obtain comparative data between the energy-absorbing and operational seats. Volume I describes the energy-absorbing test seat and testing conducted, and evaluates the data from both test series. Volume II presents the data obtained during the seat test series, while Volume III presents the data from the crew module test series.

17. Key Words Seat, Crew Module, Crashworthiness, Escape Systems, Impact Protection, Restraint Systems, Impact Tests	18. Distribution Statement Unclassified - Unlimited Subject Category 05

19. Security Classif. (of this report)	20. Security Classif. (of this page)	21. No. of Pages	22. Price
Unclassified	Unclassified	150	A07

N-305

For sale by the National Technical Information Service, Springfield, Virginia 22161

NASA-Langley, 1985

National Aeronautics and
Space Administration

Washington, D.C.
20546

Official Business
Penalty for Private Use, $300

BULK RATE
POSTAGE & FEES PAID
NASA Washington, DC
Permit No. G-27

NASA

POSTMASTER: **If Undeliverable (Section 158 Postal Manual) Do Not Return**